AD-A086 456 CALIFORNIA UNIV LOS ANGELES SCHOOL OF ENGINEERING A--ETC F/G 20/9
STUDIES OF NONLINEAR PHENOMENA IN PLASMAS.(U)
MAR 80 P K WANG AFOSR-79-0050
UNCLASSIFIED UCLA-ENG-8012 AFOSR-TR-80-0502 NL

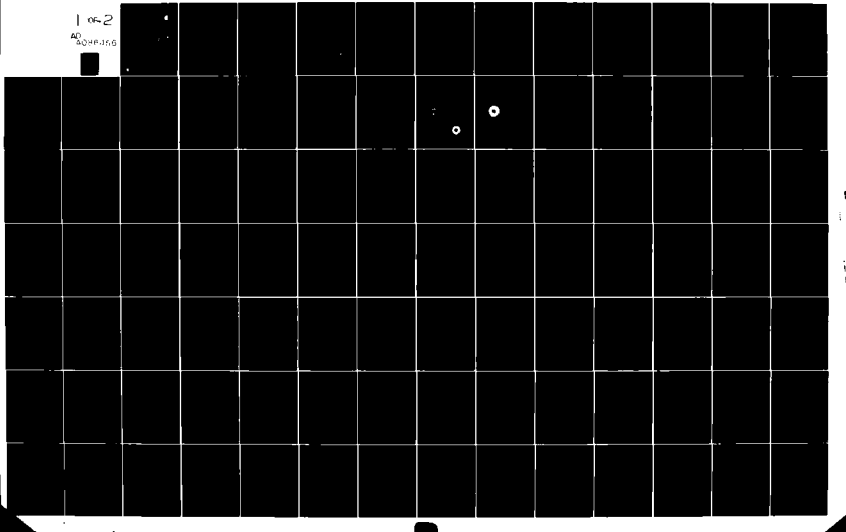

AFOSR-TR- 80-0502

(3)

LEVEL II

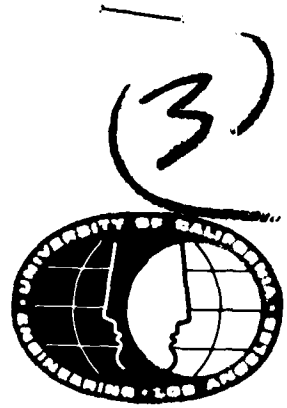

ADA086456

UCLA-ENG-8012
MARCH 1980

STUDIES OF NONLINEAR PHENOMENA IN PLASMAS

PRINCIPAL INVESTIGATOR:
P.K.C. WANG

Final Technical Report
for
AFOSR Grant No. AFOSR-79-0060

Period of Coverage: January 1, 1979 – March 31, 1980

Approved for public release;
distribution unlimited.

UNCLASSIFIED

SECURITY CLASSIFICATION OF THIS PAGE (When Data Ent...)

REPORT DOCUMENTATION PAGE

READ INSTRUCTIONS BEFORE COMPLETING FORM

1. REPORT NUMBER: AFOSR-TR-80-0502	2. GOVT ACCESSION NO.: AD-A086456
3. RECIPIENT'S CATALOG NUMBER	
4. TITLE (and Subtitle): STUDIES OF NONLINEAR PHENOMENA IN PLASMAS	5. TYPE OF REPORT & PERIOD COVERED: FINAL rept 1 Jan 79-31 Mar 80
6. PERFORMING ORG. REPORT NUMBER: UCLA-ENG-8012	
7. AUTHOR(s): P.K.C. Wang	8. CONTRACT OR GRANT NUMBER(s): AFOSR-79-0050
9. PERFORMING ORGANIZATION NAME AND ADDRESS: School of Engineering and Applied Science, University of California, Los Angeles CA 90024	10. PROGRAM ELEMENT, PROJECT, TASK AREA & WORK UNIT NUMBERS: 61102F 2301/A7
11. CONTROLLING OFFICE NAME AND ADDRESS: AFOSR/NP, Bolling AFB, Bldg.#410, Wash DC 20332	12. REPORT DATE: Mar 80
	13. NUMBER OF PAGES: 149
14. MONITORING AGENCY NAME & ADDRESS (if different from Controlling Office)	15. SECURITY CLASS. (of this report): unclassified
	15a. DECLASSIFICATION/DOWNGRADING SCHEDULE: UNCLASSIFIED

16. DISTRIBUTION STATEMENT (of this Report)

Approved for Public Release; Distribution Unlimited

17. DISTRIBUTION STATEMENT (of the abstract entered in Block 20, if different from Report)

18. SUPPLEMENTARY NOTES

19. KEY WORDS (Continue on reverse side if necessary and identify by block number)

plasma turbulence -- chaotic oscillations -- strange attractors -- soliton -- nonlinear systems

20. ABSTRACT (Continue on reverse side if necessary and identify by block number)

This report summarizes the result of a study on nonlinear phenomena in plasmas with main emphasis on developing deterministic theories for plasma turbulence based on the Ruelle-Takens theory of strange attractors, and on the interaction of solitons. The main results include the demonstration of the occurrence of turbulence-like solutions in a simplified Zakharov model for Langmuir turbulence and a number of nonlinear three-wave interactions. The stability of mode-converted lower-hybrid solitons is also studied.

DD FORM 1 JAN 73 1473 EDITION OF 1 NOV 65 IS OBSOLETE S/N 0102-LF-014-6601

404637

UNCLASSIFIED

SECURITY CLASSIFICATION OF THIS PAGE (When Data Entered)

3

STUDIES OF NONLINEAR PHENOMENA IN PLASMAS

FINAL TECHNICAL REPORT

for

US AIR FORCE GRANT No. AFOSR 79-0050

Period of Coverage: 1 January 1979 - 31 March 1980

PRINCIPAL INVESTIGATOR:

P.K.C. WANG

School of Engineering and Applied Science
University of California
Los Angeles, California 90024

March 1980

TABLE OF CONTENTS

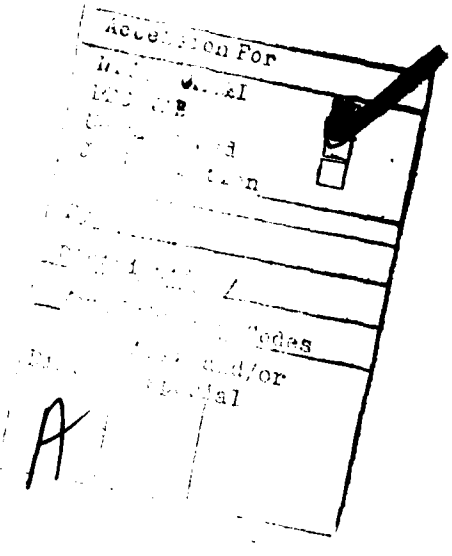

ABSTRACT

This report summarizes the results of a study on nonlinear phenomena in plasmas with the main emphasis on developing deterministic theories for plasma turbulence based on the Ruelle-Takens theory of strange attractors and on the interaction of solitons. The main results include a demonstration of the occurrence of turbulence-like solutions in a simplified Zakharov model for Langmuir turbulence and a number of nonlinear three-wave interactions. The stability of mode-converted lower-hybrid solitons is also studied.

I. INTRODUCTION

Recently, a considerable amount of work has been performed on plasma turbulence. This was partially motivated by the observance of various forms of turbulence phenomena in plasma heating experiments conducted both in this country and abroad.

Since plasma turbulence is primarily due to the nonlinear excitation of collective oscillations having a broad spectrum of frequencies, nonlinear plasma models must be used in the development of theories for such phenomena. The classical approach to the theory of plasma turbulence is to regard the phenomena as stochastic processes. Thus, the description of turbulence quantities is given in terms of their statistical averages [1],[2]. In existing theories for plasma turbulence, certain basic assumptions are introduced, such as ergodicity or stationarity of the processes. The validity of these assumptions is extremely difficult, if not impossible, to establish by experiments. Furthermore, various phenomena at the onset of turbulence cannot be explained by statistical theories.

Motivated by such deficiences in the statistical theories of turbulence, attempts have been made to develop turbulence theory using deterministic models. In 1973, Kingsep, Rudakov and Sudan [3] suggested that strong Langmuir turbulence could be described in terms of a system of interacting Langmuir solitary waves. Subsequently, a considerable amount of analytical and numerical work has been done based on this idea for the one-dimensional case [4],[5]. It was suggested that a similar theory could be developed for the multi-dimensional case. Goldman and Nicholson, however, showed that multi-dimensional spherically symmetric Langmuir solitons, under adiabatic conditions and negligible ion inertia effects, are unstable [6]. Similar

conclusions have been deduced for other cases [7]-[11]. Therefore, further studies are necessary before definite conclusions can be drawn from the approach suggested by Kingsep et al.

In early 1978, under the support of AFOSR Grant No. 74-2662, we began to explore a new direction for developing a deterministic theory for plasma turbulence. This approach was motivated by the work of Lorenz on deterministic nonperiodic flows pertaining to atmospheric turbulence [1] and the theory of "strange attractors" proposed by Ruelle and Takens [13]. A remarkable feature of Lorenz's work is his demonstration of the existence of turbulence-like solutions of a simple nonlinear third-order ordinary differential equation with quadratic nonlinear terms. His equation is a highly simplified model of an incompressible fluid with heat transfer. The results suggest the possibility of modeling atmospheric turbulence by deterministic nonlinear differential equations.

The main objective of this study is to develop *deterministic* theories for plasma turbulence from the standpoint of the Ruelle and Takens theory of strange attractors and the interaction of solitary waves. The results of this study will be summarized categorically in the subsequent section.

II. RESEARCH SUMMARY

In the study of plasma turbulence via the Ruelle-Takens approach, attention has been focused on Langmuir turbulence and nonlinear wave-wave interactions in plasmas. The study of plasma turbulence via the interaction of solitary waves has been limited to mode-converted lower-hybrid solitons. The results are summarized below.

A. Nonperiodic Oscillations of Langmuir Waves

In 1978, under the support of AFOSR Grant No. 74-2662, we discovered that single-mode equations, derived from Zakharov's model for Langmuir turbulence in a plasma in the presence of an external spatially homogeneous electric field oscillating at the electron plasma frequency, have non-periodic chaotic solutions whose power spectra have turbulence-like features [14]. In this simplified model, phenomenological damping terms are introduced; such dissipative terms are essential for the existence of chaotic oscillations.

During the period covered by this report, we explored further the observed chaotic oscillations with the objective of achieving some understanding of the nature of the onset of these oscillations and their qualitative behavior. Our first results consist of estimates for the amplitudes of the chaotic oscillations. We showed that the magnitude of the high-frequency electric field oscillations, about some real scalar multiple of the external electric field E_0, satisfies a bound which grows linearly with $\|E_0\|$. In addition, the ion density oscillations are contained in a ball whose radius grows with $\|E_0\|^2$. These bounds are consistent with the numerical solutions. The results were combined with those in [14] and published recently in the *Journal of Mathematical Physics* (see Appendix A).

In order to understand the onset of chaotic oscillations, we determined numerically the Poincaré mappings associated with various hyperplanes in the system's state space. It was found that the mappings are quasi-one-dimensional, but their structures are not sufficiently simple to permit meaningful analytical studies. Finally, a bifurcation analysis of the system was performed with respect to the damping coefficients. The results are described in the report [P9] (see Appendix B).

B. Chaotic Solutions of Resonant Three-Wave Interactions

This study began with the following well-known simplified model governing the nonlinear resonant interaction of three waves with both linear growth and damping terms:

$$\left.\begin{aligned} dA_1/dt &= \gamma_1 A_1 - iVA_2A_2 \ , \\ dA_2/dt &= -\gamma_2 A_2 - iVA_1A_3^* \ , \\ dA_3/dt &= -\gamma_3 A_3 - iVA_1A_2^* \ , \end{aligned}\right\} \qquad (1)$$

where the A_j's correspond to the normalized complex wave amplitudes, V is a real coupling coefficient and the γ_j's are positive numbers. This model includes a number of important resonant wave-wave interactions in plasmas. It was shown that, under certain conditions, the asymptotic behavior of the solutions of (1) for $t \to \infty$ can be described by a system of three real ordinary differential equations. Numerical studies showed that the reduced system exhibits chaotic oscillations which are sensitive to variations in the initial conditions. Moreover, the autocovariance functions associated with the chaotic solutions appear to decay as the separation time tends to ∞. This suggests that a turbulent state could be

produced through the nonlinear interaction of a linearly unstable wave with two linearly damped waves. The preliminary results of this study are described in the report [P7] (see Appendix C) published in November, 1979. Since then, further studies have been made in categorizing general three-wave interactions which are capable of producing chaotic oscillations. The results will be described in a forthcoming thesis by K. Masui [P8].

C. Mode-Converted Lower-Hybrid Solitons

It is well known that one-dimensional Langmuir solitons are modulationally unstable to transverse perturbations. The instability causes the solitons to collapse and form bunches resembling a turbulent state. Here, it was shown that the planar mode-converted lower-hybrid solitons are also unstable to transverse perturbations. Moreover, two distinct classes of modes are found. In the lowest order. the stability of each class is related to a particular term of the equation governing the nonlinear evolution of these waves. The details are described in the report [P5] (see Appendix D).

D. Chaotic Oscillations in Bilinear Systems

It was observed that the mathematical models of may physical processes, including certain nonlinear wave-wave interactions and the Lorenz equation, can be written in the form: $dx/dt = Ax + f(x)$, where A is a real $n \times n$ matrix and f is a bilinear function of x . During 1979, chaotic oscillations in this class of systems were explored from the viewpoint of feedback control theory. A simple and sufficient condition for the nonexistence of such oscillations was derived. Ellipsoidal bounds for the amplitudes of chaotic oscillations were also obtained. The results are applicable to the Lorenz equation and other equations which are known to have chaotic oscillations. The details are given in report [P6] (see Appendix E).

III. CONCLUDING REMARKS

Since the initiation of this study, there appears to be a growing interest in the theory of chaotic oscillations in deterministic nonlinear dynamical systems and its application to turbulence, as proposed by Ruelle and Takens. During the period covered by this report, the following conferences and symposia were held both in the US and abroad at which papers on chaotic oscillations were presented:

(1) International Workshop on Intrinsic Stochasticity in Plasmas, June 17-23, 1973, Institut d'Etudes Scientifiques de Cargese, Corse, France.

(2) Annual Meeting of the Plasma Physics Division, American Physical Society, November 12-16, 1979, Boston.

(3) Engineering Foundation Converence on New Approaches to Nonlinear Problems in Dynamics, December 9-14, 1979, Asilomar, California.

(4) International Conference on Nonlinear Dynamics, December 17-21, 1979, New York City.

So far, chaotic oscillations in nonlinear systems have been discovered mostly through bifurcation analysis and numerical experimentation. There are no general mathematical conditions of ensuring the existence of chaotic oscillations in systems described by ordinary or partial differential equations. Moreover, it is very difficult to verify that a numerically computed apparently chaotic solution is indeed chaotic in some sense. Until these basic questions are resolved, there remains a gap between the mathematical theory of chaotic oscillations and turbulence phenomena as observed in the physical world.

IV. REFERENCES

[1] V.N. Tystovich, *Theory of Turbulent Plasma*, Consultants Bureau, NY, 1977.

[2] S. Ichimaru, *Basic Principles of Plasma Physics: A Statistical Approach*, W.A. Benjamin, Inc., London, 1973.

[3] A.S. Kingsep, L.I. Rudakov and R.N. Sudan, *Phys.Rev.Lett., 31* (1973) p.1482.

[4] L.M. Degtyarev et al, *Soviet Physics JETP, 40* (1975) p.264.

[5] V.I. Karpman, *Physica Scripta, 11* (1975) p.263.

[6] M.V. Goldman and D.R. Nicholson, *Phys.Rev.Lett., 41* (1978) p.406.

[7] V.E. Zakharov and V.S. Synakh, *Soviet Physics JETP, 41* (1976) p.465.

[8] J. Gibbons et al., *J.Plasma Physics, 17* (1977) p.153.

[9] J. Denavit et al., *Phys.Rev.Lett., 33* (1974) p.1435.

[10] J.Z. Wilcox and T.J. Wilcox, *Phys.Rev.Lett., 34* (1975) p.1160.

[11] E. Infeld and G. Rowlands, *Plasma Phys., 15* (1977) p.343.

[12] E.N. Lorenz, *J.Atmospheric Sci., 20* (1963) p.130.

[13] D. Ruelle and F. Takens, *Comm.Math.Physics, 20* (1971) p.167.

[14] P.K.C. Wang, *Nonperiodic Oscillations of Langmuir Waves*, UCLA Engr. Rpt. No. *ENG-7879*, Nov. 1978.

V. PUBLICATIONS, REPORTS AND PRESENTATIONS

[P1] P.K.C. Wang, "Nonperiodic Oscillations of Langmuir Waves," *J.Math.Phys., 21:2* (1980) 398-407.

[P2] P.K.C. Wang, "Turbulent Solutions of Zakharov's Model for Langmuir Turbulence," *Annual Mtg., Plasma Physics Div., Am.Phys.Soc., Boston, Nov. 1979,* Paper No. 1R2 (Abstract: *Bull.Am.Phys.Soc., 24:8* (1979)p.934).

[P3] K. Masui and P.K.C. Wang, "Turbulent Solutions of Resonant Three-Wave Interactions," *Annual Mtg., Plasma Physics Div., Am.Phys.Soc, Boston, Nov. 1979,* Paper 1R1 (Abstract: *Bull.Am.Phys.Soc, 24:8* (1979) p.933).

[P4] P.K.C. Wang, "Chaotic Oscillations in Plasmas," *Symp. on New Approaches to Nonlinear Problems, Asilomar, CA, Dec. 1979* (Presentation).

[P5] L.C. Himmell, "Stability of Mode-Converted Lower-Hybrid Solitons," UCLA Engr.Rpt.No. *ENG-7913*, Feb. 1979.

[P6] P.K.C. Wang, "Chaotic Oscillations of Bilinear Systems with Linear Feedback Controls," UCLA Engr.Rpt.No. *ENG-7948*, Aug. 1979.

[P7] K. Masui and P.K.C. Wang, "Chaotic Solutions of Resonant Three-Wave Interactions," UCLA Eng.Rpt.No. *ENG-7976,* Nov. 1979.

[P8] K. Masui, "Chaotic Solutions of Nonlinear Wave-Wave Interacting Systems in Plasmas," *Ph.D. Dissertation*, Univ. of California, Los Angeles (to be completed in June, 1980).

[P9] P.K.C. Wang, "Further Study of Chaotic Oscillations of a Simplified Zakharov Model for Langmuir Turbulence", UCLA Engr.Rpt.No. *ENG-8013*, March 1980.

APPENDIX A

Nonperiodic oscillations of Langmuir waves

P. K. C. Wang
School of Engineering and Applied Science, University of California, Los Angeles, California 90024

(Received 21 December 1978; accepted for publication 15 October 1979)

It is shown that the single-mode equations derived from Zakharov's model for Langmuir turbulence in a plasma in the presence of an external spatially homogeneous electric field oscillating at the electron plasma frequency has nonperiodic chaotic solutions whose power spectra have turbulence-like features. Bounds for these chaotic solutions are derived. Typical numerical results are presented for the one-dimensional case.

1. INTRODUCTION

It has been observed that certain nonlinear ordinary differential equations have chaotic or turbulence-like solutions.[1-4] A simple example is the Lorenz model for thermal convection in a fluid layer.[1] Recently, Ruelle and Takens proposed that fluid turbulence can be mathematically characterized by this class of solutions whose trajectories in the state space are attracted to a nonempty set ("strange attractor") which is neither an equilibrium set nor a periodic orbit.[5] On this set, the trajectories exhibit chaotic oscillations. Moreover, they are sensitive to variations in the initial conditions. Here, we shall demonstrate that the single-mode equations derived from the Zakharov's model for Langmuir turbulence in a plasma have nonperiodic chaotic solutions.

We begin with the following dimensionless form of Zakharov's equations describing the nonlinear interaction of high-frequency electron oscillations with an ion fluid in the presence of an external spatially homogeneous electric field oscillating at the electron plasma frequency ω_p:[6-8]

$$\nabla\cdot\left[i\frac{\partial \mathbf{E}}{\partial t}+\nabla^2\mathbf{E}-n(\mathbf{E}+\mathbf{E}_0)\right]=0, \tag{1}$$

$$\frac{\partial^2 n}{\partial t^2}-\nabla^2 n=\nabla^2\left[|\mathbf{E}|^2+\mathbf{E}_0\cdot(\mathbf{E}+\mathbf{E}^*)\right], \tag{2}$$

where $i=\sqrt{-1}$; $(\cdot)^*$ denotes complex conjugation, and $\mathbf{a}\cdot\mathbf{b}$ the usual scalar product of two real or complex vectors $\mathbf{a}$ and $\mathbf{b}$. $\mathbf{E}=(E_1,\ldots,E_N)$ is the complex amplitude of the high-frequency electric field $\mathscr{E}$ given by

$$\mathscr{E}(t,\mathbf{x})=\mathrm{Re}[\mathbf{E}(t,\mathbf{x})\exp(-i\omega_p t)]; \tag{3}$$

and n is a real quantity corresponding to the low-frequency perturbation in the ion density from its constant equilibrium value n_0. The units of time t, spatial coordinates $\mathbf{x}=(x_1,\ldots,x_N)$, electric fields $\mathbf{E}_0$ and $\mathbf{E}$, and ion density perturbation are respectively, $3/(2\alpha\omega_p)$, $(3/2)\alpha^{-1/2}\lambda_D$, $[(64/3)\pi n_0 m_e c_s^2]^{1/2}$, and $(4/3)\alpha n_0$, where α is the electron-ion mass ratio m_e/m_i, λ_D the Debye length, and c_s is the ion acoustic speed. Here, $\mathbf{E}_0=(E_{01},\ldots,E_{0N})$ is a real constant vector corresponding to the normalized amplitude of the external electric field. It is of interest to determine the behavior of the solutions of (1) and (2) (with appropriate damping terms) as a function of the parameter $\mathbf{E}_0$, in particular, the existence of turbulence-like solutions for some $\mathbf{E}_0$, and the onset of such solutions as $\mathbf{E}_0$ tends to some threshold values.

2. SIMPLIFIED MODEL

Let the spatial domain Ω be a bounded open subset of the N-dimensional Euclidean space $\mathbf{R}^N$, and $L^2(\Omega)$ denote the Hilbert space of real square-integrable functions defined on Ω with inner product $\langle u,v\rangle=\int_\Omega u(\mathbf{x})v(\mathbf{x})\,d\Omega$. Let $\{\phi_k\}$ be a countable orthonormal basis for $L^2(\Omega)$. We seek solutions to (1) and (2) in the form:

$$\mathbf{E}(t,\mathbf{x})=\sum_k \mathbf{E}_k(t)\phi_k(\mathbf{x}),\quad n(t,\mathbf{x})=\sum_k n_k(t)\phi_k(\mathbf{x}). \tag{4}$$

If the boundary of Ω is sufficiently smooth, then the Laplacian with suitable homogeneous boundary conditions is a negative operator with a countable point spectrum. We may take ϕ_k to be the orthonormalized eigenfunction of ∇^2 corresponding to the eigenvalue $\lambda_k=-\mu_k^2$. In this case, we may substitute (4) into (1) and (2), multiply both sides of the equations by $\phi_m(\mathbf{x})$, and integrate over Ω to give a countably infinite system of ordinary differential equations for $\mathbf{E}_m$ and n_m:

$$i\frac{d\mathbf{E}_m}{dt}-\mu_m^2\mathbf{E}_m=n_m\mathbf{E}_0+\sum_k\sum_{k'}\alpha_{mkk'}n_k\mathbf{E}_{k'}, \tag{5}$$

$$\frac{d^2 n_m}{dt^2}+\mu_m^2 n_m=-\mu_m^2\mathbf{E}_0\cdot(\mathbf{E}_m+\mathbf{E}_m^*)+\sum_k\sum_{k'}\beta_{mkk'}\mathbf{E}_k\cdot\mathbf{E}_{k'}, \tag{6}$$

where $\mathbf{E}_k\cdot\mathbf{E}_{k'}=\sum_j E_{kj}E_{k'j}^*$ and

$$\alpha_{mkk'}=\int_\Omega \phi_k(\mathbf{x})\phi_{k'}(\mathbf{x})\phi_m(\mathbf{x})\,d\Omega. \tag{7}$$

$$\beta_{mkk'}=\int_\Omega \nabla^2[\phi_k(\mathbf{x})\phi_{k'}(\mathbf{x})]\phi_m(\mathbf{x})\,d\Omega. \tag{8}$$

By retaining only the terms involving $\mathbf{E}_m$ and n_m in (5) and (6), we obtain the following simplified equations for a single mode m:

$$i\frac{d\mathbf{E}_m}{dt}-(\mu_m^2-i\gamma_m)\mathbf{E}_m=n_m(\mathbf{E}_0+\alpha_m\mathbf{E}_m), \tag{9}$$

$$\frac{d^2 n_m}{dt^2}+2\Gamma_m\frac{dn_m}{dt}+\mu_m^2 n_m=-\mu_m^2\mathbf{E}_0\cdot(\mathbf{E}_m+\mathbf{E}_m^*)+\beta_m|\mathbf{E}_m|^2, \tag{10}$$

where

 0022-2488/80/020398-10$1.00

$$\alpha_m = \int_\Omega \phi_m^\dagger(\mathbf{x})\,d\Omega, \quad \beta_m = \int_\Omega \nabla^2[\phi_m^\dagger(\mathbf{x})]\phi_m(\mathbf{x})\,d\Omega\,. \tag{11}$$

Also, we have added the phenomenological damping coefficients γ_m and Γ_m. They may represent Landau damping of the high- and low-frequency waves. In what follows, we shall analyze the behavior of the solutions of (9) and (10) as $\mathbf{E}_0$ varies. For brevity, the subscript m in (9) and (10) will be omitted in places where ambiguity does not arise.

A starting point for searching the strange attractor or chaotic solutions is to study the nature of the equilibrium points as $\mathbf{E}_0$ varies. It is known that chaotic solutions could arise after finite number of Hopf bifurcations,[5] therefore we shall establish the existence of Hopf bifurcation points.

3. EQUILIBRIUM POINTS

Consider the following equations for determining the equilibrium points of (9) and (10) for any given $\mathbf{E}_0$:

$$(i\gamma - \mu^2)\mathbf{E} = n(\mathbf{E}_0 + \alpha\mathbf{E})\,, \tag{12}$$

$$\mu^2 n = -\mu^2\mathbf{E}_0\cdot(\mathbf{E} + \mathbf{E}^*) + \beta\,|\mathbf{E}|^2\,. \tag{13}$$

Using (13) to eliminate n in (12), we obtain an equation for $\mathbf{E}$:

$$(i\gamma - \mu^2)\mathbf{E} = [-\mathbf{E}_0\cdot(\mathbf{E} + \mathbf{E}^*) + \beta\mu^{-2}\,|\mathbf{E}|^2](\mathbf{E}_0 + \alpha\mathbf{E})\,. \tag{14}$$

Evidently, since $\mathbf{E}_0$ is a real N-dimensional vector and n is real, a solution of (14) must be a complex scalar multiple of $\mathbf{E}_0$ (i.e., $\mathbf{E} = \xi\,\mathbf{E}_0$ for some $\xi = \xi_R + i\xi_I$). Thus, the solution of (14) reduces to finding ξ. Note that $\mathbf{E} = 0$ is a solution of (14) for any $\mathbf{E}_0$. Substituting $\mathbf{E} = \xi\,\mathbf{E}_0$ into (14) leads to the following equations for ξ_R and ξ_I:

$$-(\mu^2\xi_R + \gamma\xi_I) = \{\beta\mu^{-2}(\xi_R^2 + \xi_I^2) - 2\xi_R\}(1 + \alpha\xi_R)\|\mathbf{E}_0\|^2, \tag{15}$$

$$\gamma\xi_R - \mu^2\xi_I = \{\beta\mu^{-2}(\xi_R^2 + \xi_I^2) - 2\xi_R\}\alpha\xi_I\|\mathbf{E}_0\|^2, \tag{16}$$

and

$$n = \{\beta\mu^{-2}(\xi_R^2 + \xi_I^2) - 2\xi_R\}\|\mathbf{E}_0\|^2, \tag{17}$$

where $\|\mathbf{E}_0\|^2 = \mathbf{E}_0\cdot\mathbf{E}_0$.

Dividing (15) by (16) gives

$$\xi_R^2 + \xi_I^2 = (\alpha\gamma)^{-1}(\mu^2\xi_I - \gamma\xi_R)\,, \tag{18}$$

which implies that a solution must lie on the circle:

$$\left(\xi_R + \frac{1}{2\alpha}\right)^2 + \left(\xi_I - \frac{\mu^2}{2\alpha\gamma}\right)^2 = \frac{(\mu^4 + \gamma^2)}{(2\alpha\gamma)^2}\,. \tag{19}$$

Now, we substitute (18) into (16) and solve for ξ_R in terms of ξ_I:

$$\xi_R = \xi_I(\mu^2 + \beta\gamma^{-1}\|\mathbf{E}_0\|^2\xi_I) \times [\gamma + (2\alpha + \beta\mu^{-2})\|\mathbf{E}_0\|^2\xi_I]^{-1}\,. \tag{20}$$

Finally, using (20) to eliminate ξ_R in (18) leads to the following quadratic equation for ξ_I:

$$A\xi_I^2 + B\xi_I + C = 0\,, \tag{21}$$

where

$$A = [(\beta/\gamma)^2 + \delta^2]\|\mathbf{E}_0\|^4\,, \tag{22}$$

$$B = 2(\mu^2\beta\gamma^{-1} + \gamma\delta)\|\mathbf{E}_0\|^2 - 2\mu^2\delta\gamma^{-1}\|\mathbf{E}_0\|^4\,, \tag{23}$$

$$C = \mu^4 + \gamma^2 - 2\mu^2\|\mathbf{E}_0\|^2 \tag{24}$$

$$\delta = (2\alpha + \beta\mu^{-2})\,. \tag{25}$$

If $B^2 - AC > 0$ or

$$\|\mathbf{E}_0\|^4 - 4\alpha\beta\delta^{-2}\|\mathbf{E}_0\|^2 - (2\alpha\gamma/\delta)^2 > 0\,, \tag{26}$$

then (21) has real roots given explicitly by

$$\xi_I^{\pm} = \frac{\delta\gamma\mu^2}{(\beta^2 + \delta^2\gamma^2)\|\mathbf{E}_0\|^2}\left\{\|\mathbf{E}_0\|^2 - \frac{(\mu^2\beta + \gamma^2\delta)}{\delta\mu^2} \pm \left[\|\mathbf{E}_0\|^4 - 4\alpha\beta\delta^{-2}\|\mathbf{E}_0\|^2 - \left(\frac{2\alpha\gamma}{\delta}\right)^2\right]^{1/2}\right\} \tag{27}$$

For $\|\mathbf{E}_0\|^2 > 0$, condition (26) is satisfied if and only if

$$\|\mathbf{E}_0\|^2 > E_{oc}^2 \triangleq 2\alpha\delta^{-2}[\beta + (\beta^2 + \delta^2\gamma^2)^{1/2}]\,. \tag{28}$$

Thus, we conclude that for $0 \le \|\mathbf{E}_0\| < E_{oc}$, the origin $(\mathbf{E},n,\dot{n}) = (0 + j0,0,0)$ is the only equilibrium state of system (9) and (10), where $\dot{n}$ denotes dn/dt. When $\|\mathbf{E}_0\| = E_{oc}$, a new equilibrium state $(\mathbf{E},n,\dot{n}) = (\mathrm{Re}(\mathbf{E}) + i\mathrm{Im}(\mathbf{E}),n,0)$ emerges, where $\mathrm{Re}(\mathbf{E}) = \xi_R\,\mathbf{E}_0$, $\mathrm{Im}(\mathbf{E}) = \xi_R\,\mathbf{E}_0$ with ξ_I given by

$$\xi_I = \frac{\delta\gamma\mu^2}{(\beta^2 + \delta^2\gamma^2)E_{oc}^2}\left(E_{oc}^2 - \frac{(\mu^2\beta + \gamma^2\delta)}{\delta\mu^2}\right), \tag{29}$$

and ξ_R, n are given by (20) and (17) respectively. As $\|\mathbf{E}_0\|$ increases from E_{oc}, the foregoing nonzero equilibrium state bifurcates into two distinct equilibrium states $(\xi_R^+\mathbf{E}_0 + i\xi_I^+\mathbf{E}_0, n^+, 0)$ and $(\xi_R^-\mathbf{E}_0 + i\xi_I^-\mathbf{E}_0, n^-, 0)$ where $\xi_I^\pm$ are given by (27), whose corresponding $\xi_R^\pm$ and $n^\pm$ are determined respectively by (20) and (17). We note that ξ_R and ξ_I depend on $\|\mathbf{E}_0\|^2$. Also, the coefficient C defined by (24) vanishes when

$$\|\mathbf{E}_0\|^2 = \bar{E}_{oc}^2 \triangleq (\mu^4 + \gamma^2)/(2\mu^2)\,. \tag{30}$$

Consequently, ξ_I^- also vanishes. Thus, in this case, the equilibrium set consists of the origin and the point $[(\xi_R^+ + i\xi_I^+)\mathbf{E}_0, n^+, 0]$. When $\|\mathbf{E}_0\|$ increases from $\bar{E}_{oc}$, we have again three distinct equilibrium points.

4. STABILITY OF EQUILIBRIUM

Let $\mathbf{E}_R = \mathrm{Re}(\mathbf{E})$, $\mathbf{E}_I = \mathrm{Im}(\mathbf{E})$, and $\mathbf{z}$ denote the $2(N+1)$-dimensional real vector $(n,\dot{n},\mathbf{E}_R,\mathbf{E}_I)^T$, where $(\cdot)^T$ denotes transposition. We rewrite (9) and (10) in the form:

$$\frac{d\mathbf{z}}{dt} = \mathbf{f}(\mathbf{z};\mathbf{E}_0) \triangleq \begin{bmatrix} \dot{n} \\ -\mu^2 n - 2\Gamma\dot{n} - 2\mu^2\,\mathbf{E}_0\cdot\mathbf{E}_R + \beta\,(\|\mathbf{E}_R\|^2 + \|\mathbf{E}_I\|^2) \\ -\gamma\mathbf{E}_R + (\mu^2 + \alpha n)\mathbf{E}_I \\ -\gamma\mathbf{E}_I - (\mu^2 + \alpha n)\mathbf{E}_R - n\mathbf{E}_0 \end{bmatrix}. \tag{31}$$

Let $\mathbf{z}_e = (n^e, 0, \mathbf{E}_R^e, \mathbf{E}_I^e)$ be an equilibrium point of (31) as given in Sec. 3, and $\delta\mathbf{z}(t) \triangleq \mathbf{z}(t) - \mathbf{z}_e$. We consider the following linearized system of (31) about $\mathbf{z}_e$:

$$\frac{d\delta\mathbf{z}}{dt} = \mathbf{J}_f(\mathbf{z}_e;\mathbf{E}_0)\delta\mathbf{z}, \tag{32}$$

where $\mathbf{J}_f(\mathbf{z}_e;\mathbf{E}_0)$ is the Jacobian matrix of $\mathbf{f}$ at $\mathbf{z}_e$ given by

$$\mathbf{J}_f(\mathbf{z}_e;\mathbf{E}_0) = \begin{bmatrix} 0 & 1 & \mathbf{O}_N^T & \mathbf{O}_N^T \\ -\mu^2 & -2\Gamma & 2(\beta\mathbf{E}_R^e - \mu^2\mathbf{E}_0)^T & 2\beta(\mathbf{E}_I^e)^T \\ \alpha\mathbf{E}_I^e & 0 & -\gamma\mathbf{I}_N & (\mu^2+\alpha n^e)\mathbf{I}_N \\ -(\mathbf{E}_0+\alpha\mathbf{E}_R^e) & 0 & -(\mu^2+\alpha n^e)\mathbf{I}_N & -\gamma\mathbf{I}_N \end{bmatrix}, \tag{33}$$

where $\mathbf{O}_N$ and $\mathbf{I}_N$ are the N-dimensional zero vector and $N\times N$ identity matrix respectively. It can be shown (see Appendix) that the characteristic polynomial of $\mathbf{J}_f(\mathbf{z}_e;\mathbf{E}_0)$ is given by

$$\begin{aligned}\det[\mathbf{J}_f(\mathbf{z}_e;\mathbf{E}_0) - \lambda\,\mathbf{I}_{2(N+1)}] &= [(\gamma+\lambda)^2 + (\mu^2+\alpha n^e)^2]^N(\lambda^2 + 2\Gamma\lambda + \mu^2) + 2[(\gamma+\lambda)^2 + (\mu^2+\alpha n^e)^2]^{N-1} \\ &\times [(\mu^2+\alpha n^e)\{(\beta\mathbf{E}_R^e - \mu^2\mathbf{E}_0)\cdot(\mathbf{E}_0+\mathbf{E}_R^e) + \alpha\beta\|\mathbf{E}_I^e\|^2\} + (\gamma+\lambda)(\alpha\mu^2+\beta)\mathbf{E}_0\cdot\mathbf{E}_I^e]. \end{aligned} \tag{34}$$

For the case where $\mathbf{z}_e = \mathbf{0}$, the above expression reduces to

$$\det[\mathbf{J}_f(\mathbf{0};\mathbf{E}_0) - \lambda\,\mathbf{I}_{2(N+1)}] = [(\gamma+\lambda)^2+\mu^4]^{N-1}[(\lambda^2+2\Gamma\lambda+\mu^2)\{(\gamma+\lambda)^2+\mu^4\} - 2\mu^4\|\mathbf{E}_0\|^2] \tag{35}$$

Evidently, when $\mathbf{E}_0 = \mathbf{0}$, the spectrum of $\mathbf{J}_f(\mathbf{0};\mathbf{0})$ is given by $\{-\gamma \pm i\mu^2$ (multiplicity N), $-\Gamma \pm (\Gamma^2-\mu^2)^{1/2}\}$, which implies the asymptotic stability of the origin for $\gamma,\Gamma > 0$. For $\mathbf{E}_0 \neq 0$, the eigenvalues $\lambda = -\gamma \pm i\mu^2$ [multiplicity $(N-1)$] remain invariant, while the remaining eigenvalues are roots of the quartic equation:

$$\lambda^4 + 2(\gamma+\Gamma)\lambda^3 + (\mu^4+\mu^2+4\gamma\Gamma+\gamma^2)\lambda^2 + 2[\Gamma(\gamma^2+\mu^4) + \gamma\mu^2]\lambda + \mu^2[(\gamma^2+\mu^4) - 2\mu^2\|\mathbf{E}_0\|^2] = 0. \tag{36}$$

Obviously, $\mathbf{J}_f(\mathbf{0};\mathbf{E}_0)$ has a zero eigenvalue when $\|\mathbf{E}_0\|^2 = \bar{E}_{oc}^2 \triangleq (\mu^4+\gamma^2)/(2\mu^2)$. This coincides with condition (30) for which one of the equilibrium points returns to the origin. It can be readily shown by using Routh's criterion[9] that the origin becomes unstable when $\|\mathbf{E}_0\| > \bar{E}_{oc}$. In fact, (36) has only one unstable root and it is real and positive. Thus, the origin has a saddle point structure in a two-dimensional manifold. So we conclude that Hopf bifurcation cannot occur at the origin for any value of $\|\mathbf{E}_0\|$.

For the case where $\|\mathbf{E}_0\| > E_{oc}$, there exist nonzero equilibrium states $\mathbf{z}_e$ which depend on $\|\mathbf{E}_0\|$. We observe from (34) that $\lambda = -\gamma \pm i(\mu^2+\alpha n^e)$ are stable eigenvalues of $\mathbf{J}_f(\mathbf{z}_e;\mathbf{E}_0)$ with a multiplicity of $(N-1)$. The remaining eigenvalues are given by the roots of the quartic equation:

$$\lambda^4 + a_3\lambda^3 + a_2(\|\mathbf{E}_0\|)\lambda^2 + a_1(\|\mathbf{E}_0\|)\lambda + a_0(\|\mathbf{E}_0\|) = 0. \tag{37}$$

where

$$\begin{aligned} a_3 &= 2(\gamma+\Gamma), \quad a_2(\|\mathbf{E}_0\|) = \gamma^2+\mu^2+4\gamma\Gamma + (\mu^2+\alpha n^e)^2, \\ a_1(\|\mathbf{E}_0\|) &= 2\{\Gamma[\gamma^2+(\mu^2+\alpha n^e)^2] + \gamma\mu^2 + (\alpha\mu^2+\beta)\mathbf{E}_0\cdot\mathbf{E}_I^e\}, \\ a_0(\|\mathbf{E}_0\|) &= \mu^2[\gamma^2+(\mu^2+\alpha n^e)^2] + 2\{(\mu^2+\alpha n^e)[(\beta\mathbf{E}_R^e - \mu^2\mathbf{E}_0)\cdot(\mathbf{E}_0+\alpha\mathbf{E}_R^e) \\ &\quad + \alpha\beta\|\mathbf{E}_I^e\|^2] + \gamma(\alpha\mu^2+\beta)\mathbf{E}_0\cdot\mathbf{E}_I^e\}, \end{aligned} \tag{38}$$

where $\mathbf{E}_R^e$, $\mathbf{E}_I^e$, and n^e (given in Sec. 3) depend on $\|\mathbf{E}_0\|$. To determine the value of $\|\mathbf{E}_0\|$ for which Hopf bifurcation occurs, it is necessary to determine the existence of purely imaginary roots of (37) for some value of $\|\mathbf{E}_0\|$. From Routh's criterion, we can deduce that if

$$a_3a_2(\|\mathbf{E}_0\|) > a_1(\|\mathbf{E}_0\|) \tag{39}$$

and

$$a_1(\|\mathbf{E}_0\|)[a_3a_2(\|\mathbf{E}_0\|) - a_1(\|\mathbf{E}_0\|)] = a_3^2a_0(\|\mathbf{E}_0\|), \tag{40}$$

then (38) has a pair of purely imaginary roots given by $\lambda = \pm\{a_3a_0[a_3a_2(\|\mathbf{E}_0\|) - a_1(\|\mathbf{E}_0\|)]\}^{1/2}i$.

Let E_{0H} be the value of $\|\mathbf{E}_0\|$ such that both (39) and (40) are satisfied; and $\tilde{\lambda}_\pm(\|\mathbf{E}_0\|) = \tilde{\lambda}_R(\|\mathbf{E}_0\|) \pm i\tilde{\lambda}_I(\|\mathbf{E}_0\|)$ be the roots of (37) such that $\tilde{\lambda}_R(E_{0H}) = 0$. By a lengthy but straightforward computation, it can be shown that $\tilde{\lambda}_R'$, the derivative of $\tilde{\lambda}_R$ with respect to the parameter $\|\mathbf{E}_0\|$, is given by

$$\begin{aligned}\tilde{\lambda}_R'(\|\mathbf{E}_0\|) &= [a_3^2a_0'(\|\mathbf{E}_0\|) + 2a_1(\|\mathbf{E}_0\|)a_1'(\|\mathbf{E}_0\|) - a_3a_2'(\|\mathbf{E}_0\|)a_1(\|\mathbf{E}_0\|) \\ &\quad - a_3a_2(\|\mathbf{E}_0\|)a_1'(\|\mathbf{E}_0\|)]\{2a_3[a_3a_1(\|\mathbf{E}_0\|) + a_2^2(\|\mathbf{E}_0\|) - 4a_0(\|\mathbf{E}_0\|)]\}^{-1}, \end{aligned} \tag{41}$$

where a_j' denotes the derivative of a_j with respect to $\|\mathbf{E}_0\|$. For Hopf bifurcation,[10] $\tilde{\lambda}_R'(E_{0H}) > 0$. Due to the complicated dependence of a_2, a_1, and a_0 on $\|\mathbf{E}_0\|$, it is difficult to determine the threshold values of $\|\mathbf{E}_0\|$ for Hopf bifurcation. We shall resort to numerical computation at this point.

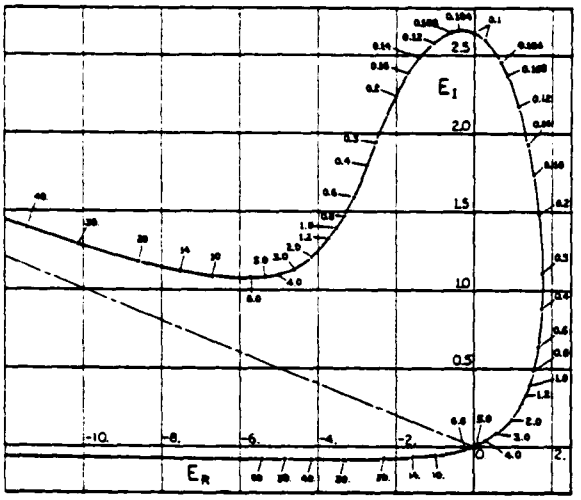

FIG. 1. Locus of equilibrium electric field $E^e = E_R^e + iE_I^e$ with E_0^2 as a parameter. ($E_+^e = \xi^+ E_0$ and $E_-^e = \xi^- E_0$ are denoted by solid dots and circles respectively.

We note here that the Hopf bifurcation problem for (9) and (10) with spatial dimension N or $\dim(\mathbf{E}) > 1$ can be completely studied by considering only (37) which is the characteristic equation for the case with $N = 1$. Since for $\gamma > 0$ and $\Gamma > 0$, the additional eigenvalues $\lambda = -\lambda \pm i(\mu^2 + \alpha n^2)$ for $N > 1$ are stable, and a_2, $a_3(\|\mathbf{E}_0\|) > 0$ for all $\|\mathbf{E}_0\|$, the dimension of the unstable manifold associated with a nonzero equilibrium state is at most three.

5. BOUNDS FOR CHAOTIC OSCILLATIONS

The existence of chaotic oscillations depends on the manner in which the stable and unstable manifolds associated with the equilibrium points intersect with each other. At present, there are no readily verifiable analytical sufficient conditions for the existence of chaotic solutions for finite dimensional systems of ordinary differential equations. Here, we assume the existence of chaotic oscillations and proceed to derive bounds for their amplitudes, thus providing estimates for the size of the invariant manifold generated by the chaotic oscillations.

First, we shall make use of a function V of the form:

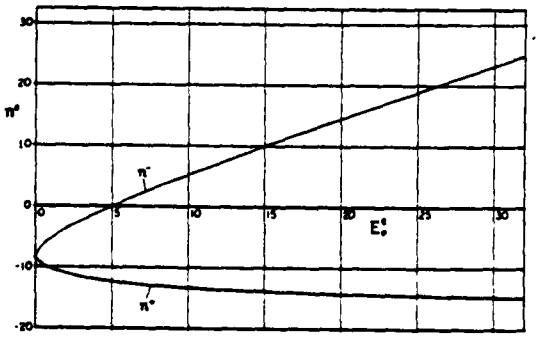

FIG. 2. Locus of equilibrium ion densitities n^+ and n^- with E_0^2 as a parameter.

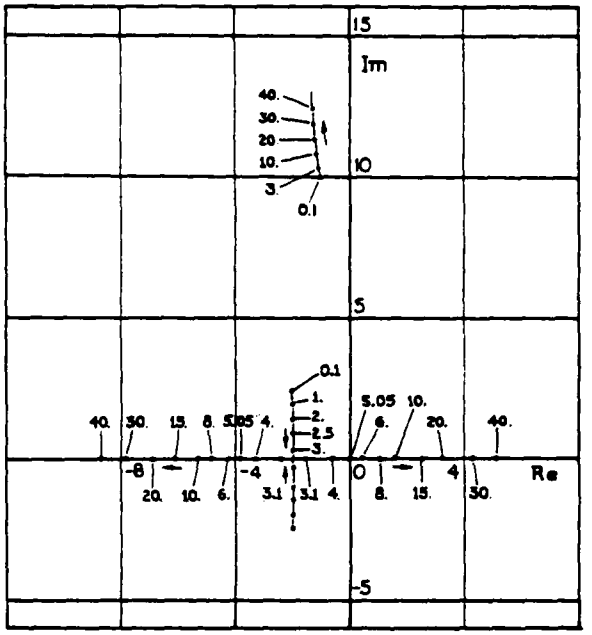

FIG. 3. Locus of the eigenvalues of $J_f(0;E_0)$ with E_0^2 as a parameter.

$$V(\mathbf{E}) = |\mathbf{E} - \tilde{\mathbf{E}}|^2/2\,, \tag{42}$$

to estimate the magnitude of chaotic oscillations of the electric field where $\tilde{\mathbf{E}} = \mathrm{Re}\tilde{\mathbf{E}} + i\mathrm{Im}\tilde{\mathbf{E}}$ is to be determined. By direct computation:

$$\begin{aligned}\frac{dV}{dt} = &-\gamma\{\|\mathbf{E}_R + (\tfrac{1}{2})[\gamma^{-1}(\mu^2 + \alpha n)\mathrm{Im}\tilde{\mathbf{E}} - \mathrm{Re}\tilde{\mathbf{E}}]\|^2 \\ &+ \|\mathbf{E}_I + (\tfrac{1}{2})[\gamma^{-1}(\mu^2 + \alpha n)\mathrm{Re}\tilde{\mathbf{E}} - \mathrm{Im}\tilde{\mathbf{E}} + \gamma^{-1} n\mathbf{E}_0]\|^2 \\ &- \tfrac{1}{4}[\|\gamma^{-1}(\mu^2 + \alpha n)\mathrm{Im}\tilde{\mathbf{E}} - \mathrm{Re}\tilde{\mathbf{E}}\|^2 \\ &+ \|\gamma^{-1}(\mu^2 + \alpha n)\mathrm{Re}\tilde{\mathbf{E}} - \mathrm{Im}\tilde{\mathbf{E}} + \gamma^{-1} n\mathbf{E}_0\|^2]\}\,. \end{aligned} \tag{43}$$

If we set $\mathrm{Re}\tilde{\mathbf{E}} = -\alpha^{-1}\mathbf{E}_0$ and $\mathrm{Im}\tilde{\mathbf{E}} = \mathbf{0}$, then (43) reduces to

$$\frac{dV}{dt} = -\gamma\{\|\mathbf{E}_R + (2\alpha)^{-1}\mathbf{E}_0\|^2 + \|\mathbf{E}_I - \mu^2\mathbf{E}_0/(2\alpha\gamma)\|^2$$

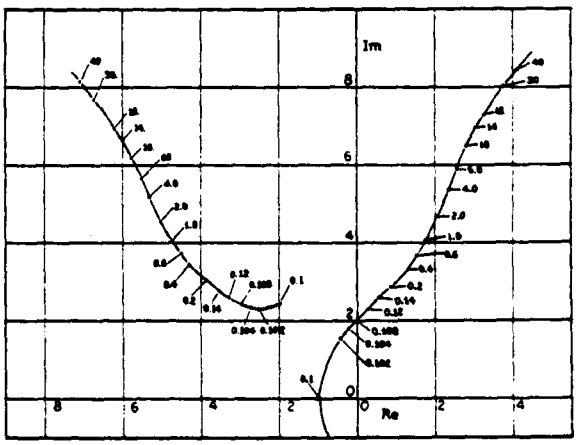

FIG. 4. Locus of the eigenvalues of $J_f(z_i^+;E_0)$ with E_0^2 as a parameter.

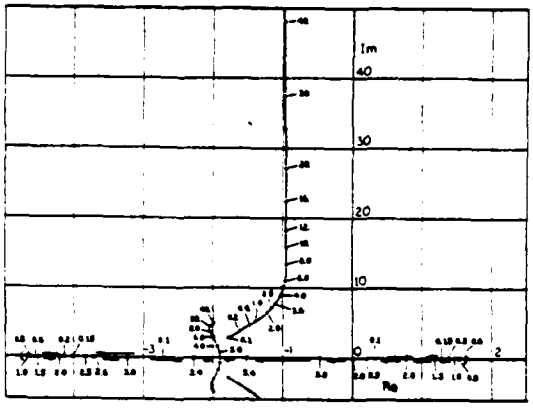

FIG. 5. Locus of the eigenvalues of $\mathbf{J}_1(\mathbf{z}_0; E_n)$ with E_n^2 as a parameter.

$$-(2\alpha)^{-2}(1+\mu^4\gamma^{-2})\|\mathbf{E}_0\|^2\}$$
$$= -\gamma\left[|\mathbf{E}-\mathbf{E}_*|^2-(2\alpha)^{-2}(1+\mu^4\gamma^{-2})\|\mathbf{E}_0\|^2\right], \quad (44)$$

where $\mathbf{E}_* = -(2\alpha)^{-1}\mathbf{E}_0 + i\mu^2\mathbf{E}_0/(2\alpha\gamma)$. We note that with the foregoing choice of $\bar{\mathbf{E}}$, n does not appear in (44). Moreover, for $\gamma>0$, $dV/dt<0$ at any point $\mathbf{E}$ exterior to the set $\Xi=\{\mathbf{E}:|\mathbf{E}-\mathbf{E}_*|\le(2\alpha)^{-1}(1+\mu^4\gamma^{-2})^{1/2}\|\mathbf{E}_0\|\}$. Let $\Xi_\delta=\{E: V(E)=\frac{1}{2}|E+\alpha^{-1}E_0|^2\le\delta^2\}$. Since for any $\delta>0$, Ξ_δ is a ball in E-space centered about the point $-\alpha^{-1}\mathbf{E}_0$ with radius $\sqrt{2}\delta$, it is possible to select a δ such that $\bar{\Xi}\subset\Xi_\delta$. In fact, elementary geometric considerations show that the smallest δ having the foregoing inclusion property is given by $\check{\delta}=(\sqrt{2}\alpha)^{-1}(1+\mu^4\gamma^{-2})^{1/2}\|\mathbf{E}_0\|$. Evidently, $dV/dt<0$ at any point $\mathbf{E}$ exterior to $\Xi_{\check{\delta}}$. This implies that for a solution of (31) initiated from any point $\mathbf{z}(0)=(n(0),\dot{n}(0),\mathbf{E}_R(0),\mathbf{E}_I(0))$ at $t=0$ with $\mathbf{E}(0)=\mathbf{E}_R(0)+i\mathbf{E}_I(0)$ exterior to $\Xi_{\check{\delta}}$, its corresponding $\mathbf{E}(t)$, $t>0$ either eventually enters $\Xi_{\check{\delta}}$ at some finite time $t_1>0$ and remains in $\Xi_{\check{\delta}}$ for all $t>t_1$ or tends to $\Xi_{\check{\delta}}$ as $t\to\infty$. Clearly, $\Xi_{\check{\delta}}$ contains all the points $\mathbf{E}(t)$ along any chaotic solution of (31) when it exists.

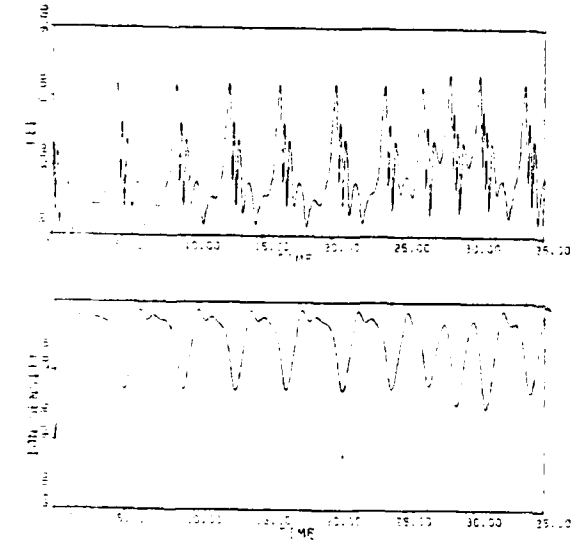

FIG. 6. $|E(t)|$ and $n(t)$ vs time t corresponding to the solution of (53) and (54) with $m=1$, $L=\pi/\sqrt{10}$, $\Gamma=2.0$, $\gamma_1=1.0$, $E_n^2=1.625$; initial data: $E(0)=1.426+0.5071i$, $n(0)=-40.75$ and $\dot{n}(0)=34.58$.

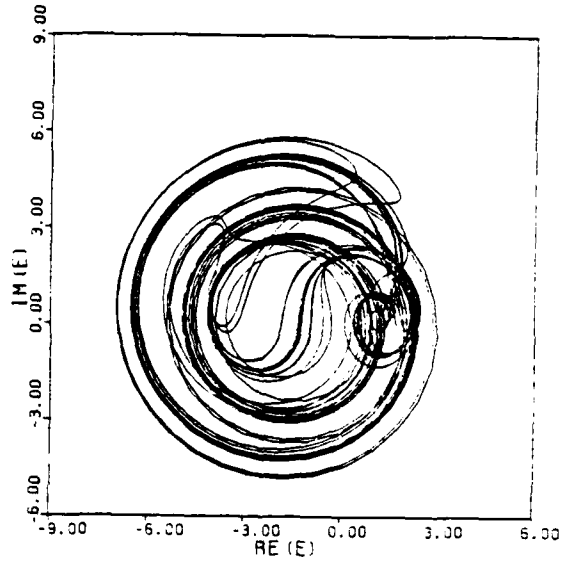

FIG. 7. Projection of the trajectory of (53) and (54) (with parameters as given in Fig. 6) onto the (E_R,E_I)-plane.

Next, we derive a bound for the magnitude of ion density oscillations. Let $\bar{n}=n+\mu^2\beta^{-1}\|\mathbf{E}_0\|^2$. We can rewrite the first two equations in (31) as

$$\frac{d\mathcal{N}}{dt}=\mathcal{A}\mathcal{N}+[0,\beta|\mathbf{E}-\mu^2\beta^{-1}\mathbf{E}_0|^2]^T, \quad (45)$$

where $\mathcal{N}=(\bar{n},\dot{\bar{n}})^T$ and

$$\mathcal{A}=\begin{bmatrix}0 & 1\\ -\mu^2 & -2\Gamma\end{bmatrix}. \quad (46)$$

Given $\mathcal{N}(0)$, the initial data for $\mathcal{N}$ at $t=0$, (45) is equivalent to the integral equation:

$$\mathcal{N}(t)=[\exp\mathcal{A}t\,]\mathcal{N}(0)+\int_0^t\exp[\mathcal{A}(t-\tau)]\times[0,\beta|\mathbf{E}(\tau)-\mu^2\beta^{-1}\mathbf{E}_0|^2]^T d\tau. \quad (47)$$

Thus,

$$\|\mathcal{N}(t)\|\le\|\exp\mathcal{A}t\|\|\mathcal{N}(0)\|+\int_0^t|\beta|\|\exp\mathcal{A}(t-\tau)\|\times|\mathbf{E}(\tau)-\mu^2\beta^{-1}\mathbf{E}_0|^2 d\tau. \quad (48)$$

For $\mu^2>\Gamma>0$, we can find a constant $\mathscr{C}>0$ such that $\|\exp(\mathcal{A}t)\|<\mathscr{C}\exp(-\Gamma t)$. Also, we have already established that along any chaotic solution $\mathbf{E}(t)\subset\Xi_{\check{\delta}}$ or $|\mathbf{E}(t)+\alpha^{-1}\mathbf{E}_0|<\check{\delta}=(\sqrt{2}\alpha)^{-1}(1+\mu^4\gamma^{-2})^{1/2}\|\mathbf{E}_0\|$ for all t. Hence,

$$\begin{aligned}&|\mathbf{E}(\tau)-\mu^2\beta^{-1}\mathbf{E}_0|\\ &\quad=|\mathbf{E}(\tau)+\alpha^{-1}\mathbf{E}_0-(\alpha^{-1}+\mu^2\beta^{-1})\mathbf{E}_0|\\ &\quad\le|\mathbf{E}(\tau)+\alpha^{-1}\mathbf{E}_0|+|\alpha^{-1}+\mu^2\beta^{-1}|\|\mathbf{E}_0\|\\ &\quad<\check{\delta}+|\alpha^{-1}+\mu^2\beta^{-1}|\|\mathbf{E}_0\|<\Psi\|\mathbf{E}_0\|, \end{aligned}\quad (49)$$

where $\Psi=(\sqrt{2}\alpha)^{-1}(1+\mu^4\gamma^{-2})^{1/2}+|\alpha^{-1}+\mu^2\beta^{-1}|$. It follows from (48) that

$$\|\mathcal{N}(t)\|<\mathscr{C}\{\Psi|\beta|\|\mathbf{E}_0\|^2\Gamma^{-1}+[\|\mathbf{z}(0)\|-\Psi|\beta|\|\mathbf{E}_0\|^2\Gamma^{-1}]\exp(-\Gamma t)\}$$

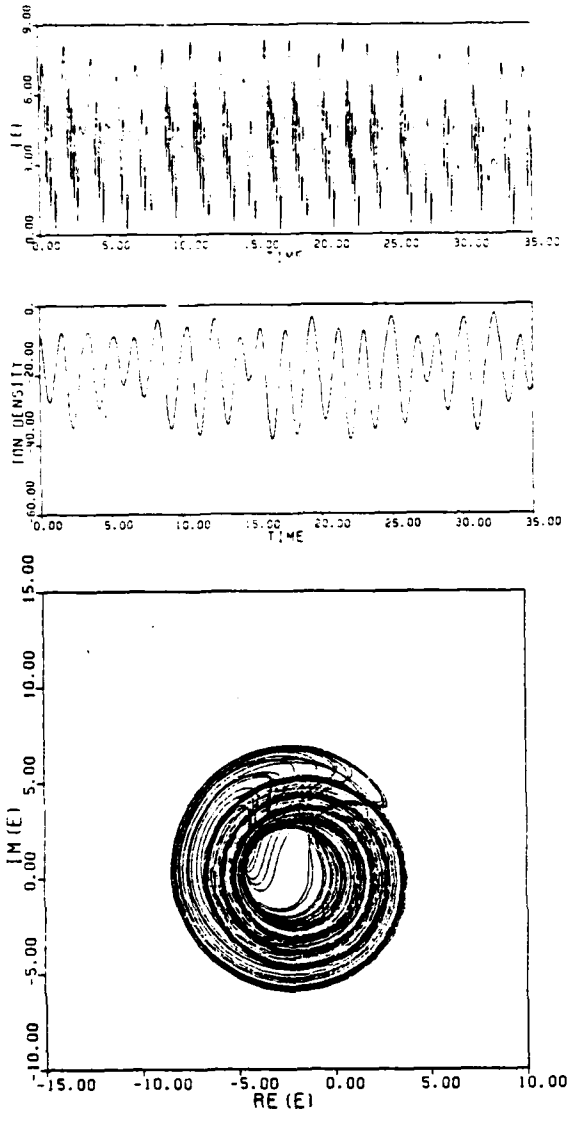

FIG. 8. Solution of (53) and (54) with $E_0^* = 2.669$, $E(0) = -3.07656 + 4.22328i$, $n(0) = -8.38056$, $\dot{n}(0) = -8.25344$, and other parameters as given in Fig. 6.

$$< \mathcal{C} \max\{\|\mathbf{z}(0)\|, \Psi \mid \beta \mid \|\mathbf{E}_0\|^2 \Gamma^{-1}\}, \tag{50}$$

for all $t > 0$ and $\mathbf{E}(0) \in \Xi_\delta$. When $\|\mathbf{z}(0)\| < \Psi \mid \beta \mid \|\mathbf{E}_0\|^2 \Gamma^{-1}$, we have $\|\mathcal{N}(t)\| < \mathcal{C} \Psi \mid \beta \mid \|\mathbf{E}_0\|^2 \Gamma^{-1}$ for all $t > 0$, a bound which is independent of $\mathbf{z}(0)$.

6. ONE-DIMENSIONAL EXAMPLE

Consider the case where $N = 1$ with a bounded spatial domain $\Omega = [0, L]$. Assuming that both E and n vanish at the boundary points $x = 0$ and $x = L$, we can take $\phi_k(x) = (2/L)^{1/2} \sin(k\pi x/L)$, $\mu_k = k\pi/L$, $k = 1, 2, \cdots$. For this case, the coefficients α_m and β_m defined in (11) become

$$\alpha_m = \int_0^L (2/L)^{3/2} \sin^3(m\pi x/L)\, dx = \begin{cases} 0 & \text{for } m \text{ even}, \\ (2^7/L)^{1/2}/(3m\pi) & \text{for } m \text{ odd}, \end{cases} \tag{51}$$

$$\beta_m = \int_0^L \left(\frac{2}{L}\right)^{3/2} \frac{d^2}{dx^2} [\sin^2(m\pi x/L)] \sin(m\pi x/L)\, dx = \begin{cases} 0 & \text{for } m \text{ even}, \\ -8m\pi (2/L^5)^{1/2}/3 & \text{for } m \text{ odd}. \end{cases} \tag{52}$$

Thus, for an odd integer m, Eqs. (9) and (10) have the form:

$$i \frac{dE_m}{dt} - \left(\frac{m\pi}{L}\right)^2 E_m + i\gamma_m E_m = n_m \left[E_0 + \left(\frac{2^7}{L}\right)^{1/2} / (3m\pi) E_m\right], \tag{53}$$

$$\frac{d^2 n_m}{dt^2} + 2\Gamma_m \frac{dn_m}{dt} + \left(\frac{m\pi}{L}\right)^2 n_m = -\left(\frac{m\pi}{L}\right)^2 E_0 (E_m + E_m^*) - \left[8m\pi \frac{(2/L^5)^{1/2}}{3}\right] |E_m|^2, \tag{54}$$

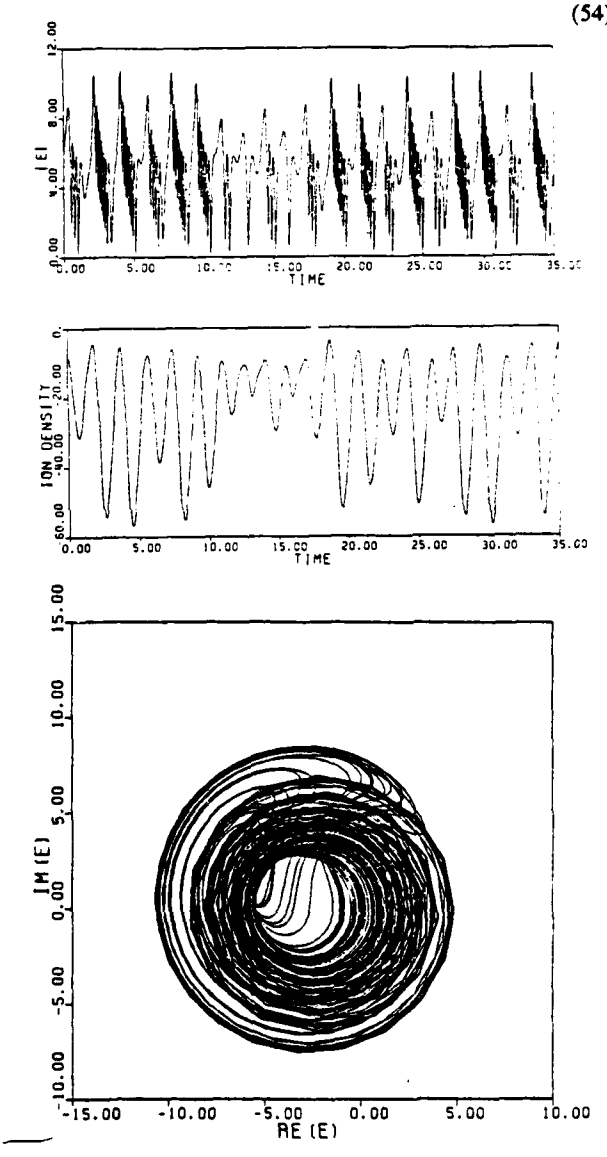

FIG. 9. Solution of (53) and (54) with $E_0^* = 5.05$, $E(0) = -5.0069 + 3.26742i$, $n(0) = -8.63114$, $\dot{n}(0) = 1.86353$, and other parameters as given in Fig. 6.

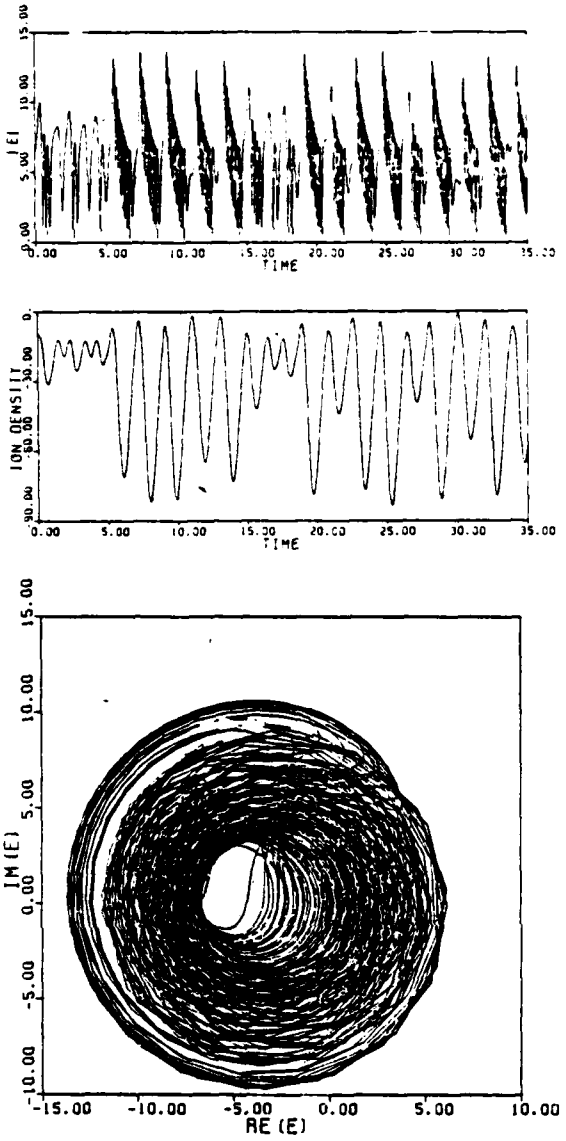

FIG. 10. Solution of (53) and (54) with $E_0^2 = 10.0$, $E(0) = -6.0 + 2.0i$, $n(0) = -10$, $\dot{n}(0) = 0$, and other parameters as given in Fig. 6.

where E_0 is a real nonnegative parameter.

To illustrate the qualitative features of the solutions of the above equations, numerical results are obtained for the case where $m = 1$, $L = \pi/\sqrt{10}$, $\Gamma_1 = 2.0$, and $\gamma_1 = 1.0$. These values are chosen to simplify the numerical computation. They may not correspond to any particular physical situation. Numerical results for specific physical situations will be presented elsewhere.

First, we compute the locus of the equilibrium electric field E^e as a function of E_0^2 using (27) and (20). Figure 1 shows the locus in the (E_R, E_I)-plane. It can be seen that bifurcation occurs at $E_0^2 = E_{0c}^2 = 0.09974$. At $E_0^2 = \tilde{E}_{0c}^2 = 5.05$, one of the equilibrium points E^e returns to the origin. As $E_0^2 \to \infty$, the locus of one of the equilibrium points is asymptotic to the line $E_I = \gamma\beta^{-1}(2\alpha_1 + \beta_1\mu_1^{-1})E_R = -0.1\,E_R$, while the other one tends to $(E_R, E_I) = (-\infty, 0)$. Figure 2 shows the equilibrium ion densities n^e as a function of E_0^2.

Next, we examine the nature of each equilibrium state $\mathbf{z}_e$ for various values of E_0^2 by determining the roots of (37) or the eigenvalues of $\mathbf{J}_f(\mathbf{z}_e; E_0)$. Figure 3 shows the locus of the eigenvalues of $\mathbf{J}_f(0; E_0)$ as E_0^2 varies. As established in Sec. 4, when $E_0^2 < \tilde{E}_{0c}^2 = 5.05$, all the eigenvalues have negative real parts implying that the origin is asymptotically stable. When E_0^2 exceeds $\tilde{E}_{0c}^2$, one of the real eigenvalues crosses the imaginary axis. Consequently, the origin becomes unstable. Figure 4 shows the eigenvalue locus of $\mathbf{J}_f(\mathbf{z}_e^+; E_0)$ for $0.1 < E_0^2 < 40.0$, where the components of $\mathbf{z}_e^+ = (n^+, 0, \xi_R^+ E_0, \xi_I^+ E_0)$ are given by (17), (20), and (27). We note that for $0.1 < E_0^2 < 0.108$, all the eignevalues have negative real parts, and at $E_0^2 \simeq 0.108$, a complex conjugate pair of eigenvalues cross the imaginary axis into the right-half plane. It can be verified that Hopf bifurcation takes place at this point. The locus of the eigenvalues of $\mathbf{J}_f(\mathbf{z}_e^-; E_0)$ is shown in Fig. 5. Here, for $0.1 < E_0^2 < 2.669$, $\mathbf{J}_f(\mathbf{z}_e^-; E_0)$ has a positive real eigenvalue. When $E_0^2 > 2.67$, all the eigenvalues of $\mathbf{J}_f(\mathbf{z}_e^-; E_0)$ are in the left-half plane.

An inspection of the eigenvalue loci given by Figs. 3–5 suggests that one might search for the existence of chaotic solutions in the neighborhood of $\mathbf{z}_e^+$ for $E_0^2 > 0.108$ (Hopf bifurcation point). Numerical integration of (53) and (54) with various initial conditions was performed for progressively larger values of E_0^2. The results suggest that the periodic solutions in the neighborhood of $\mathbf{z}_e^+$ (whose existence is ensured by the Hopf bifurcation theorem) are unstable and the bifurcation is subcritical. Figure 6 shows the time-domain buildup of a nearly periodic solution which evolves into chaotic oscillations. The projection of the trajectory onto the (E_R, E_I)-plane is shown in Fig. 7. Figures 8–10 show the chaotic solutions for various values of E_0^2. It was found that

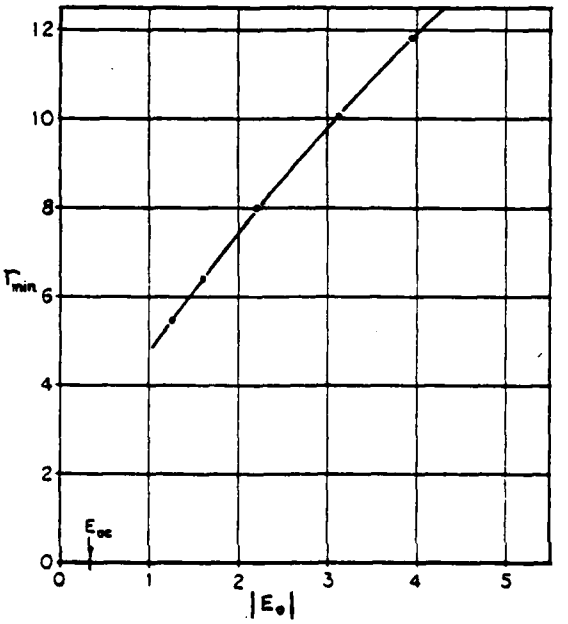

FIG. 11. Variation of r_{min} as a function of $|E_0|$.

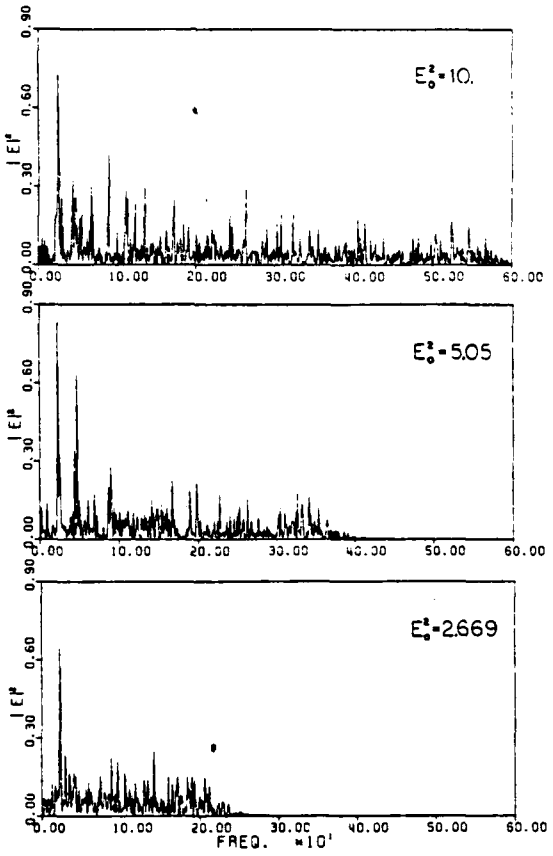

FIG. 12. Power spectra of the electric field corresponding to the solutions of (53) and (54) as shown in Figs. 8–10; frequency scale: 1/40.96 normalized unit.

these solutions are highly sensitive to initial conditions. Also, not all trajectories in the z space tend to the chaotic solutions as $t \to \infty$. This is apparent from the fact that for $0.108 < E_0^2 < \tilde{E}_{0c}^2 = 5.05$, the origin $z = 0$ is a stable equilibrium point, and for any $E_0^2 > \tilde{E}_{0c}^2$, z_e^- is always a stable equilibrium point. We note from Figures 8b–10b that in each case, there exists a circle with minimum radius r_{min} which encloses the projection of the trajectories onto the (E_R, E_I)-plane. Figure 11 shows the variation of r_{min} as a function $|E_0|$ as obtained from the numerical solutions. Evidently, r_{min} can be bounded by a linear fundtion of $|E_0|$. This is consistent with the estimate δ given in Sec. 5. It can be readily verified that in each case, the projection of the trajectories of the chaotic oscillations onto the (E_R, E_I)-plane is completely contained in $\Xi_\delta = \{E: |E + \alpha^{-1} E_0| < \sqrt{2\delta} = 8.3445 |E_0|\}$, where $\alpha = 1.204367$. Also, we observe from these solutions that the maximum depth of the ion density troughs increases with E_0^2, and the electric field oscillates more rapidly during the ion density dips. This can be roughly explained by considering the following equations for E_R and E_I derived from (31):

$$\frac{d^2E_R}{dt^2} + \left(2\gamma - \frac{\alpha\dot{n}}{(\mu^2+\alpha n)}\right)\frac{dE_R}{dt} + \left(\gamma^2 + (\mu^2+\alpha n)^2 - \frac{\alpha\gamma\dot{n}}{(\mu^2+\alpha n)}\right)E_R = -n(\mu^2+\alpha n)E_0, \tag{55}$$

$$\frac{d^2E_I}{dt^2} + \left(2\gamma - \frac{\alpha\dot{n}}{(\mu^2+\alpha n)}\right)\frac{dE_I}{dt} + \left(\gamma^2 + (\mu^2+\alpha n)^2 - \frac{\alpha\gamma\dot{n}}{(\mu^2+\alpha n)}\right)E_I = -\left(\dot{n} + \left(\gamma - \frac{\alpha\dot{n}}{(\mu^2+\alpha n)}\right)n\right)E_0. \tag{56}$$

Considering n as a slowly time-varying parameter, the frequency of electric-field oscillations is roughly equal to $\omega = [\gamma^2(\mu^2+\alpha n)^2 - \alpha\gamma\dot{n}(\mu^2+\alpha n)^{-1}]^{1/2}$, and the effective damping coefficient is $2\gamma - \alpha\dot{n}(\mu^2+\alpha n)^{-1}$. Let T denote the time interval corresponding to an ion density dip, and t^* is the minimum point of n over T where $\dot{n}(t^*) = 0$. Then $\omega(t^*) > \omega(t)$ for all t in T such that $\dot{n}(t)$ and $\mu^2 + \alpha n(t)$ have the same sign. This condition is satisfied for the solutions shown here.

Figure 12 shows the power spectra of the electric field computed by means of the fast Fourier transform method. The results resemble those corresponding to turbulence. Also, the spectral bandwidth increases with E_0^2 as expected from physical considerations. Finally, the truncated discrete version of the autocovariance function of E given by

$$\rho(j\Delta) = \frac{1}{(N-j+1)} \sum_{i=1}^{N-j+1} [E(i\Delta) - \bar{E}] \times \{E[(i+j-1)\Delta] - \bar{E}\}^* \tag{57}$$

is computed, where $\bar{E}$ denotes the mean-value of E, and Δ is the time-step size. Figures 13a–13c show the real and imaginary parts of $\rho(j\Delta)$ for $E_0^2 = 1.669$, 5.05 and 10.0. It can be seen that both $\mathrm{Re}\,\rho(j\Delta)$ and $\mathrm{Im}\,\rho(j\Delta)$ decay from their maximum values and then fluctuate about zero. But we cannot deduce that the autocovariance function actually tends to zero as the time delay $\tau \to \infty$ as in the case of solutions on a strange attractor.

7. CONCLUDING REMARKS

It was found that the single-mode equations derived from the Zakharov's model for Langmuir turbulence in a plasma with phenomenological damping exhibit chaotic solutions whose power spectra have turbulence-like features. In the case of multiple modes, if all the mode coupling terms are omitted, then we obtain sets of uncoupled equations of the form (9) and (10). Each set is capable of producing chaotic solutions when E_0^2 exceeds a certain threshold value (generally different for each mode). The total power spectrum of the electric field is simply the sum of the single-mode power spectra. This seems to imply that energy transfer between various modes is not necessary in producing turbulence which is contrary to the cascade theory of turbulence. There are a number of computer studies' of Langmuir turbulence induced by interacting collapsing solitary waves based on Zakharov's model with phenomenological damping. Perhaps these computer results actually correspond to some form of chaotic solutions which are inherent in the model.

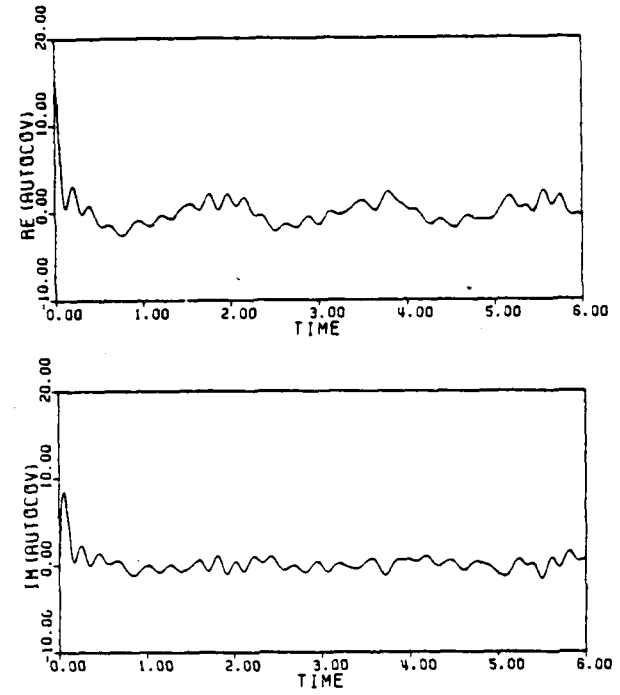

(a)

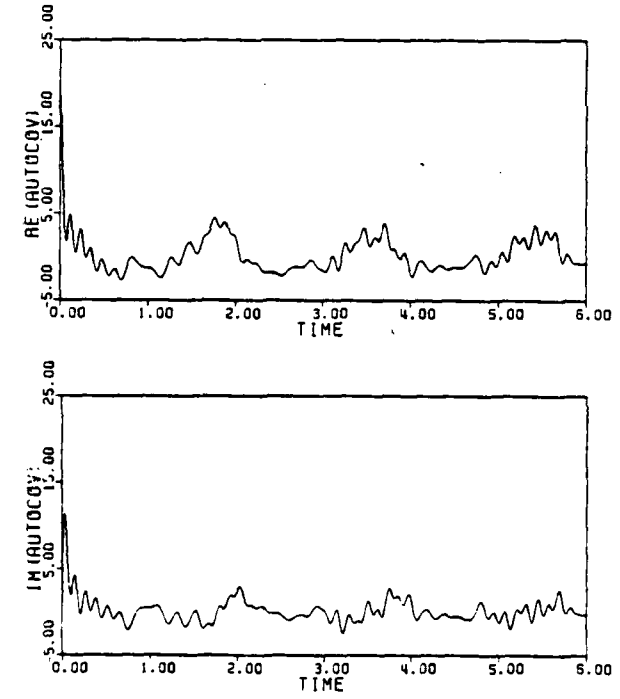

(b)

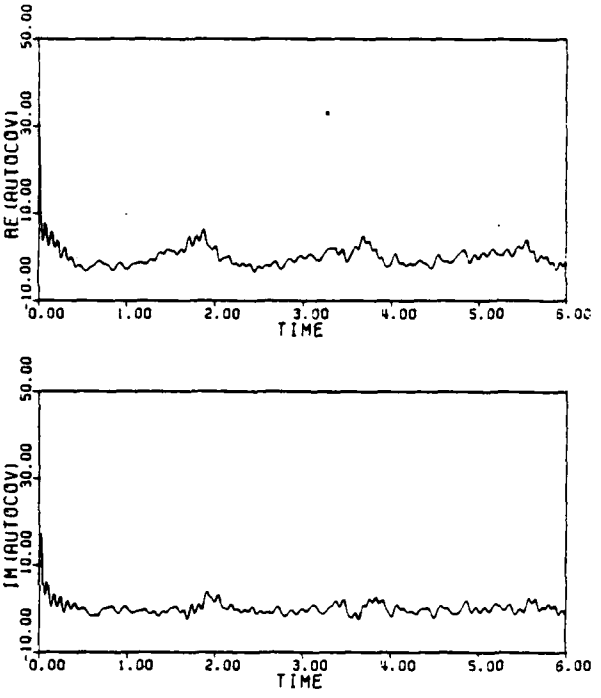

(c)

FIG. 13. Real and imaginary parts of the autocovariance function of E corresponding to the solutions shown in Figs. 8–10; (a) $E_0^2 = 2.669$, (b) $E_0^2 = 5.05$, and (c) $E_0^2 = 10$.

In this work, we have sought solutions in terms of the eigenfunctions of the Laplacian operator over a bounded spatial domain. Of course, we may expand the solutions in terms of any suitable countable basis for $L^2(\Omega)$ and arrive at a countably infinite system of ordinary differential equations similar to that given in (5) and (6). One may also consider directly the Hopf bifurcation problem for Zakharov's model (1) and (2) without resorting to modal expansions. Some results in this direction have been obtained recently. They will be reported elsewhere.

Finally, we note that the presence of the phenomenological damping coefficients γ_m and Γ_m in the simplified equations for each mode m is essential for the existence of chaotic solutions. But there does not exist a clearcut way of introducing the damping terms into the Zakharov's model based on physical considerations. Also, a detailed study of the structure of the stable and unstable manifolds associated with the equilibrium states is necessary for revealing the nature of the chaotic oscillations described here. Unfortunately, this task is complicated by the system's dimensionality.

ACKNOWLEDGMENT

The author wishes to thank the referee for his helpful comments and suggestions. This work was supported by AFOSR grants No. 74-2662 and No. 79-0050.

APPENDIX

From (33), it is evident that

$$\det[\mathbf{J}_f(\mathbf{z}^e;E_0)-\lambda\,\mathbf{I}_{2(N+1)}]=\lambda(2\Gamma+\lambda)\det\mathbf{P}-\det\mathbf{Q}, \tag{A1}$$

where

$$\mathbf{P}\begin{bmatrix}-(\gamma+\lambda)\mathbf{I}_N & (\mu^2+\alpha n^2)\mathbf{I}_N\\ -(\mu^2+\alpha n^2)\mathbf{I}_N & -(\gamma+\lambda)\mathbf{I}_N\end{bmatrix},$$

$$Q=\left[\begin{array}{c|cc} -\mu^2 & 2(\beta\mathbf{E}_R^e-\mu^2E_0)^T & 2\beta(\mathbf{E}_I^e)^T\\ \alpha\mathbf{E}_I^e & & \\ \hline & \multicolumn{2}{c}{\mathbf{P}}\\ -(E_0+\alpha\mathbf{E}_R^e) & & \end{array}\right]. \tag{A2}$$

Since $\det\mathbf{P}=[(\gamma+\lambda)^2+(\mu^2+\alpha n^2)^2]^N>0$, $\mathbf{P}^{-1}$ exists and is given by

$$\mathbf{P}^{-1}=[(\gamma+\lambda)^2+(\mu^2+\alpha n^2)^2]^{-1}\times\begin{bmatrix}-(\gamma+\lambda)\mathbf{I}_N & -(\mu^2+\alpha n^2)\mathbf{I}_N\\ (\mu^2+\alpha n^2)\mathbf{I}_N & -(\gamma+\lambda)\mathbf{I}_N\end{bmatrix}. \tag{A3}$$

Now, $\det\mathbf{Q}$ can be computed by considering the matrix

$$\mathbf{S}=\mathbf{Q}\begin{bmatrix}1 & \mathbf{O}_{2N}^T\\ \mathbf{O}_{2n} & \mathbf{P}^{-1}\end{bmatrix}=\left[\begin{array}{c|c} -\mu^2 & 2[(\beta\mathbf{E}_R^e-\mu^2E_0)^T\ \beta(\mathbf{E}_I^e)^T]\mathbf{A}^{-1}\\ \alpha\mathbf{E}_I^e & \\ \hline & \mathbf{I}_{2N}\\ -(E_0+\alpha\mathbf{E}_R^e) & \end{array}\right]. \tag{A4}$$

Since $\det\mathbf{S}=(\det\mathbf{Q})(\det\mathbf{P}^{-1})$, $\det\mathbf{P}^{-1}=[(\gamma+\lambda)^2+(\mu^2+\alpha n^2)^2]^{-N}$ and

$$\det\mathbf{S}=-\mu^2-2[(\beta\mathbf{E}_R^e-\mu^2E_0)^T]\mathbf{A}^{-1}\begin{bmatrix}\alpha\mathbf{E}_I^e\\ -(E_0+\alpha\mathbf{E}_R^e)\end{bmatrix}, \tag{A5}$$

we have $\det\mathbf{Q}=\det\mathbf{S}/\det\mathbf{P}^{-1}$. The expression (34) is obtained directly from (A1) and (A5).

[1]E.N. Lorenz, J. Atmos. Sci. 20, 130 (1972).
[2]J.B. McLaughlin and P.C. Martin, Phys. Rev. A 12, 186 (1975).
[3]O.E. Rössler, in *Synergetics, A Workshop*, edited by H. Haken (Springer-Verlag, New York, 1977), p. 184.
[4]Y. Kuramoto and T. Yamada, Prog. Theor. Phys. 55, 679 (1976).
[5]D. Ruelle and F. Takens, Commun. Math. Phys. 20, 167 (1971).
[6]V.E. Zakharov, Zh. Eksp. Teor. Fiz. 62, 1745 (1972) [Sov. Phys. JETP 35, 908 (1972)].
[7]N.R. Pereira, R.N. Sudan, and J. Denavit, Phys. Fluids 20, 271 (1977).
[8]T.A. Davydova and K.P. Shamrai, Fiz. Plazmy 3, 591 (1977) [Sov. J. Plasma Phys. 3, 333 (1978)].
[9]E.J. Routh, *Advanced Dynamics of a System of Rigid Bodies* (Dover, New York, 1955).
[10]J.E. Marsden and M. McCracken, *The Hopf Bifurcation and its Applications* (Springer-Verlag, New York, 1976).

APPENDIX B

FURTHER STUDY OF CHAOTIC OSCILLATIONS OF SIMPLIFIED ZAKHAROV'S MODEL FOR LANGMUIR TURBULENCE

P.K.C.Wang

School of Engineering and Applied Science

University of California

Los Angeles, California 90024

This work was supported by the

U.S. Air Force Office of Scientific Research

Under Grant No. AFOSR 79-0050

ABSTRACT

Further studies are made on the chaotic oscillations of the single mode equation derived from Zakharov's model for Langmuir turbulence in a plasma in the presence of an external spatially homogeneous electric field oscillating at the electron plasma frequency. First, the bifurcation of equilibrium states with respect to both the energy of the external electric field and the damping coefficient of the high-frequency waves is investigated. Then, studies are made on the onset and quenching of chaotic oscillations when damping is varied. The nature of the chaotic oscillations is explored by determining various Poincaré maps numerically.

CONTENTS

I. INTRODUCTION

Recently, it was shown[1] that the single mode equation derived from Zakharov's model[2] for Langmuir turbulence in a plasma in the presence of an external spatially homogeneous electric field oscillating at the electron plasma frequency and with phenomenological damping has nonperiodic chaotic solutions. The power spectra corresponding to these solutions have turbulence-like features. In reference 1, the chaotic solutions were discovered through bifurcation analysis and numerical experimentation. The structure and the onset of these solutions were not explored in detail. Here, further studies are made on the nature of the chaotic oscillations. First, the bifurcation of equilibrium states with respect to both the energy of the external electric field and the damping coefficient of the high-frequency waves is studied. Then, the quenching of chaotic oscillations due to increased damping is explored. Finally, some properties of the chaotic oscillations are studied by determining various Poincaré mappings numerically.

II. SIMPLIFIED MODEL

As developed in reference 1, the simplified equations for a single mode m in the Zakharov's model have the form:

$$i\frac{dE_m}{dt} - (\mu_m - i\gamma_m)E_m = n_m(E_o + \alpha_m E_m), \tag{1}$$

$$\frac{d^2n_m}{dt^2} + 2\Gamma_m\frac{dn_m}{dt} + \mu_m^2 n_m = -\mu_m^2 E_o\cdot(E_m + E_m^*) + \beta_m|E_m|^2; \tag{2}$$

with

$$\alpha_m = \int_\Omega \phi_m^3(x)\, d\Omega, \qquad \beta_m = \int_\Omega \nabla^2[\phi_m^2(x)]\phi_m(x)\, d\Omega, \tag{3}$$

where a·b denotes the usual scalar product of two vectors a and b in the

real n-dimensional Euclidean space $\mathbb{R}^N$; ϕ_m is the orthonormalized eigenfunction of the Laplacian operator corresponding to the eigenvalue $-\mu_m^2 < 0$; γ_m and Γ_m are the phenomenological damping coefficients; E_m and n_m are respectively the coefficients of expansions for the electric field E and ion density n:

$$E(t,x) = \sum_k E_k(t)\phi_k(x), \qquad n(t,x) = \sum_k n_k(t)\phi_k(x) \tag{4}$$

defined on the spatial domain $\Omega \subset \mathbb{R}^N$. $E_o = (E_{o1},\ldots,E_{oN})$ is a real constant vector representing the normalized amplitude of the external electric field. In what follows, we shall omit the subscript m in (1) and (2) for brevity.

Let $E_R = \mathrm{Re}(E)$, $E_I = \mathrm{Im}(E)$, and z denote the 2(N+1)-dimensional real vector $(n,\dot{n},E_R,E_I)^T$, where $(\cdot)^T$ denotes transposition. Equations (1) and (2) can be rewritten as:

$$\frac{dz}{dt} = f(z;\gamma,E_o) \triangleq \begin{bmatrix} \dot{n} \\ -\mu^2 n - 2\Gamma\dot{n} - 2\mu^2 E_o\cdot E_R + \beta(\|E_R\|^2 + \|E_I\|^2) \\ -\gamma E_R + (\mu^2 + \alpha n)E_I \\ -\gamma E_I - (\mu^2 + \alpha n)E_R - nE_o \end{bmatrix}, \tag{5}$$

where $\|\cdot\|$ denotes the Euclidean norm.

III. BIFURCATION OF EQUILIBRIUM STATES

The equation for the equilibrium states is given by

$$f(z;\gamma,E_o) = 0, \tag{6}$$

where γ and E_o are parameters. Evidently, $z=0 \in \mathbb{R}^{2(N+1)}$ is an equilibrium state for all γ,E_o. From the implicit function theorem, a necessary conditions for bifurcation from the main branch $\mathcal{C} = \{(0,\gamma,E_o):\gamma\in\mathbb{R}, E_o\in\mathbb{R}^N\}$ is that the Jacobian matrix $J_f(0;\gamma,E_o)$ given by

$$J_f(0;\gamma,E_o) = \begin{bmatrix} 0 & 1 & 0_N^T & 0_N^T \\ -\mu^2 & -2\Gamma & -2\mu^2 E_o^T & 0_N \\ 0 & 0 & -\gamma I_N & \mu^2 I_N \\ -E_o & 0 & -\mu I_N & -\gamma I_N \end{bmatrix} \tag{7}$$

is singular, where 0_N and I_N are the N-dimensional zero vector and N×N identity matrix respectively.

Since

$$\det J_f(0;\gamma,E_o) = (\gamma^2 + \mu^4)^{N-1}\{\mu^2(\gamma^2+ \mu^4) - 2\mu^4\|E_o\|^2\}, \tag{8}$$

bifurcation from $\mathcal{C}$ can occur only when $\det J_f(0;\gamma,E_o)=0$ or

$$\|E_o\|^2= \tilde{E}_{oc}^2 \triangleq (\gamma^2+ \mu^4)/(2\mu^2). \tag{9}$$

It can be deduced from the following exact expressions for the non-zero equilibrium states $z_e = (n_e,0,E_R^e,E_I^e)$ with

$$E_R^e = \xi_R^{\pm}E_o, \qquad E_I^e = \xi_I^{\pm}E_o, \tag{10}$$

$$\xi_R^{\pm} = \xi_I(\mu^2 + \beta\gamma^{-1}\|E_o\|^2\xi_I^{\pm})[\gamma + (2\alpha + \beta\mu^{-2})\|E_o\|^2\xi_I^{\pm}]^{-1}, \tag{11}$$

$$\xi_I^{\pm} = \frac{\delta\gamma\mu^2}{(\beta^2 + \delta^2\gamma^2)\|E_o\|^2}\left\{\|E_o\|^2 - \frac{(\mu^2\beta + \gamma^2\delta)}{\delta\mu^2} \pm [\|E_o\|^4 - 4\alpha\beta\delta^{-2}\|E_o\|^2 - \left(\frac{2\alpha\gamma}{\delta}\right)^2]^{\frac{1}{2}}\right\}, \tag{12}$$

$$n_e^{\pm} = \{\beta\mu^{-2}[(\xi_R^{\pm})^2 + (\xi_I^{\pm})^2] - 2\xi_R^{\pm}\}\|E_o\|^2, \tag{13}$$

$$\|E_o\|^2 \geq E_{oc}^2 \triangleq 2\alpha\delta^{-2}[\beta + (\beta^2+\delta^2\gamma^2)^{\frac{1}{2}}] \tag{14}$$

$$\delta = (2\alpha + \beta\mu^{-2}), \tag{15}$$

that bifurcation from $\mathcal{C}$ indeed takes place at any point $(0,\gamma,E_o)\in\mathcal{C}$ such that $\|E_o\| = \tilde{E}_{oc}$. The critical external field energy $\tilde{E}_{oc}^2$ increases with the damping coefficient γ.

For any fixed γ and $0 \leq \|E_o\|^2 < E_{oc}^2$, the origin $z = 0$ is the only equilibrium state. When $\|E_o\|^2 = E_{oc}^2$, a nonzero equilibrium state z_e

emerges, and as $\|E_o\|^2$ increases from E_{oc}^2, z_e bifurcates into two distinct equilibrium states z_e^+ and z_e^-. Moreover, the bifurcated branch corresponding to z_e^+ crosses over the main branch $\mathcal{C}$ at $\tilde{E}_{oc}^2$. Figure 1 shows the bifurcation diagram for E_I^e, the imaginary part of the equilibrium electric field, with $\|E_o\|^2$ as a variable parameter for the one dimensional case (N=1) with a bounded spatial domain $\Omega = [0,L]$ with $\phi_1(x) = (2/L)^{\frac{1}{2}}\sin(\pi x/L)$ and parameters:

$$\begin{aligned} &\mu_1 = \pi/L, \quad L = \pi/\sqrt{10}, \quad \gamma_1 = 1, \\ &\alpha_1 = (2^7/L)^{\frac{1}{2}}/(3\pi), \qquad \beta_1 = -8\pi(2/L^5)^{\frac{1}{2}}/3. \end{aligned} \tag{16}$$

Evidently, the new branch appears abruptly when $\|E_o\|^2 = E_{oc}^2$, and immediately bifurcates into two distinct branches as $\|E_o\|^2$ increases from E_{oc}^2.

Now, we consider the case where $\|E_o\|^2$ is fixed and the damping coefficient γ is a variable parameter. It can be readily verified that the trivial solution $z = 0$ is the only equilibrium point when $\gamma = 0$. From (12), it is evident that for real $\xi_I^{\pm}$, γ must satisfy:

$$\gamma \leq \gamma_c \triangleq \frac{\|E_o\|^2}{2\alpha\mu^2} \{\|E_o\|^2(2\alpha\mu^2+\beta)^2 - 4\alpha\beta\mu^4\}^{\frac{1}{2}}. \tag{17}$$

For $0 < \gamma < \gamma_c$, there exist two distinct nonzero equilibrium states and they emerge into one when $\gamma = \gamma_c$. When γ increases beyond γ_c, the nonzero equilibrium state abruptly disappears. When $\gamma = \tilde{\gamma}_c \triangleq \mu\{2\|E_o\|^2 - \mu^2\}^{\frac{1}{2}}$, there is only one nonzero equilibrium state. Figures 2 and 3 show the loci of equilibrium E_I^e and n^e as γ increases from zero for the one dimensional case with parameters given in (16) and fixed values of $\|E_o\|^2$. We observe from Fig.3 that as $\gamma \to 0$, n^e tends to nonzero values which do not correspond to equilibrium ion densities. Figure 4 shows the loci of equilibrium electric field as γ varies while keeping $\|E_o\|^2$ constant.

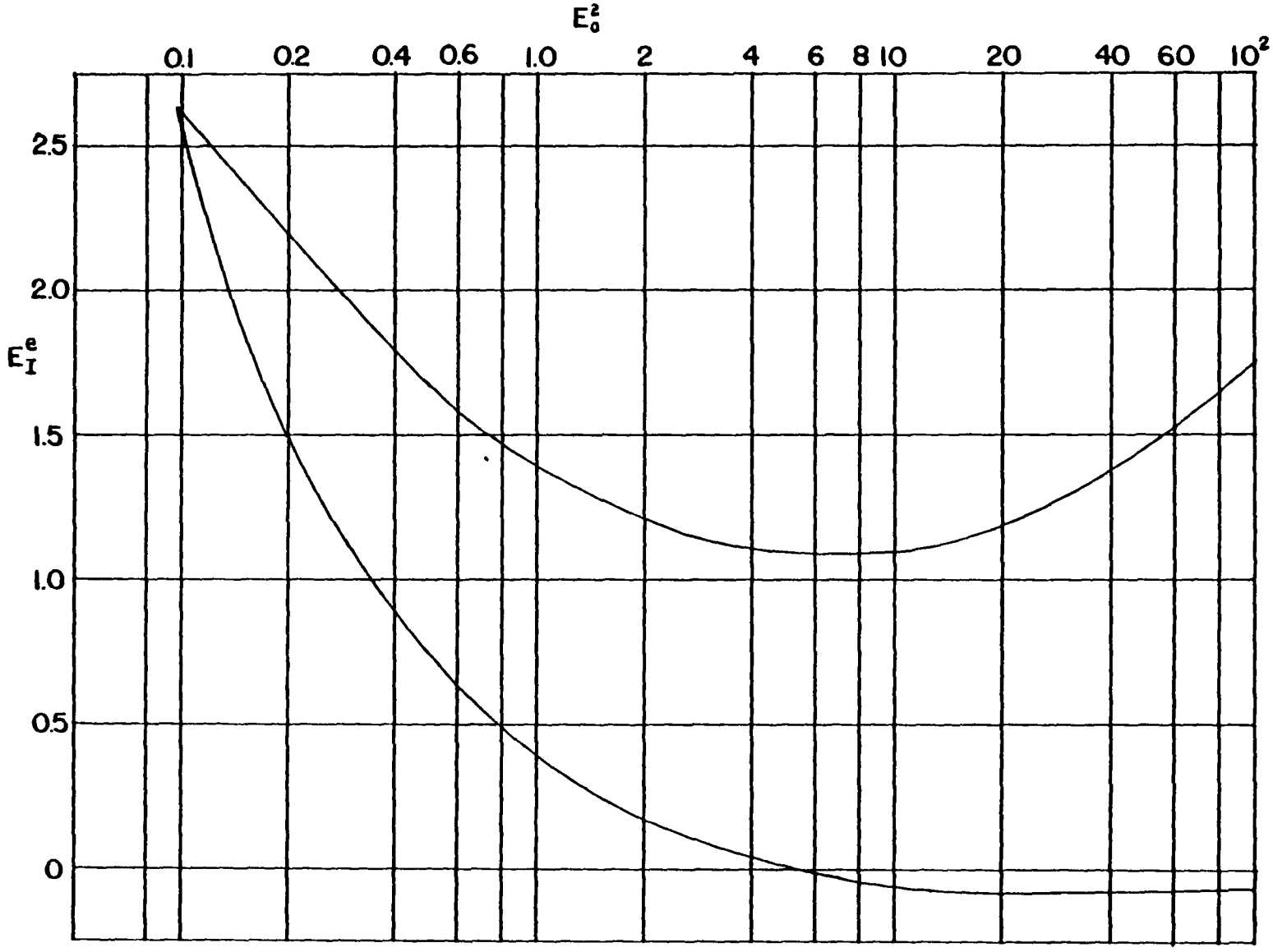

Fig.1 Bifurcation of E_I^e with respect to parameter E_o^2; $\gamma = 1.0$.

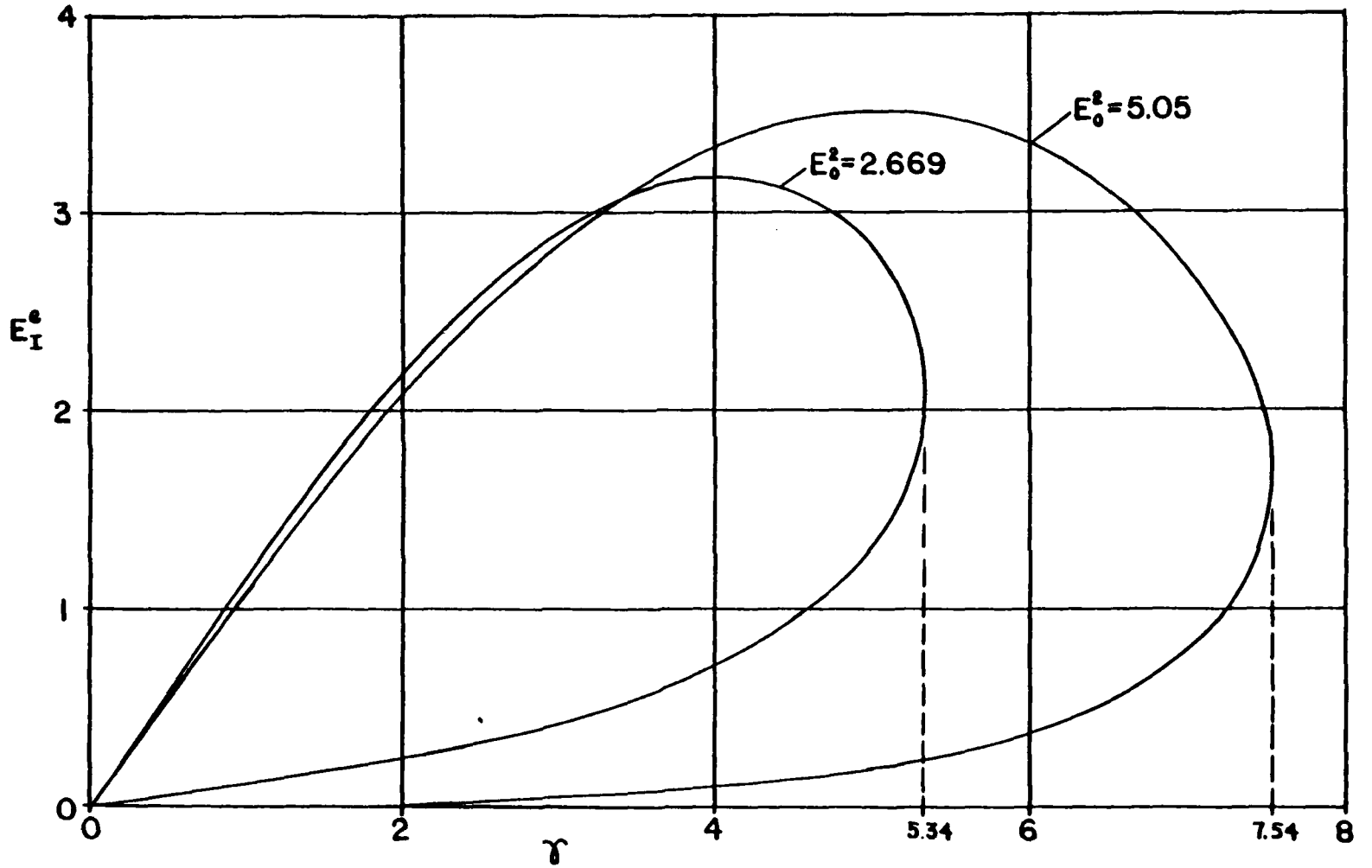

Fig.2 Bifurcation of E_I^e with respect to parameter γ; E_o^2 = 2.669, 5.05

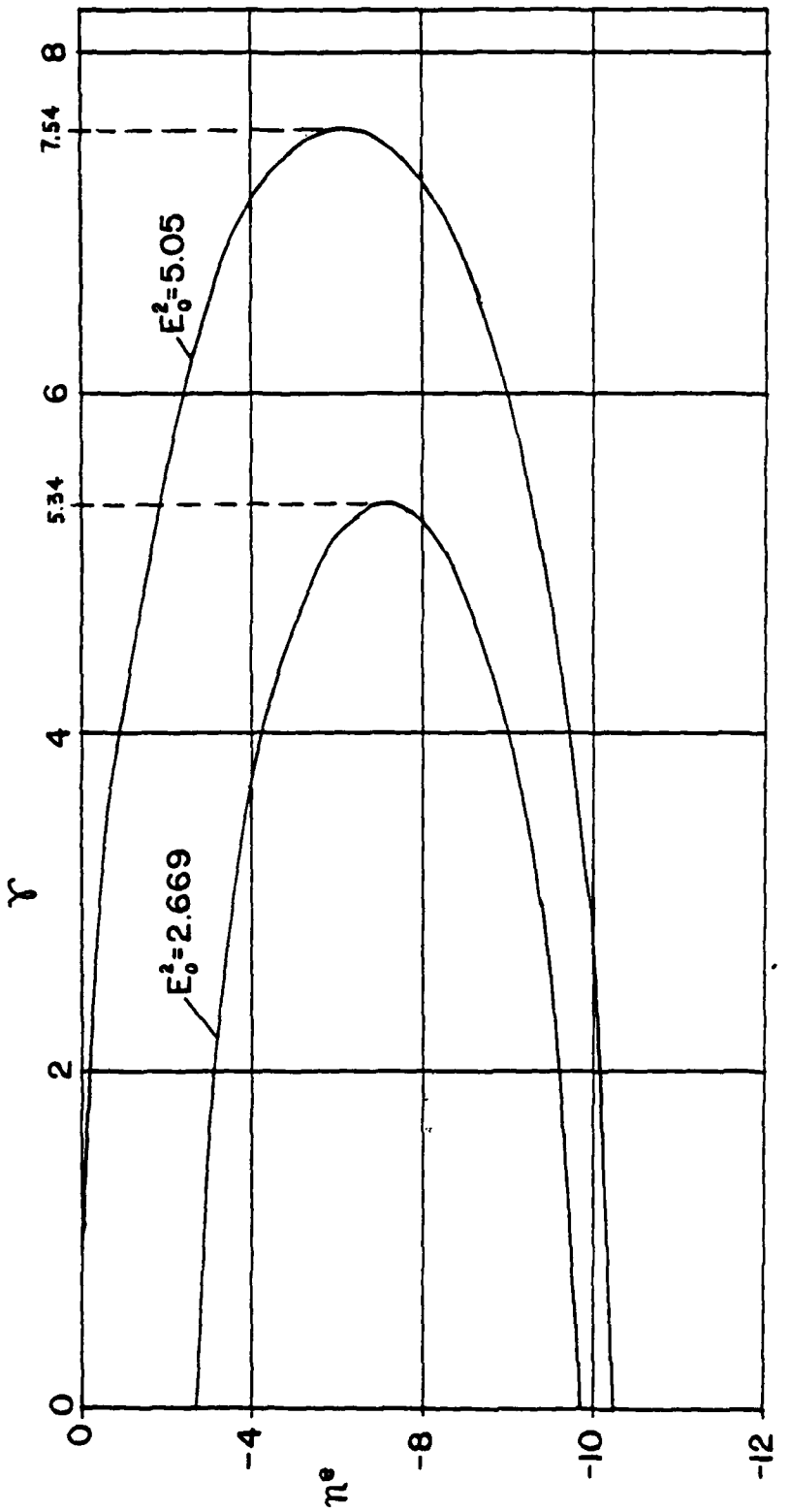

Fig.3 Bifurcation of n^e with respect to parameter γ; $E_o^2 = 2.669, 5.05$

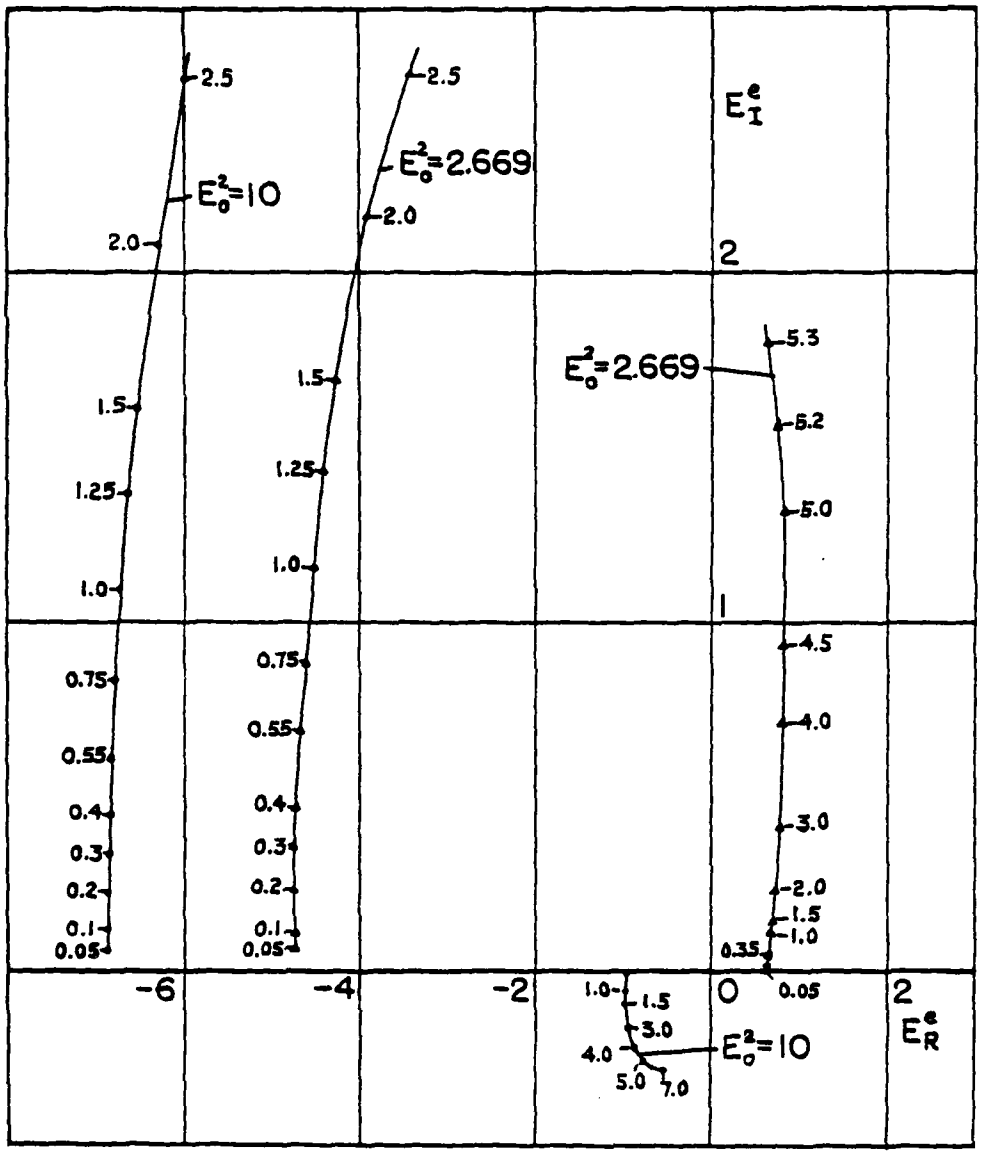

Fig.4 Loci of E_R^e and E_I^e with variable parameter γ and fixed values of E_o^2.

IV. QUENCHING OF CHAOTIC OSCILLATIONS

In the Zakharov's model for Langmuir turbulence, there does not exist a clearcut way of introducing damping terms into the equations based on physical considerations. Here, phenomenenological damping coefficient γ_m and Γ_m are introduced into the simplified model (1)-(3). They may correspond to Landau damping of the high and low frequency waves given by[3]

$$\gamma_m = \frac{3}{2}\left(\frac{m_i}{m_e}\right)\left(\frac{\pi}{8}\right)^{\frac{1}{2}}(\mu_m\lambda_D)^{-3}\exp[-\frac{1}{2}(\mu_m\lambda_D)^{-2} - \frac{3}{2}],$$
$$\Gamma_m = \frac{3}{4}\left(\frac{\pi}{8}\right)^{\frac{1}{2}}\mu_m\lambda_D, \tag{18}$$

where λ_D is the Debye length and m_i/m_e is the ion-electron mass ratio. We observe that the damping coefficient γ_m varies rapidly for small $\mu_m\lambda_D > 0$. Therefore, it is of interest to determine any change of the behavior of the solutions as γ_m is varied, in particular, the onset or quenching of chaotic oscillations when γ_m tends to some threshold value. This is studied numerically for the one-dimensional case with the fixed parameters as given in (16).

First, we study the case with $E_o^2 = 2.669$. It is known that chaotic oscillations exist for $\Gamma = 2.0$ and $\gamma = 1.0$ (see Ref.1). At these parameter values, the equilibrium states consist of the origin $z = 0$ and two distinct nonzero equilibrium states z_e^+ and z_e^- given by (10)-(15). Chaotic oscillations were found in some neighborhoood of z_e^+. Figures 5-7 show the loci of eigenvalues of $J_f(z_e,\gamma,E_o)$ with $E_o^2 = 2.669$ and variable parameter γ for each of the equilibrium states z_e. We observe that at $\gamma = 1.0$, there exist a pair of unstable complex eigenvalues for $J_f(z_e^+,\gamma,E_o)$ with $E_o^2 = 2.669$. As γ is increased, these eigenvalues cross the imaginary axis at $\gamma \approx 4.35$. When γ is increased beyond 4.35, all the eigenvalues of $J_f(z_e^+,\gamma,E_o)$, $E_o^2 = 2.669$, remain in the left-half complex plane. By defin-

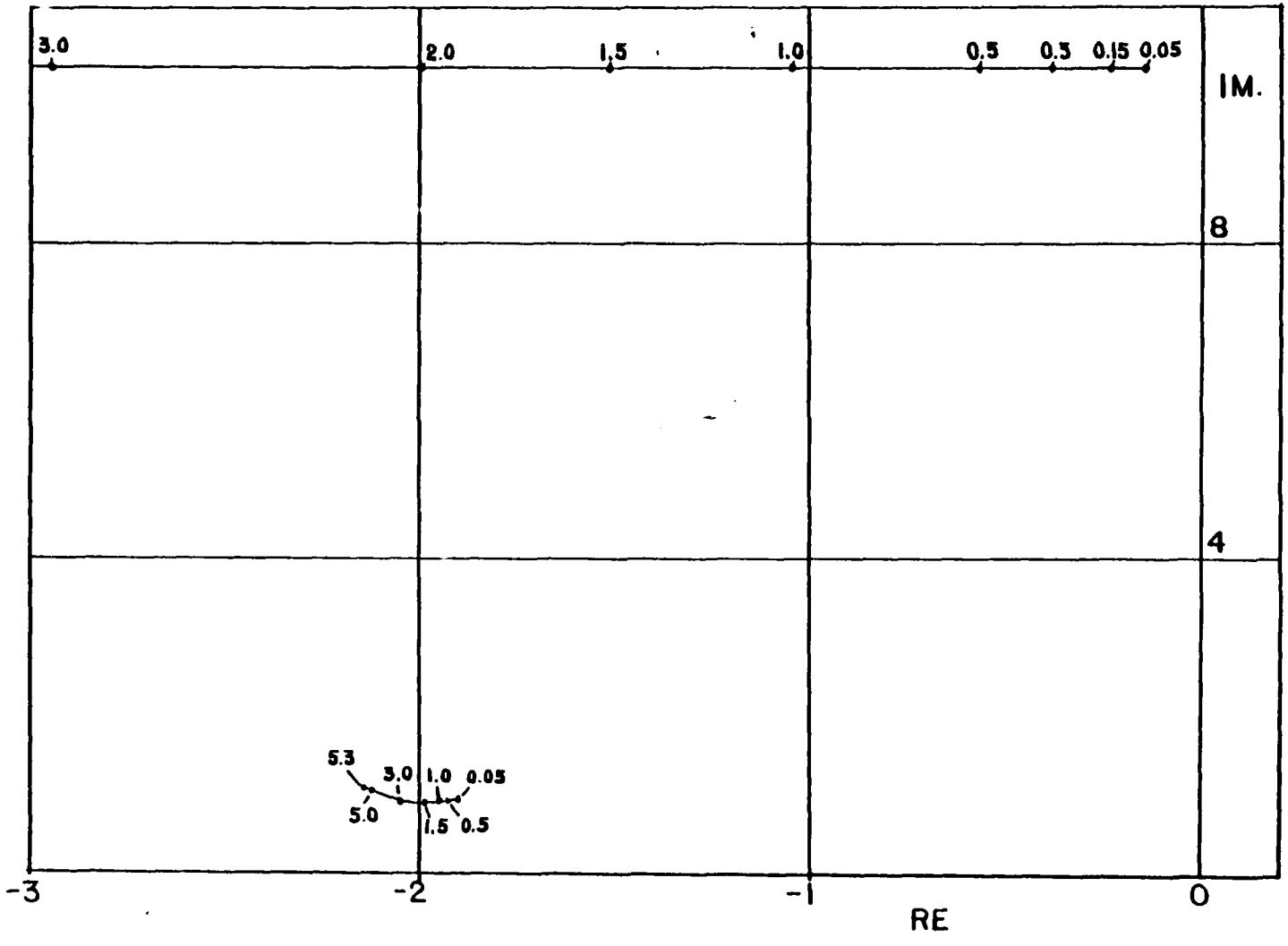

Fig.5 Loci of eigenvalues of $J_f(0,\gamma,E_o)$ with $E_o^2 = 2.669$, and variable parameter γ.

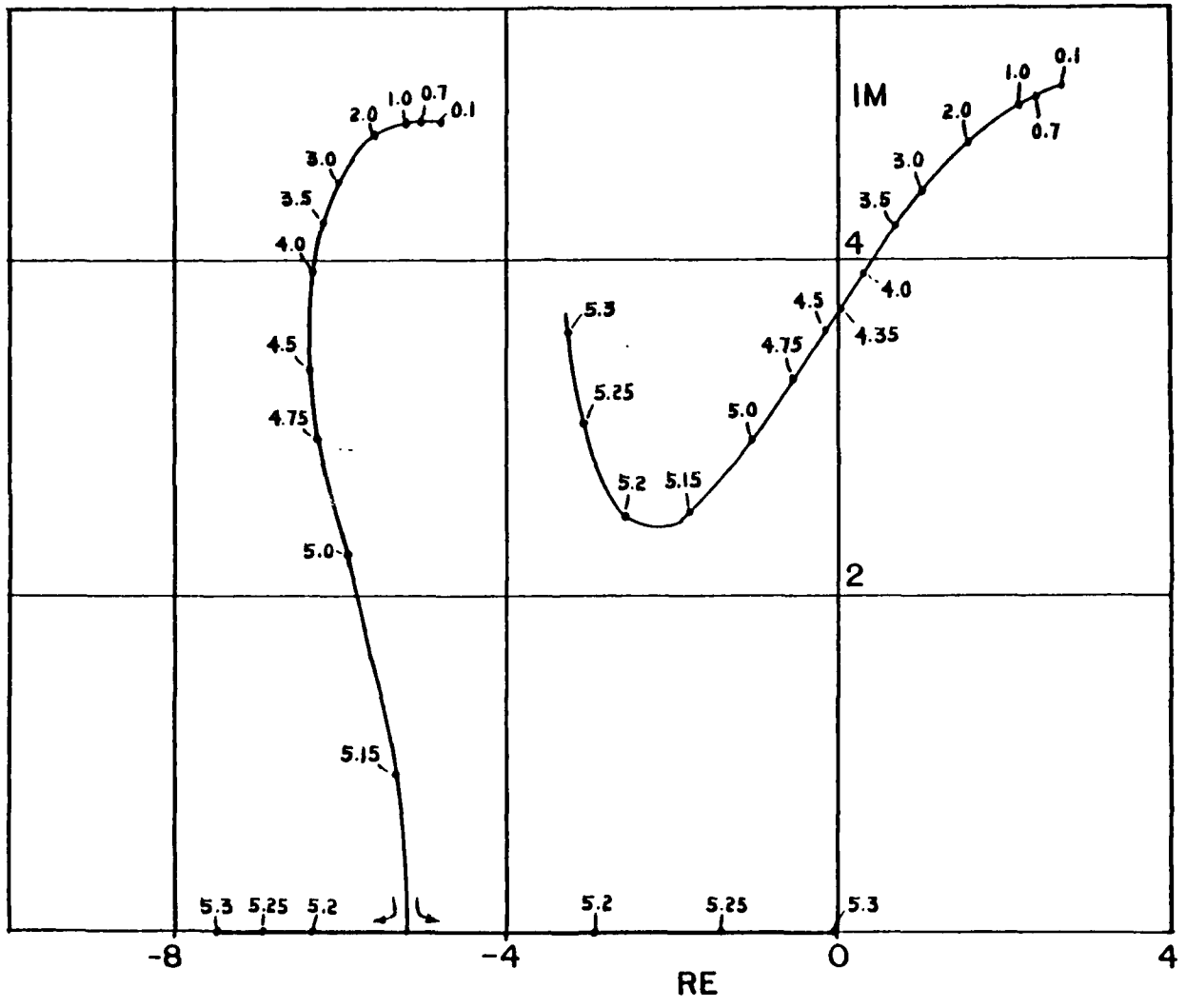

Fig.6 Loci of eigenvalues of $J_f(z_e^+, \gamma, E_o)$ with $E_o^2 = 2.669$ and variable parameter γ.

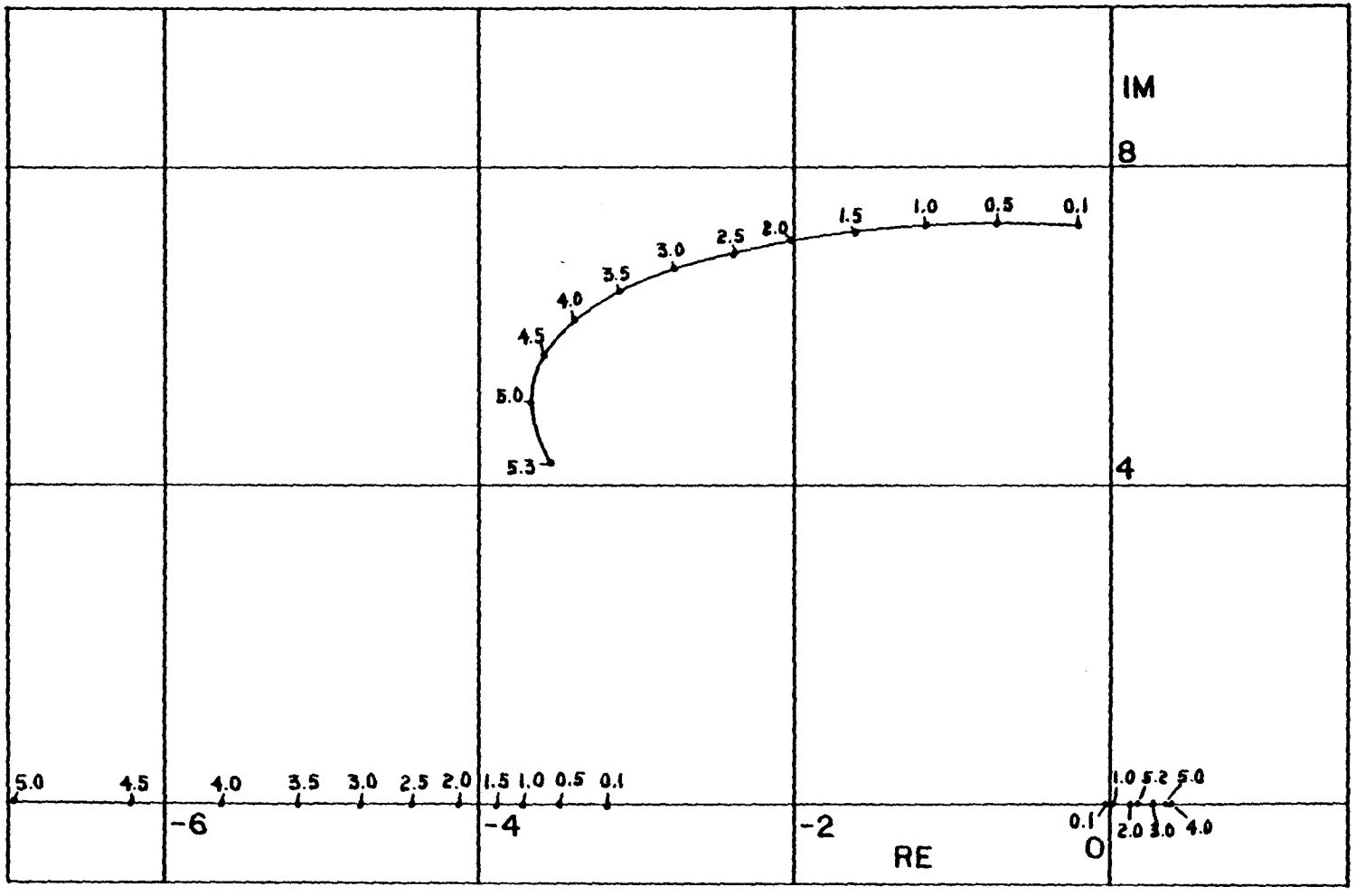

Fig.7 Loci of eigenvalues of $J_f(\bar{z_e}, \gamma, E_o)$ with $E_o^2 = 2.669$ and variable parameter γ.

ing a parameter $\gamma = 1/\hat{\gamma}$, we see that Hopf bifurcation with respect to parameter $\hat{\gamma}$ takes place at $\hat{\gamma} \approx 1/4.35$. When $\gamma = \gamma_c = 5.3358$, one of the real eigenvaues is zero. At this point, z_e^+ and z_e^- coalesce into one equilibrium state as shown in Figs. 2 and 3. Thus, we expect that quenching of the chaotic oscillations will occur when $\gamma \approx 4.35$ for $E_o^2 = 2.669$. Numerical integration of the system equations confirms our expectation. Figures 8a and 8b show the existence of a periodic solution at $\gamma = 4.35$ as predicted by the Hopf bifurcation theorem. As the damping γ is reduced, the amplitude of the periodic oscillations increases as shown in Figs. 9a and 9b with $\gamma = 4.30$. At $\gamma = 3.0$, a more complex form of periodic solutions appears (Figs.10a and 10b). As γ is further reduced, the oscillations become more complex in structure and appear to be almost periodic for $2.0 \geq \gamma \geq 1.6$ (see Figs.11-13). Finally, for $\gamma < 1.55$, the solutions become chaotic (see Figs. 14a and 14b). Figures 15-17 show the chaotic oscillations for $\gamma = 1.5, 1.4$ and 1.1. The power spectra of the electric field corresponding to the solutions in Figures 14-17 are shown in Fig.18. It can be seen that the spectra evolve from essentially discrete spectra to broadband spectra as γ crosses the threshold value $\gamma_T \approx 1.55$. Although the solutions shown in Figs.10-17 start with the same initial conditions, similar behavior has been observed for solutions starting near the equilibrium state z_e^+.

V. POINCARÉ MAPS

To obtain some idea on the nature of the chaotic oscillations, we consider various Poincaré maps associated with (4) with parameters given in (16). Let H denote a given three dimensional hyperplane in the state space $\mathbb{R}^4$ of system (4) whose flow is denoted by the family of mappings $F_t : \mathbb{R}^4 \to \mathbb{R}^4$, $t \in \mathbb{R}$. We define a Poincaré or first return map P from

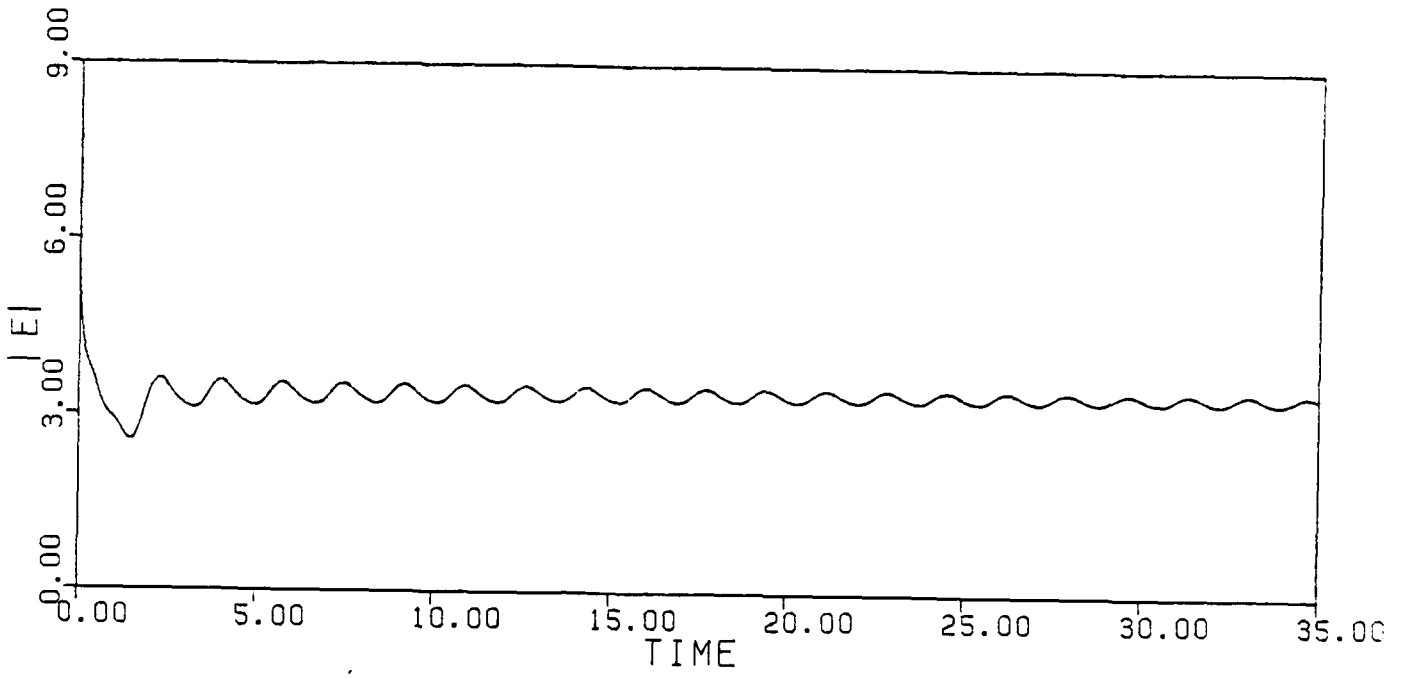
9.00
6.00
3.00
0.00
|E|
0.00
5.00
10.00
15.00
20.00
25.00
30.00
35.00
TIME

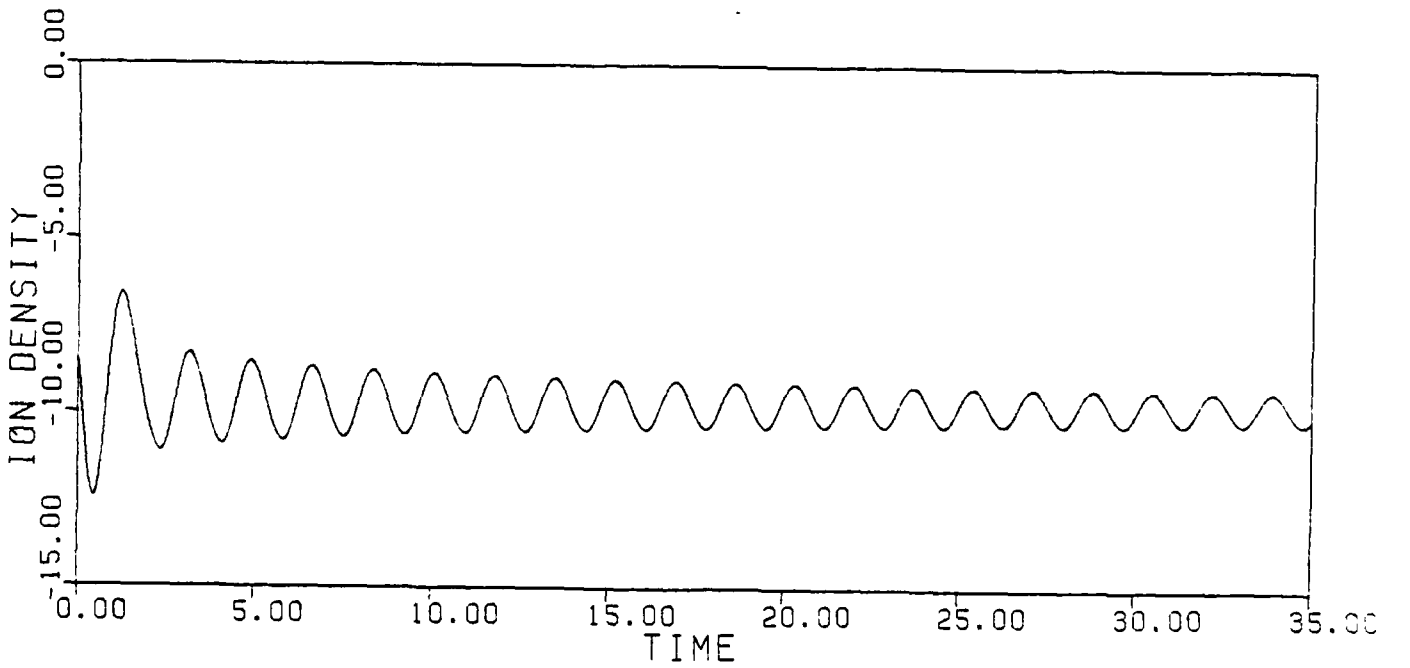
0.00
-5.00
-10.00
-15.00
ION DENSITY
0.00
5.00
10.00
15.00
20.00
25.00
30.00
35.00
TIME

Fig.8a

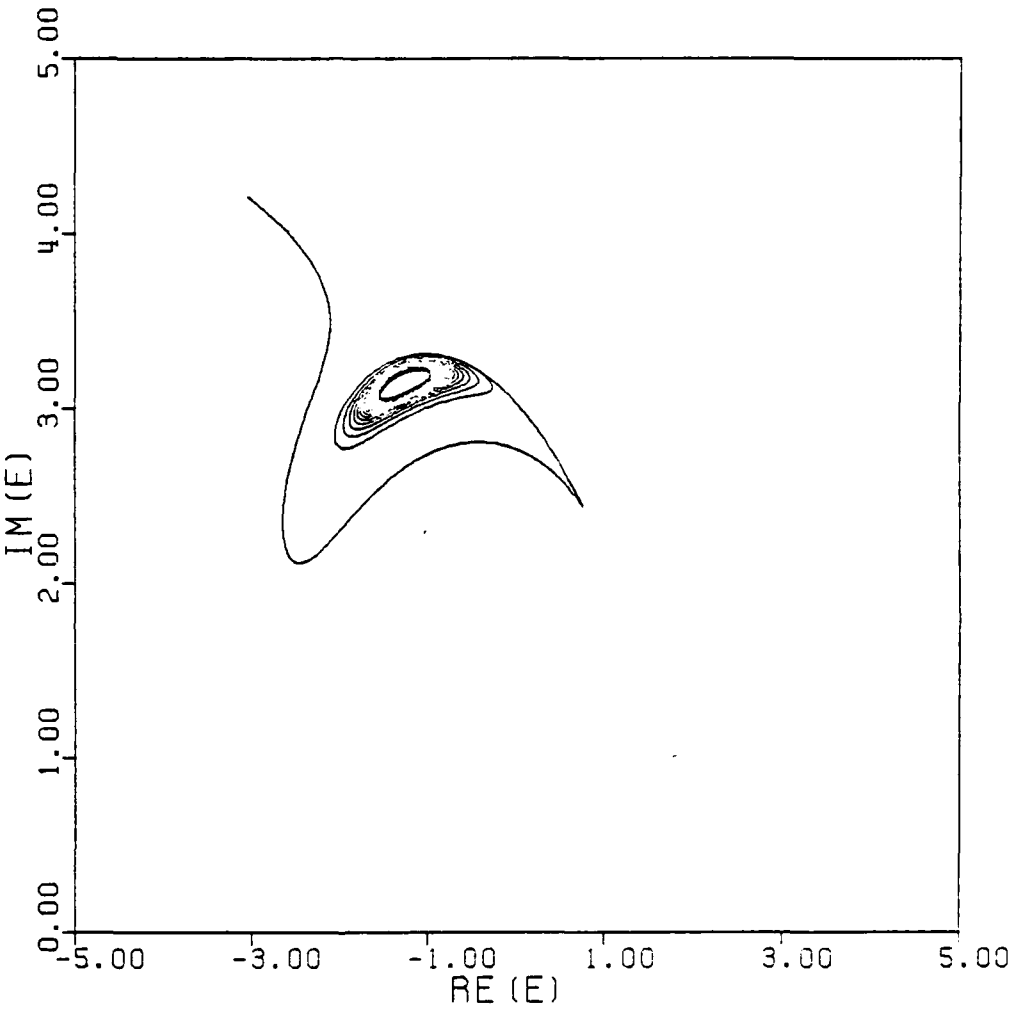

Fig.8b

Fig.8 Solution of (5) with initial condition: E(0) = -3.07656 + 4.22328i, n(0) = -8.38056, n(0) = -8.25344; E_o^2 = 2.669; γ = 4.35.

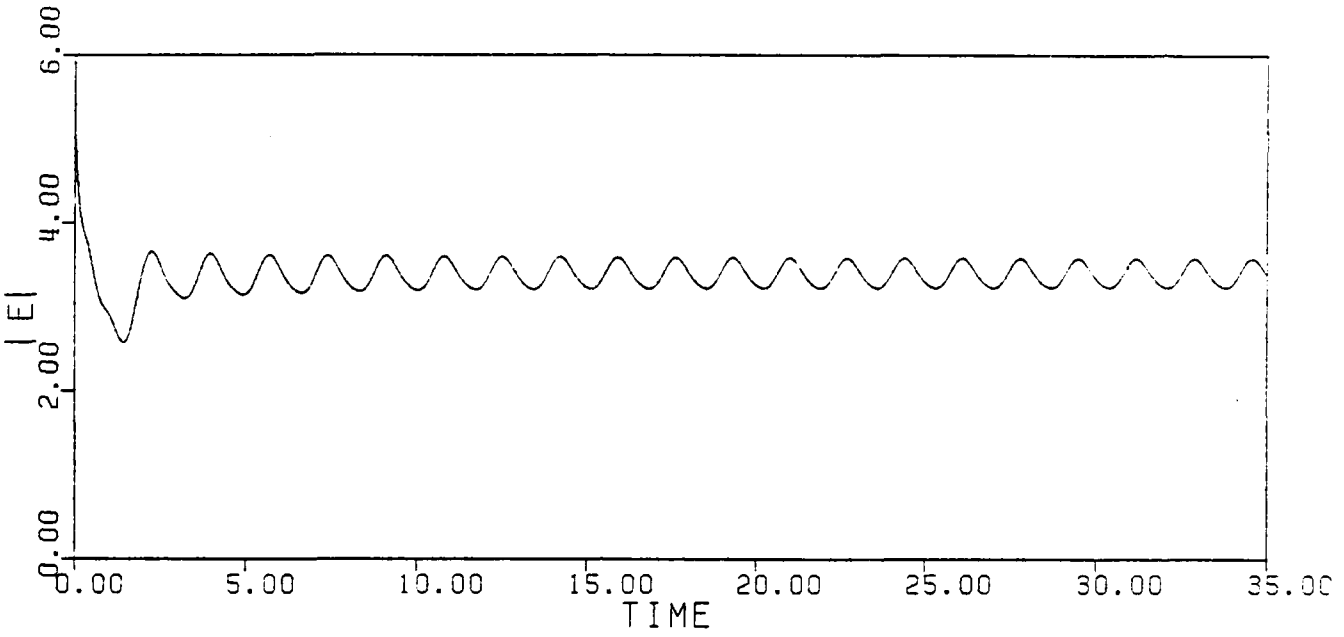
6.00
4.00
2.00
0.00
|E|
0.00
5.00
10.00
15.00
20.00
25.00
30.00
35.00
TIME

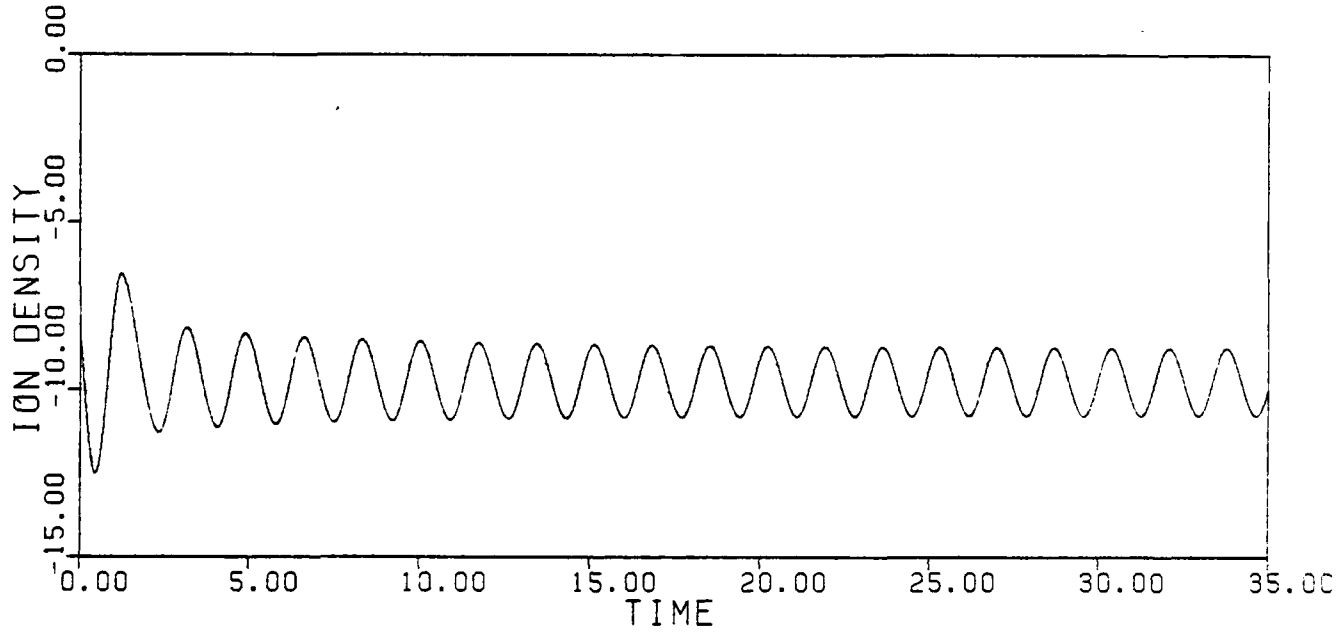
0.00
-5.00
-10.00
-15.00
ION DENSITY
0.00
5.00
10.00
15.00
20.00
25.00
30.00
35.00
TIME

Fig.9a

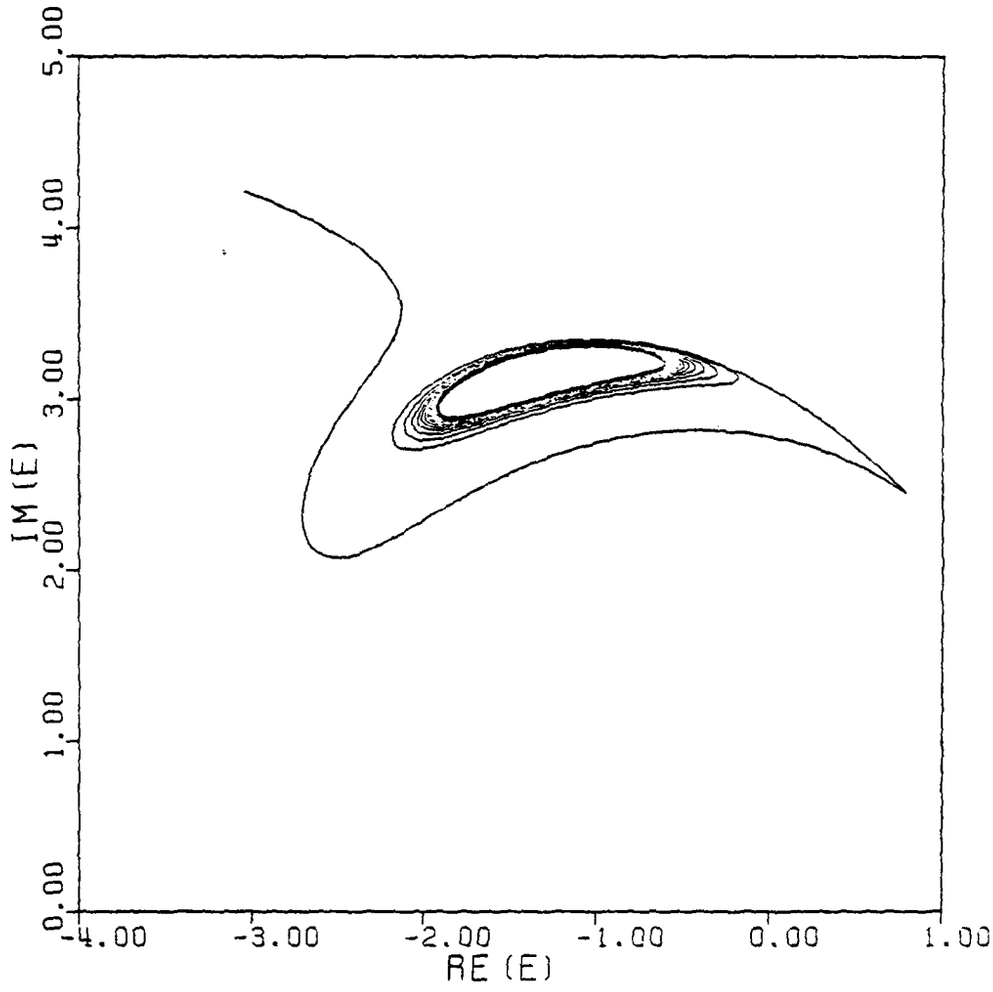

Fig.9b

Fig.9 Solution of (5) with initial condition given in Fig.8; $E_o^2 = 2.669$; $\gamma = 4.30$.

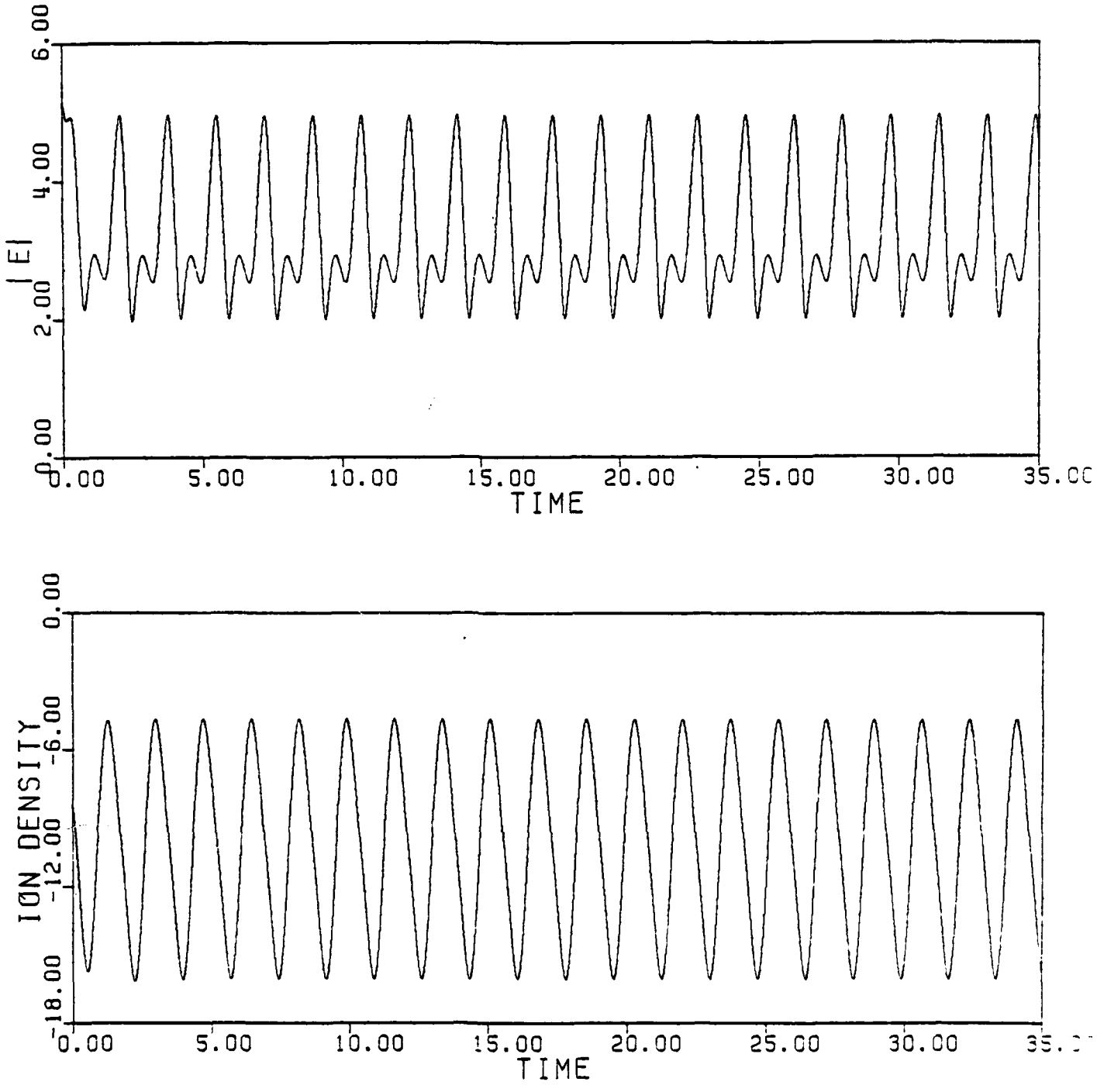
6.00
4.00
2.00
0.00
|E|
0.00
5.00
10.00
15.00
20.00
25.00
30.00
35.00
TIME
0.00
-6.00
-12.00
-18.00
ION DENSITY
0.00
5.00
10.00
15.00
20.00
25.00
30.00
TIME

Fig.10a

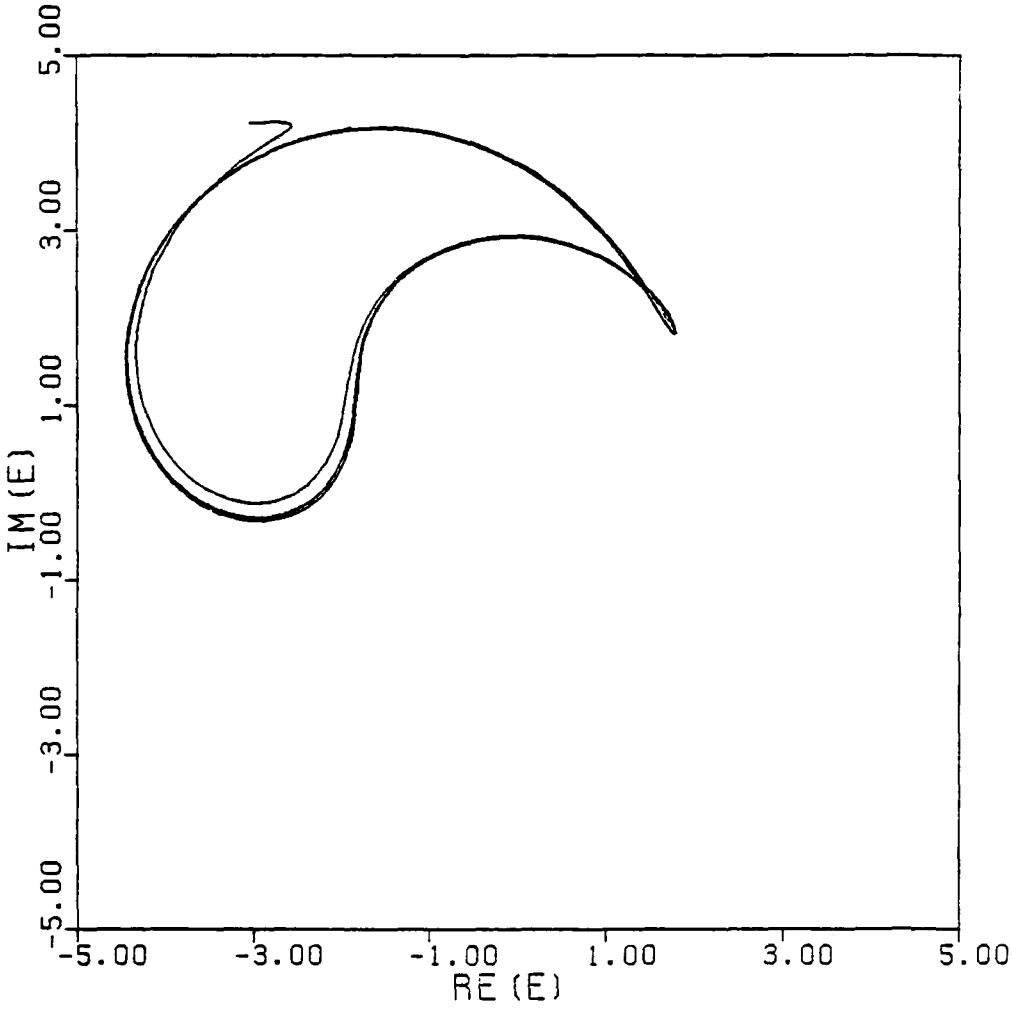

Fig.10b

Fig.10 Solution of (5) with initial condition given in Fig.8; E_o^2 =2.669; γ = 3.0.

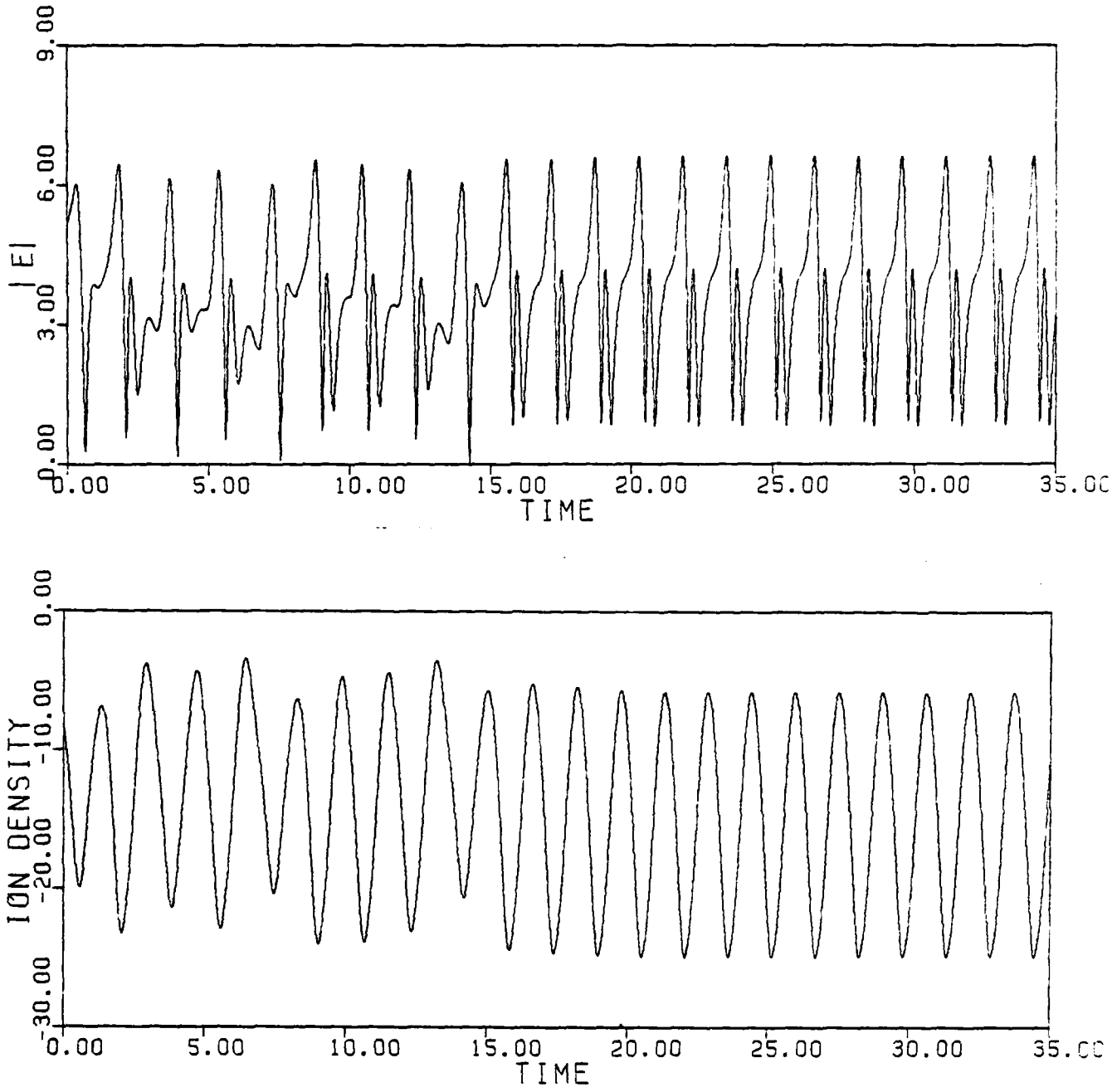
|E|
9.00
6.00
3.00
0.00
0.00
5.00
10.00
15.00
20.00
25.00
30.00
35.00
TIME
ION DENSITY
0.00
-10.00
-20.00
-30.00
0.00
5.00
10.00
15.00
20.00
25.00
30.00
35.00
TIME

Fig.11a

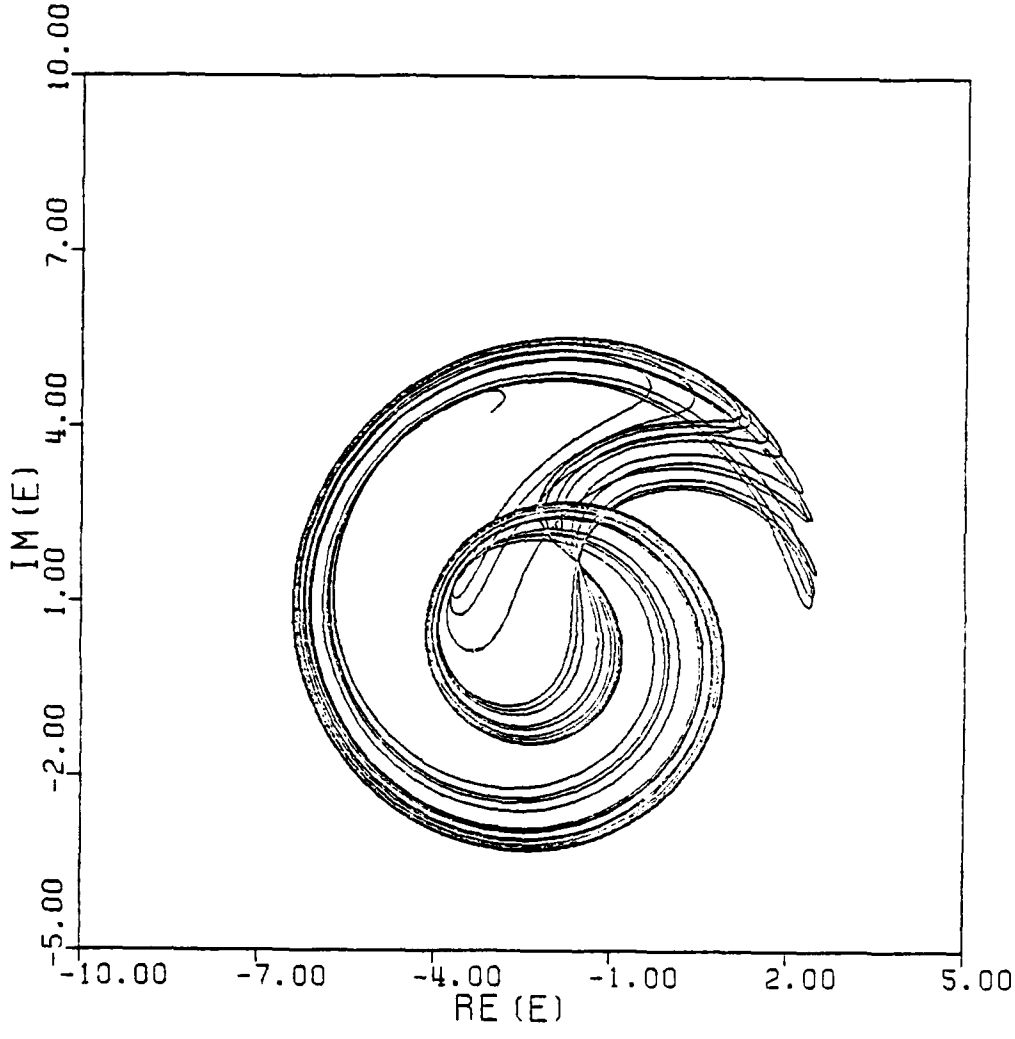

Fig.11b

Fig.11 Solution of (5) with initial condition given in Fig.8; $E_o^2 = 2.669$; $\gamma = 2.0$

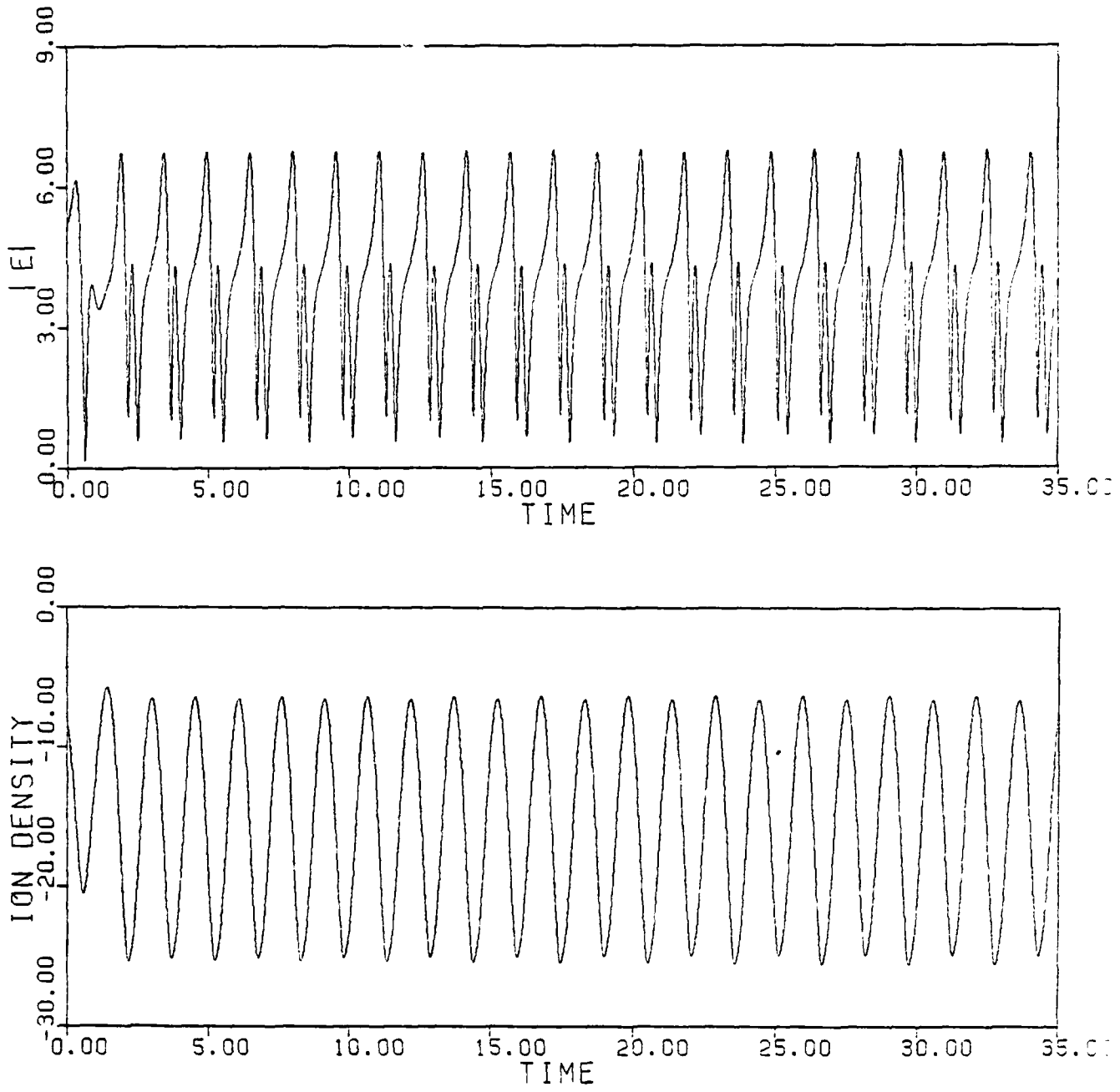
9.00
6.00
3.00
0.00
|E|
0.00
5.00
10.00
15.00
20.00
25.00
30.00
TIME
0.00
-10.00
-20.00
-30.00
ION DENSITY
0.00
5.00
10.00
15.00
20.00
25.00
30.00
TIME

Fig.12a

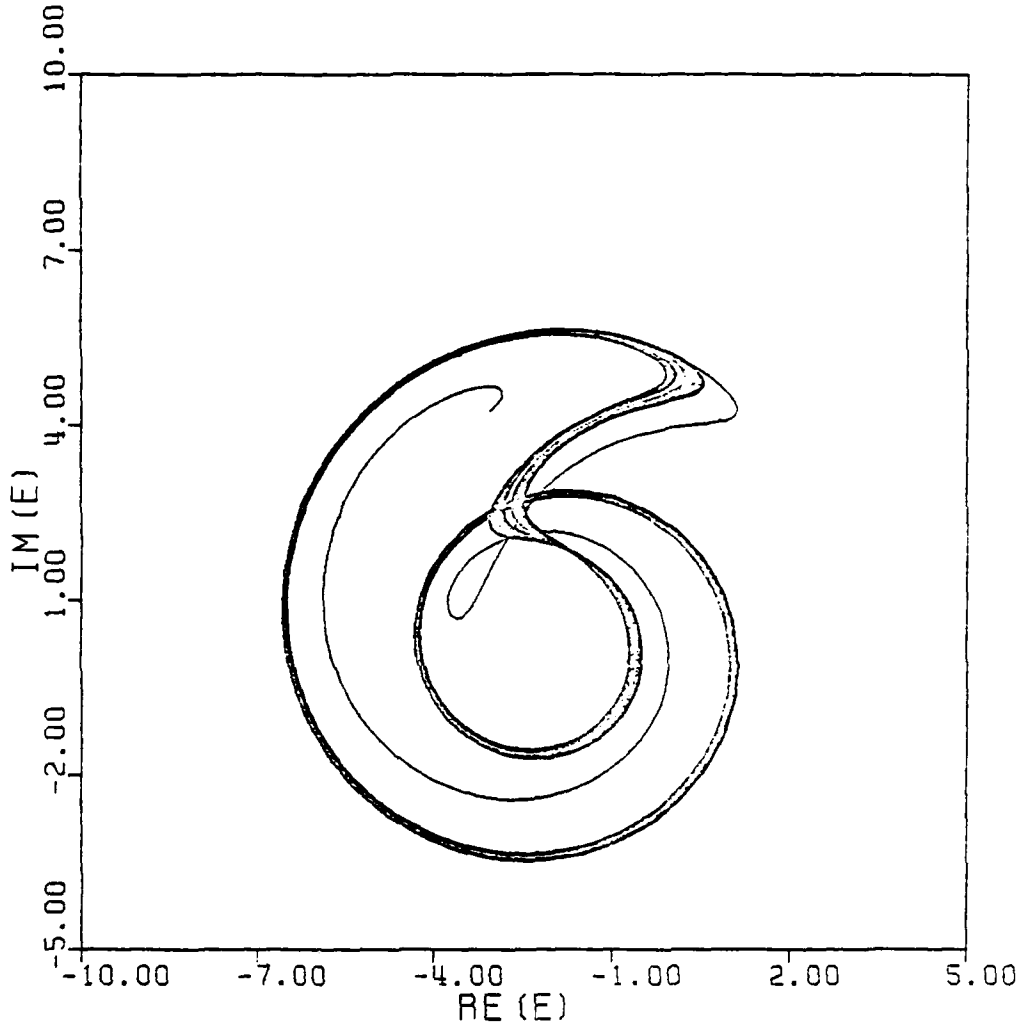

Fig.12b

Fig.12 Solution of (5) with initial condition given in Fig.8; $E_o^2 = 2.669$; $\gamma = 1.9$

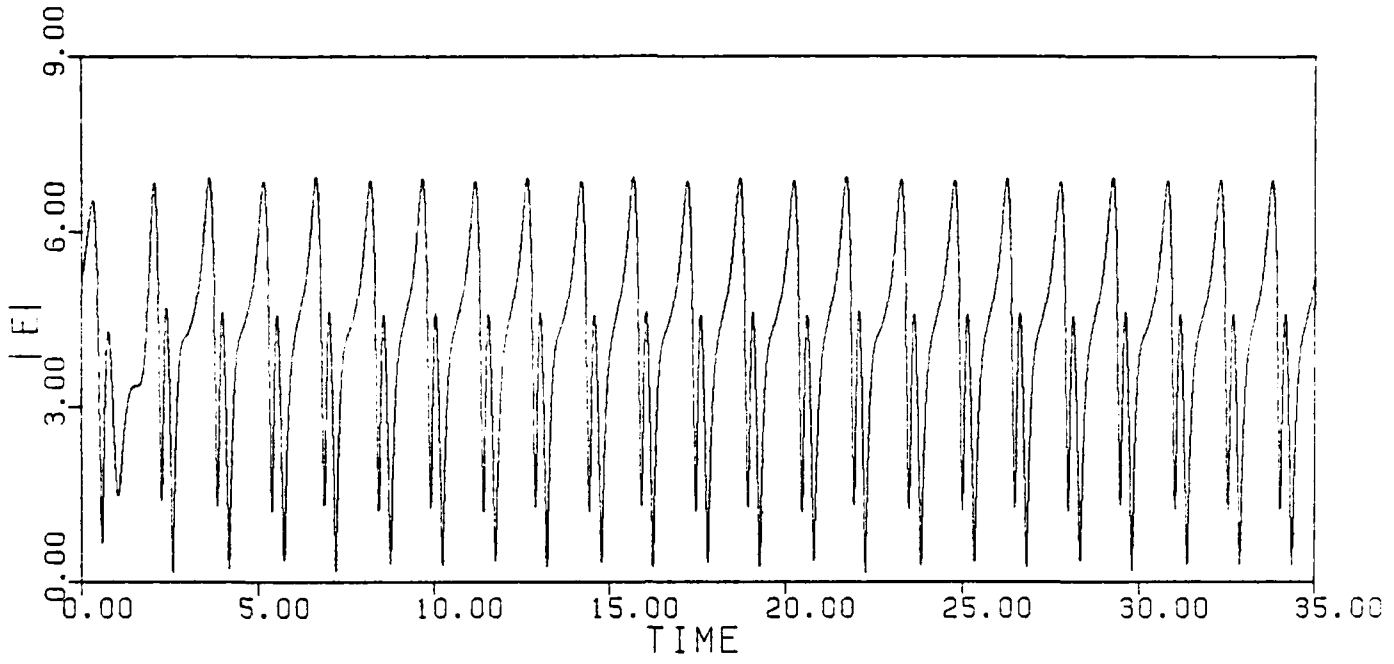
9.00
6.00
3.00
0.00
|E|
0.00
5.00
10.00
15.00
20.00
25.00
30.00
35.00
TIME

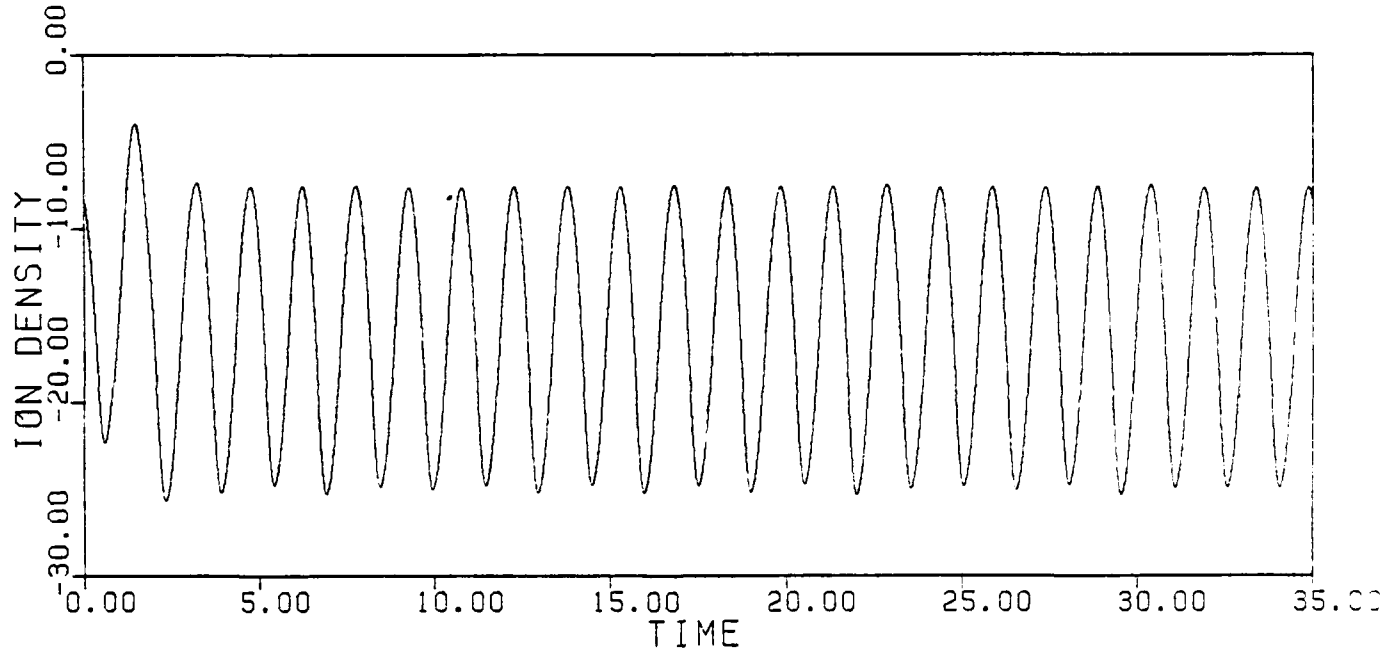
0.00
-10.00
-20.00
-30.00
ION DENSITY
0.00
5.00
10.00
15.00
20.00
25.00
30.00
35.00
TIME

Fig.13a

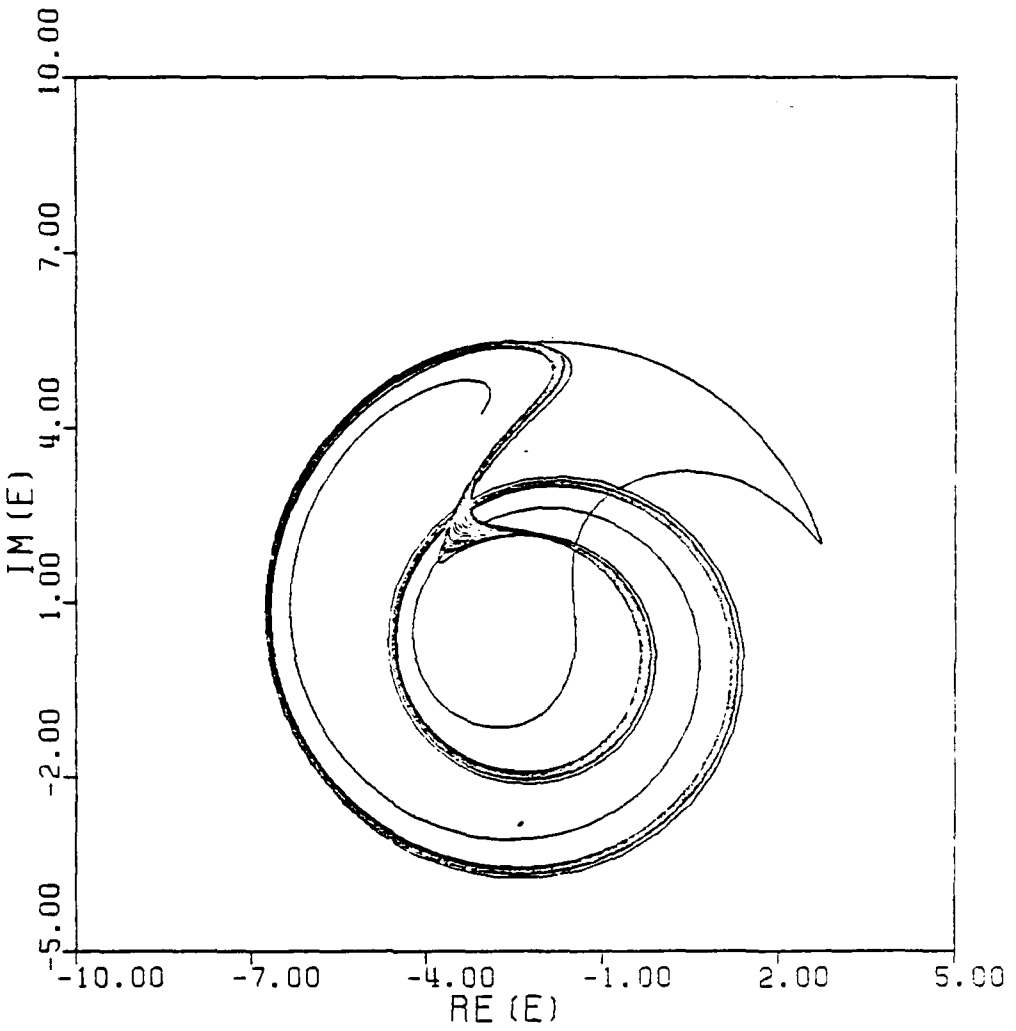

Fig.13b

Fig.13 Solution of (5) with initial condition given in Fig.8; $E_o^2 = 2.669$; $\gamma = 1.6$

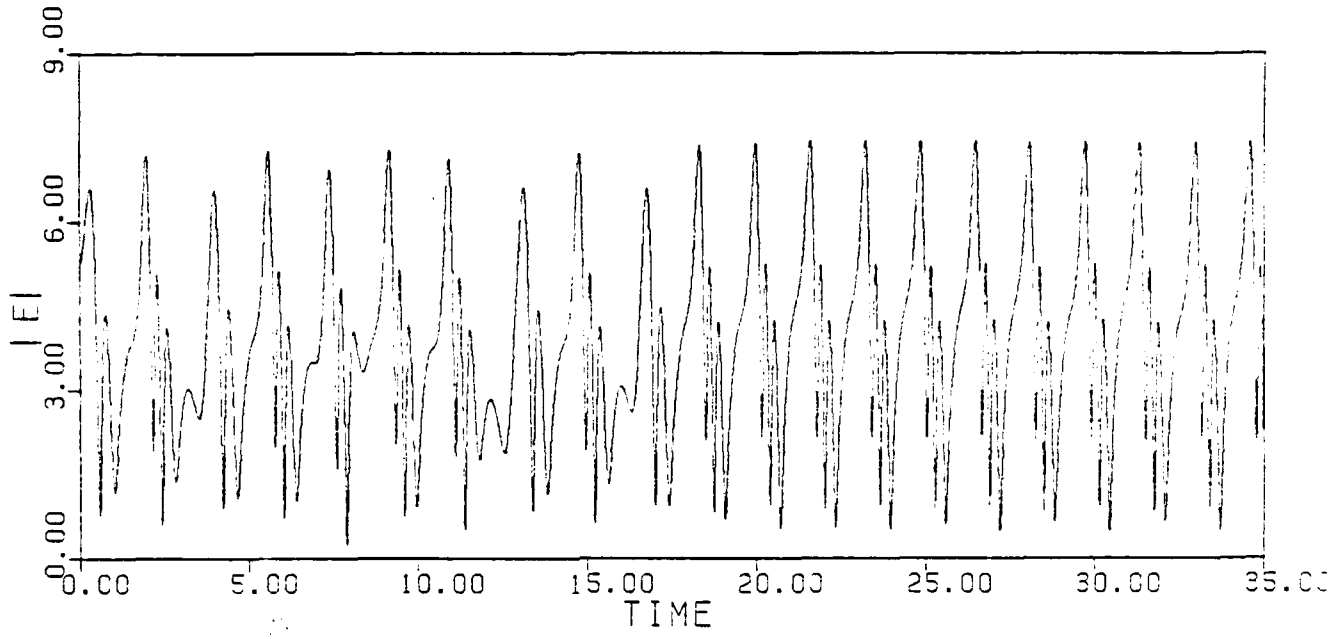
9.00
6.00
3.00
0.00
|E|
0.00
5.00
10.00
15.00
20.00
25.00
30.00
TIME

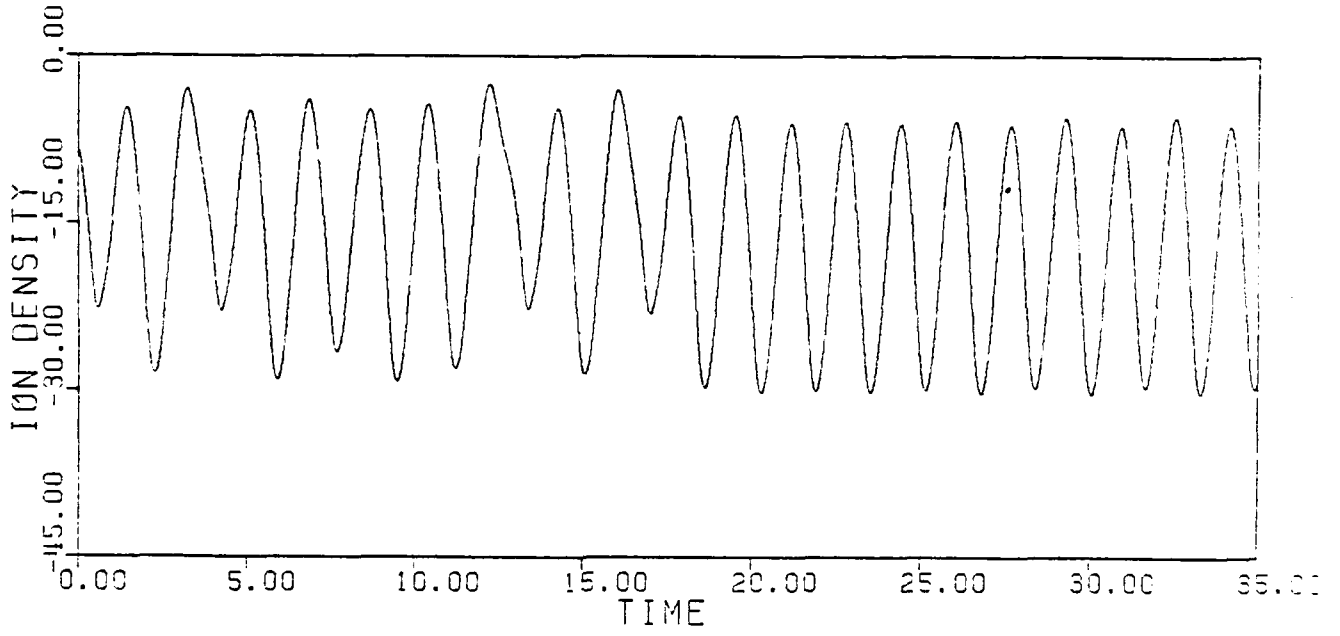
0.00
-15.00
-30.00
-45.00
ION DENSITY
0.00
5.00
10.00
15.00
20.00
25.00
30.00
TIME

Fig.14a

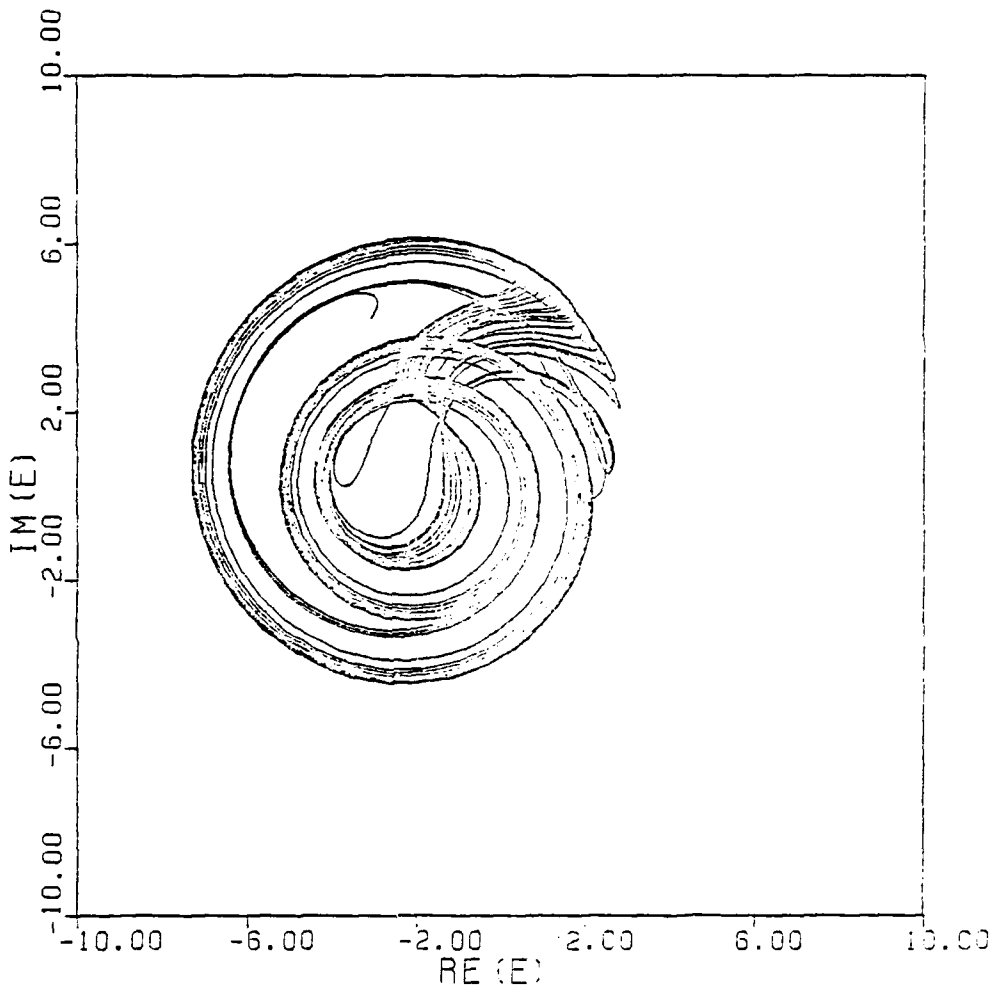

Fig.14b

Fig.14 Solution of (5) with initial condition given in Fig.8; $E_o^2 = 2.669$; $\gamma = 1.55$

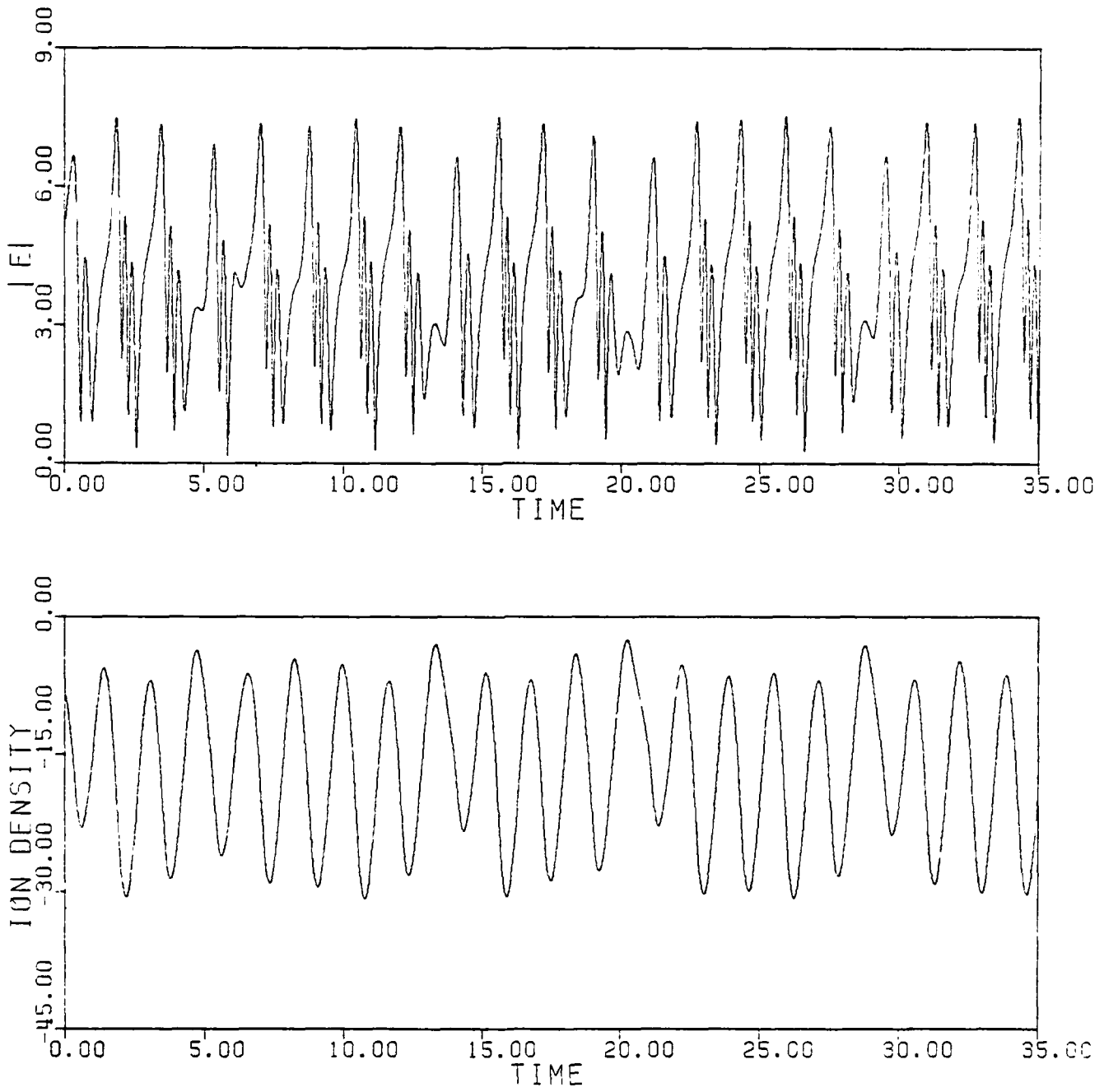
9.00
6.00
3.00
0.00
|E|
0.00
5.00
10.00
15.00
20.00
25.00
30.00
35.00
TIME
0.00
-15.00
-30.00
-45.00
ION DENSITY
0.00
5.00
10.00
15.00
20.00
25.00
30.00
35.00
TIME

Fig.15a

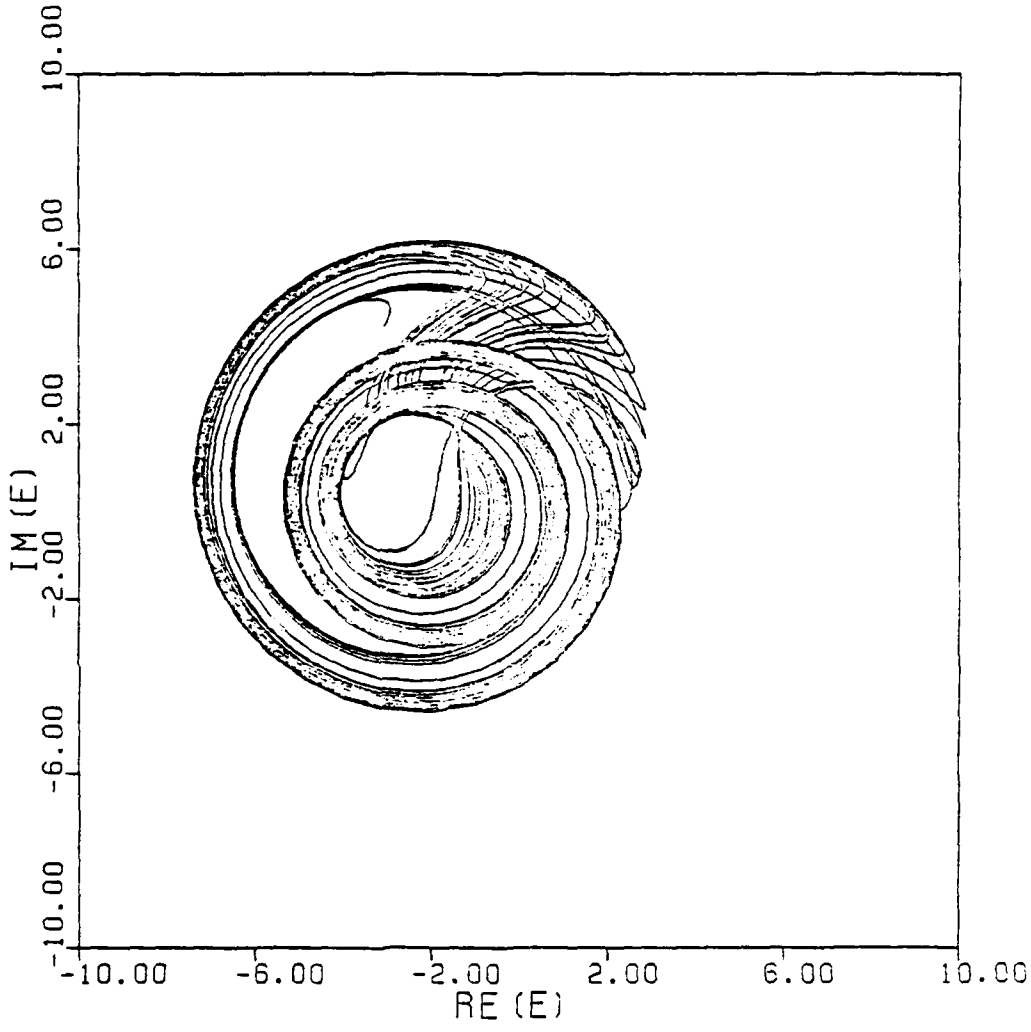

Fig.15b

Fig.15 Solution of (5) with initial condition given in Fig.8; $E_o^2 = 2.669$; $\gamma = 1.50$

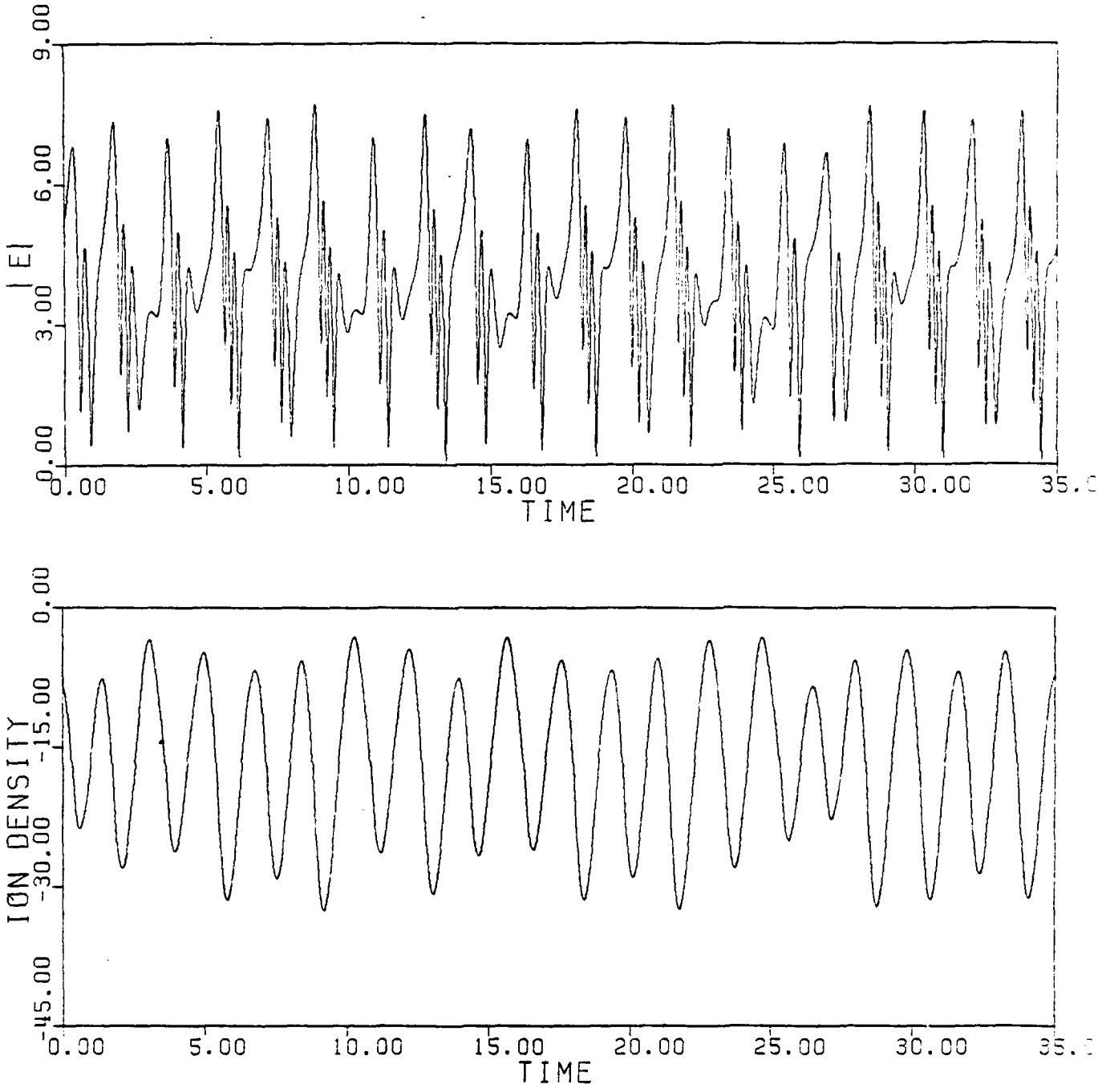
|E|
9.00
6.00
3.00
0.00
0.00
5.00
10.00
15.00
20.00
25.00
30.00
TIME
ION DENSITY
0.00
-15.00
-30.00
-45.00
0.00
5.00
10.00
15.00
20.00
25.00
30.00
TIME

Fig.16a

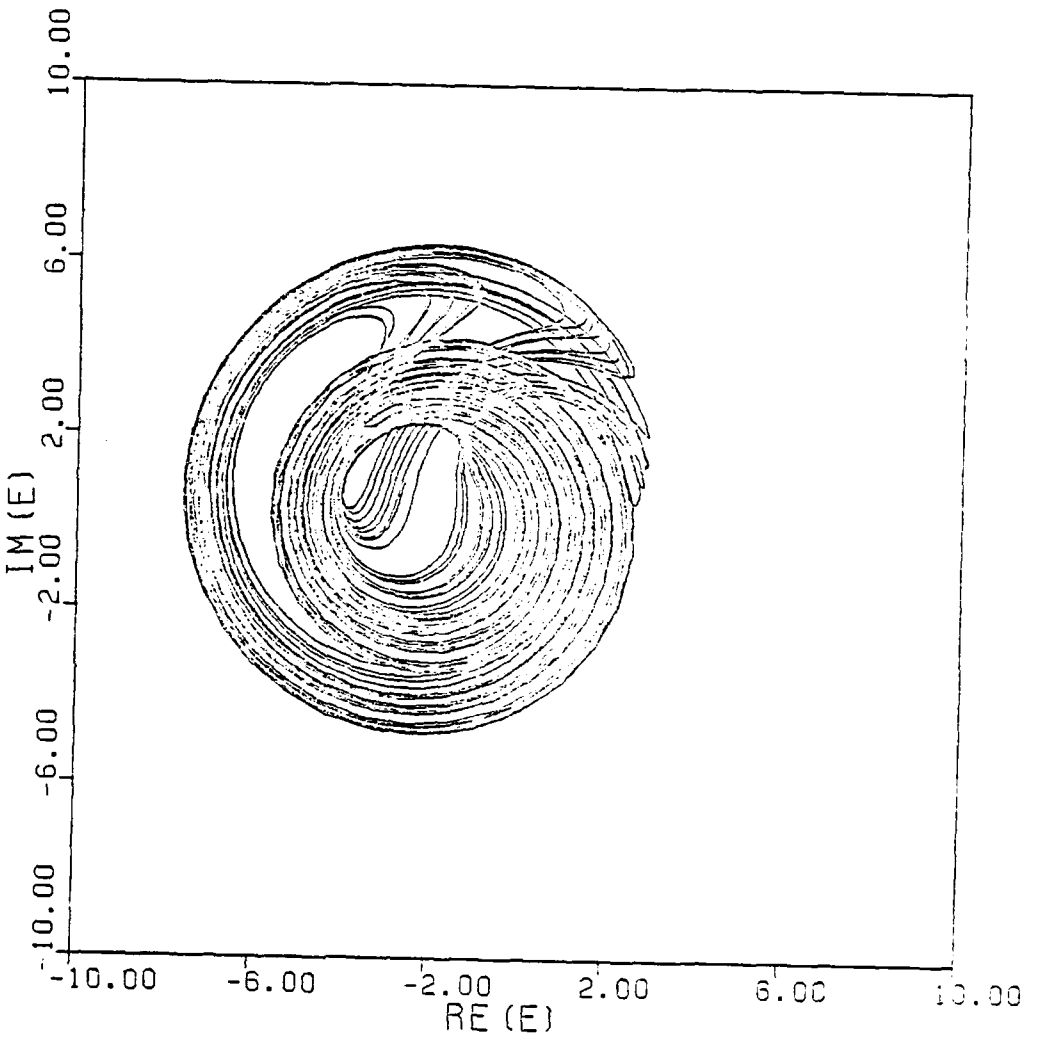

Fig.16b

Fig.16 Solution of (5) with initial condition given in Fig.8; $E_o^2 = 2.669$; $\gamma = 1.4$

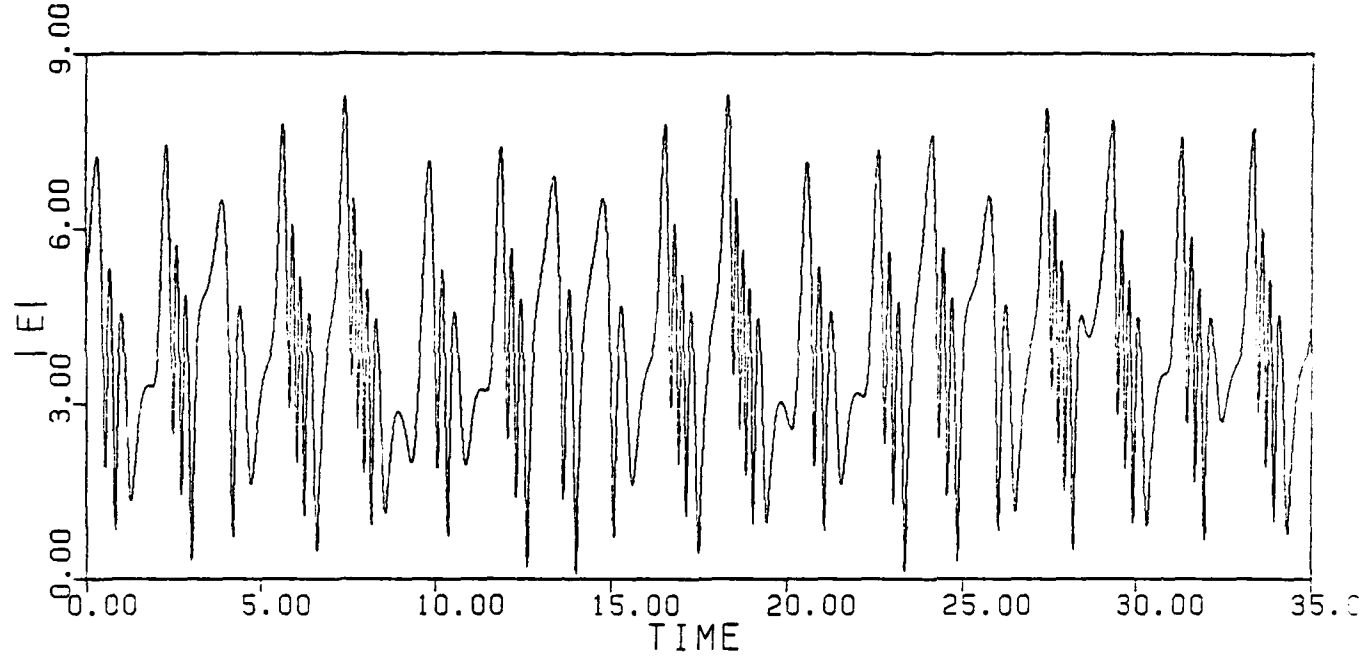
9.00
6.00
3.00
0.00
|E|
0.00
5.00
10.00
15.00
20.00
25.00
30.00
TIME

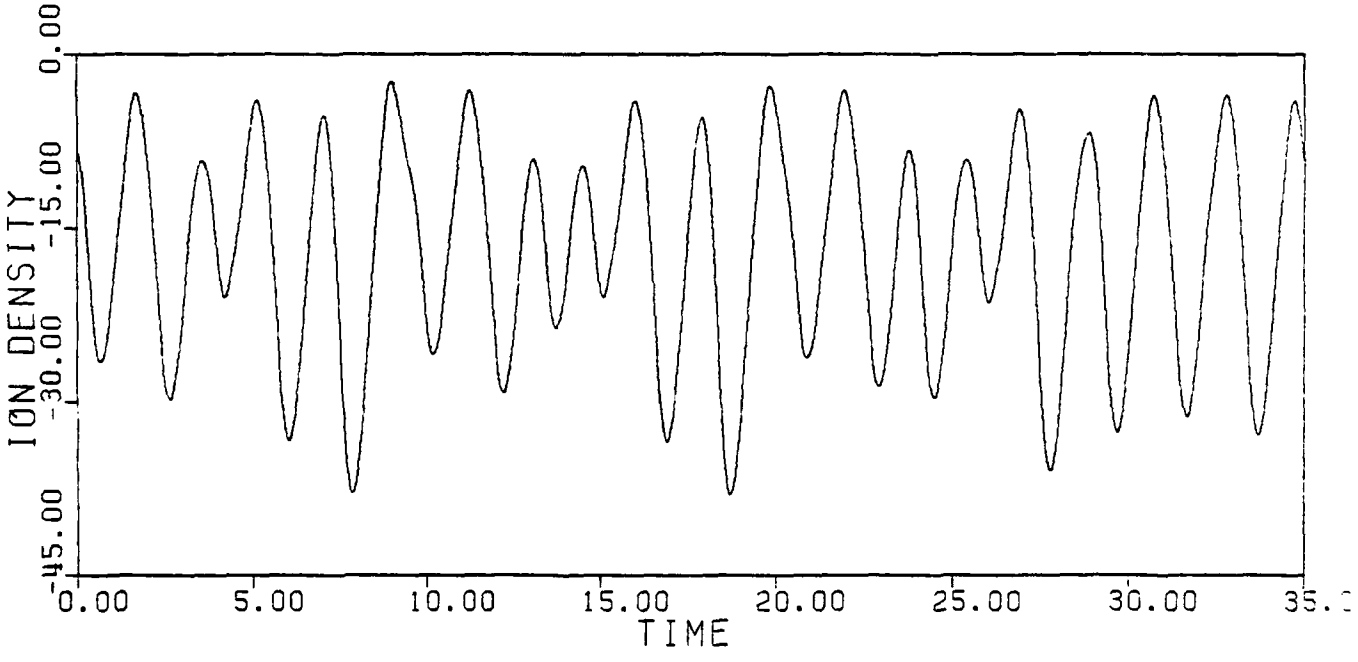
0.00
-15.00
-30.00
-45.00
ION DENSITY
0.00
5.00
10.00
15.00
20.00
25.00
30.00
TIME

Fig.17a

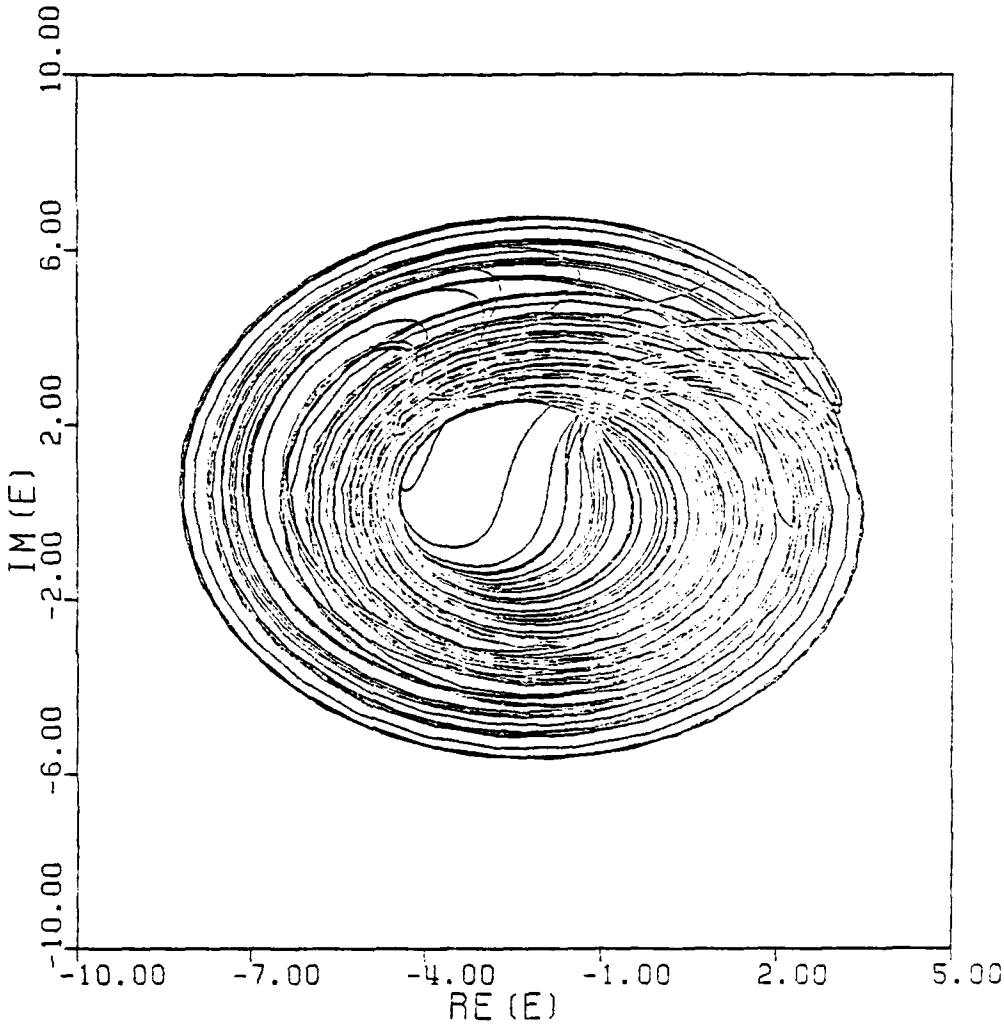

Fig.17b

Fig.17 Solution of (5) with initial condition given in Fig.8; $E_o^2 = 2.669$; $\gamma = 1.10$

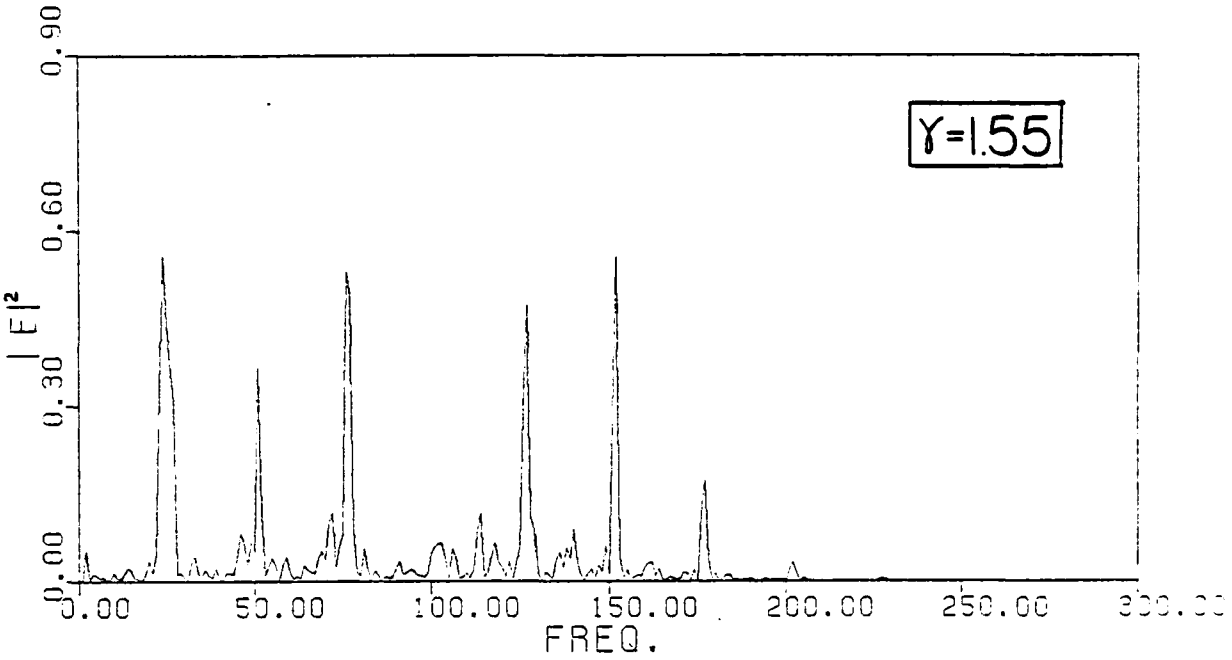
γ=1.55
0.90
0.60
0.30
0.00
|E|²
0.00
50.00
100.00
150.00
200.00
250.00
FREQ.

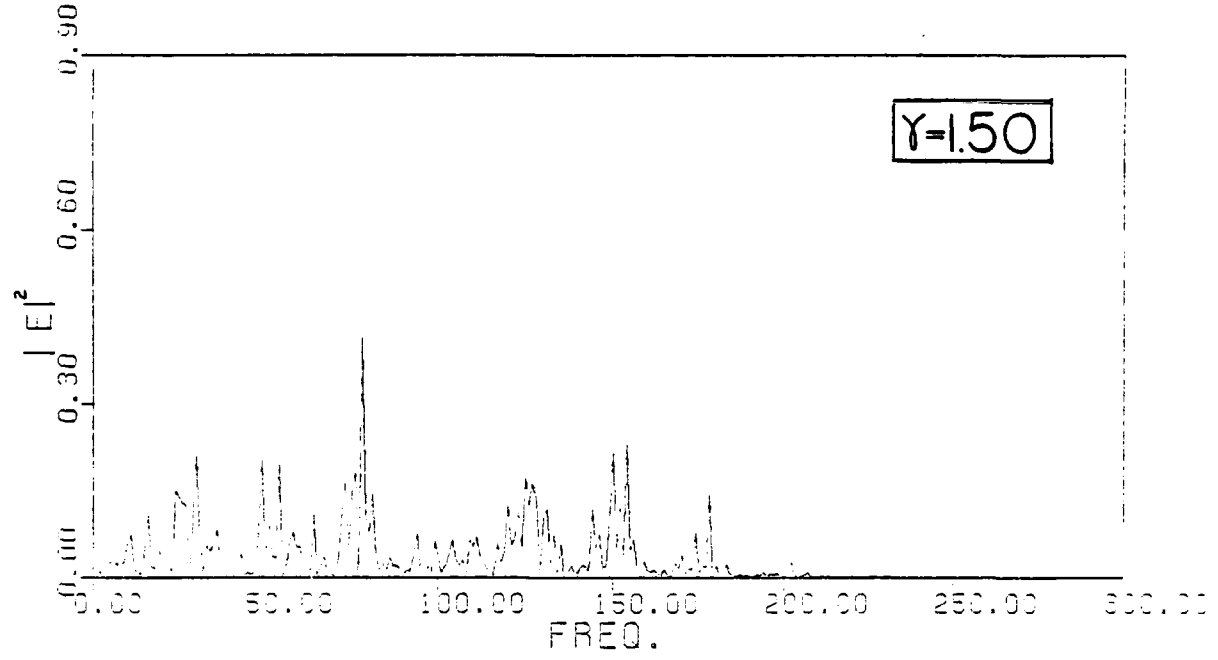
γ=1.50
0.90
0.60
0.30
|E|²
FREQ.

Fig.18a

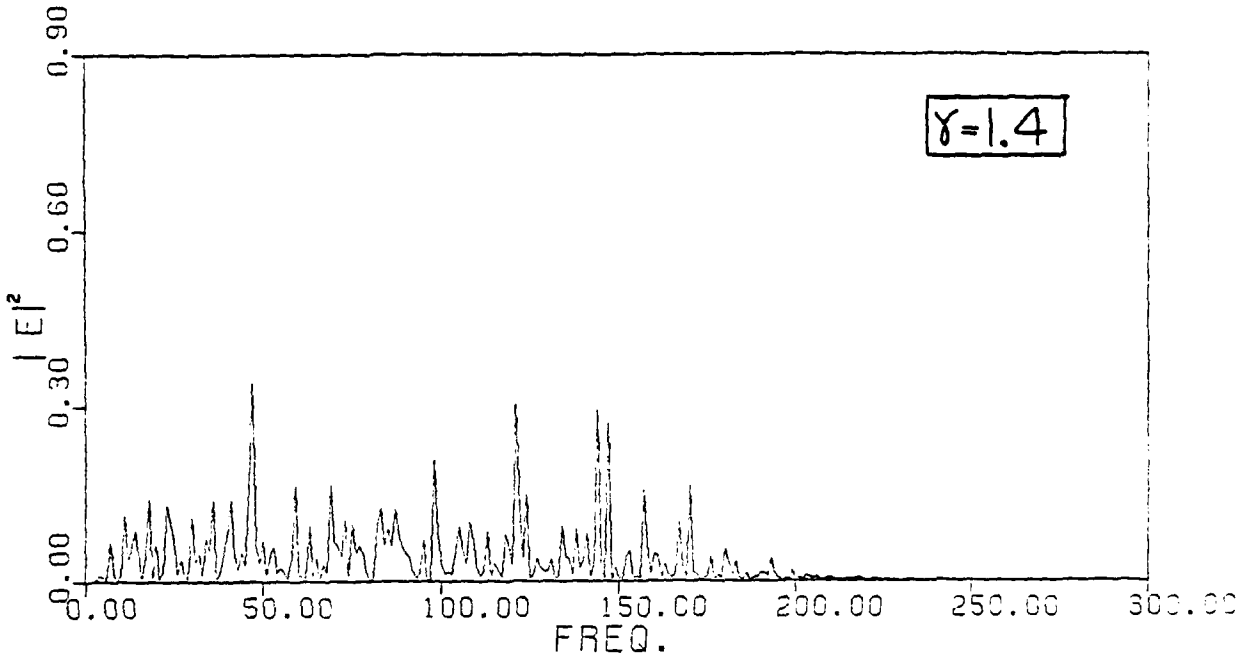

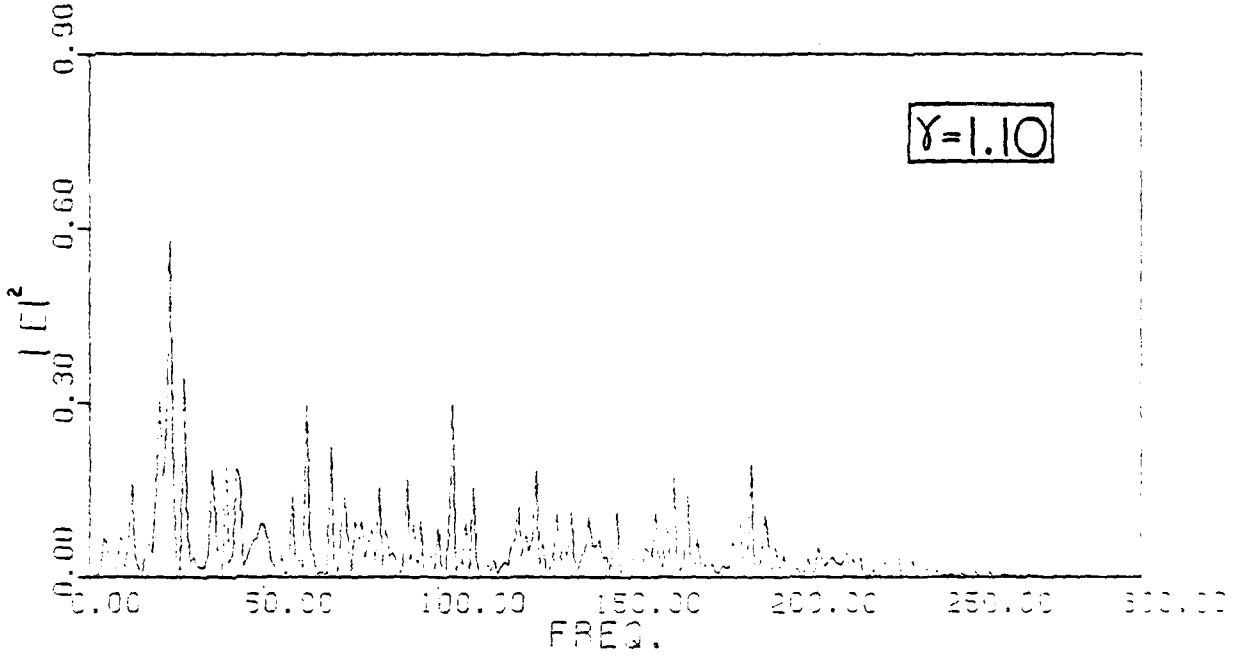

Fig.18b

Fig.18 Power spectra of electric field corresponding to solutions shown in Figs. 14-17.

$S \subsetneq H$ into S such that

$$P(z) = F_{\tau(z)}(z) \in S \quad \text{for all } z \in S, \tag{19}$$

and S is transverse to the flow (i.e. $(\partial F_t(z)/\partial t)\big|_{\tau(z)}$ has a nonzero component with respect to η, the normal vector for H), where $\tau(z)$ is the smallest time $t > 0$ such that

$$F_{\tau(z)}(z) \in S \quad \text{and} \quad \operatorname{sgn}[(z\cdot\eta)(F_{\tau(z)}(z)\cdot\eta)] > 0. \tag{20}$$

Let z(0) be a point in S at t = 0, we are interested in the sequence of states z^{k+1} generated by

$$\begin{aligned} z^{k+1} &= P(z^k), \qquad k=0,1,2,\ldots, \\ z^0 &= z(0) \in S. \end{aligned} \tag{21}$$

If there exist a point z^0 and an integer $K \geq 0$ such that $z^K = z^0$, then z^0 corresponds to a periodic solution with period $\tau = \sum_{k=0}^{K} \tau(z^k)$. For non-periodic or chaotic oscillations, there do not exist such points.

First, we obtained numerically the points generated by Poincaré maps corresponding to various hyperplanes in the state space of system (4) with parameters given in (16) and $\Gamma = 2.0$ for various values of E_o^2. Figures 19-22 show the points generated by Poincaré maps for progressively higher values of E_o^2 and fixed damping coefficients $\gamma = 1.0$ and $\Gamma = 2.0$ along chaotic solutions. A notable feature of these results is that the points appear to lie along certain curves in $\mathbb{R}^3$, which implies that the Poincaré maps associated with chaotic solutions are one dimensional in nature. But the graphs of the Poincaré maps in terms of some curve parameter are not readily obtainable.

VI. CONCLUDING REMARKS

The results of this study show more clearly the onset or quenching of

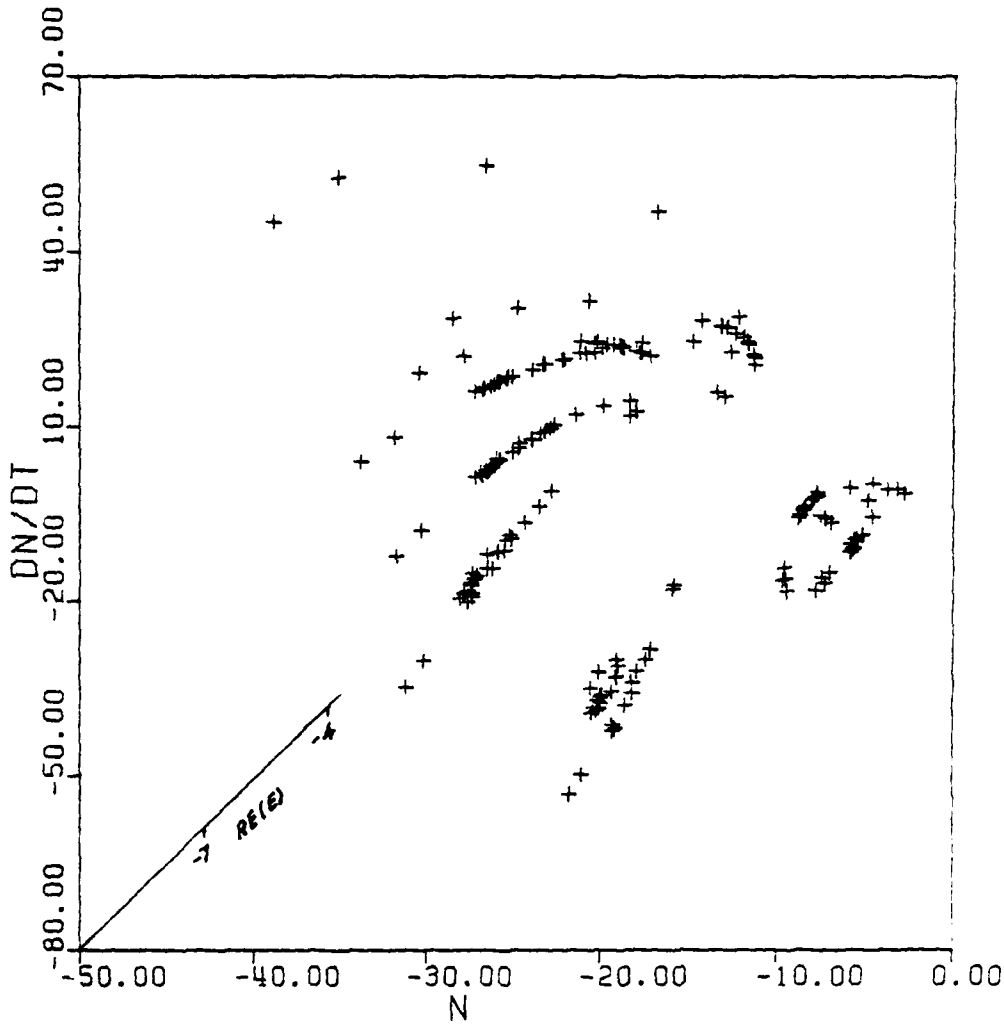
70.00
40.00
10.00
-20.00
-50.00
-80.00
DN/DT
-50.00
-40.00
-30.00
-20.00
-10.00
0.00
N
RE(E)

Fig.19a

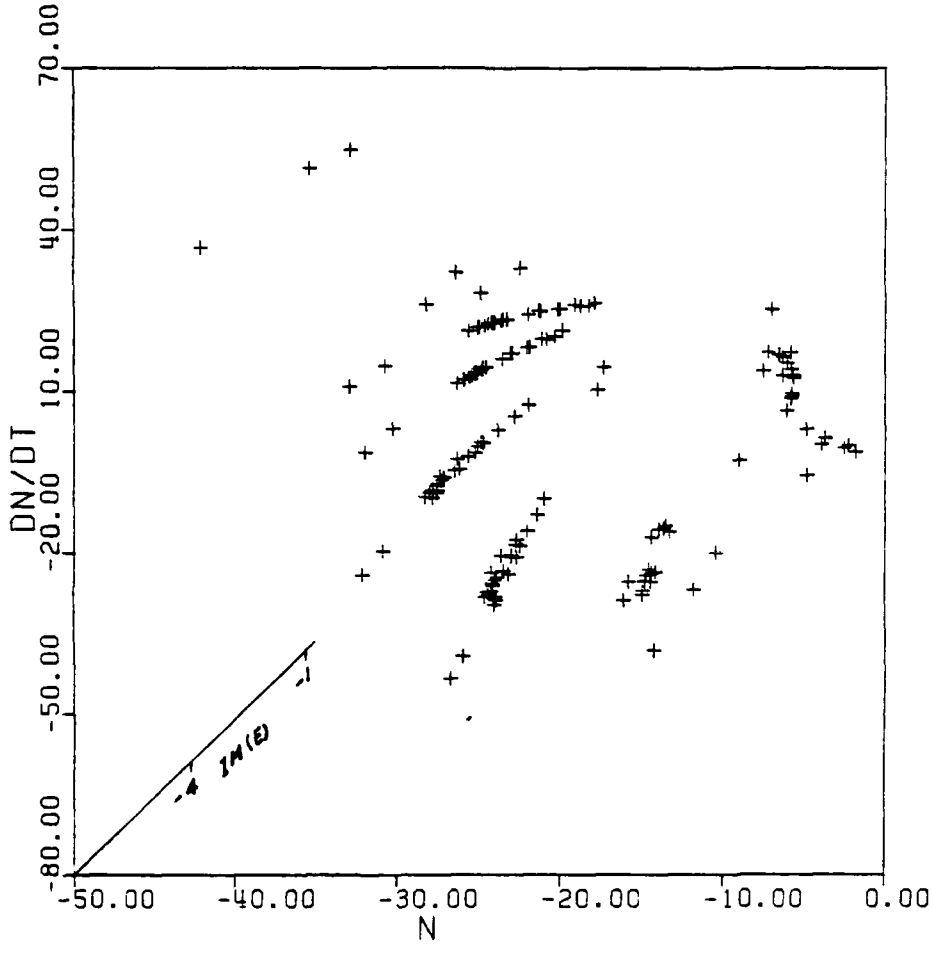
70.00
40.00
10.00
-20.00
-50.00
-80.00
DN/DT
-50.00
-40.00
-30.00
-20.00
-10.00
0.00
N
-4
IM(E)
-1

Fig.19b

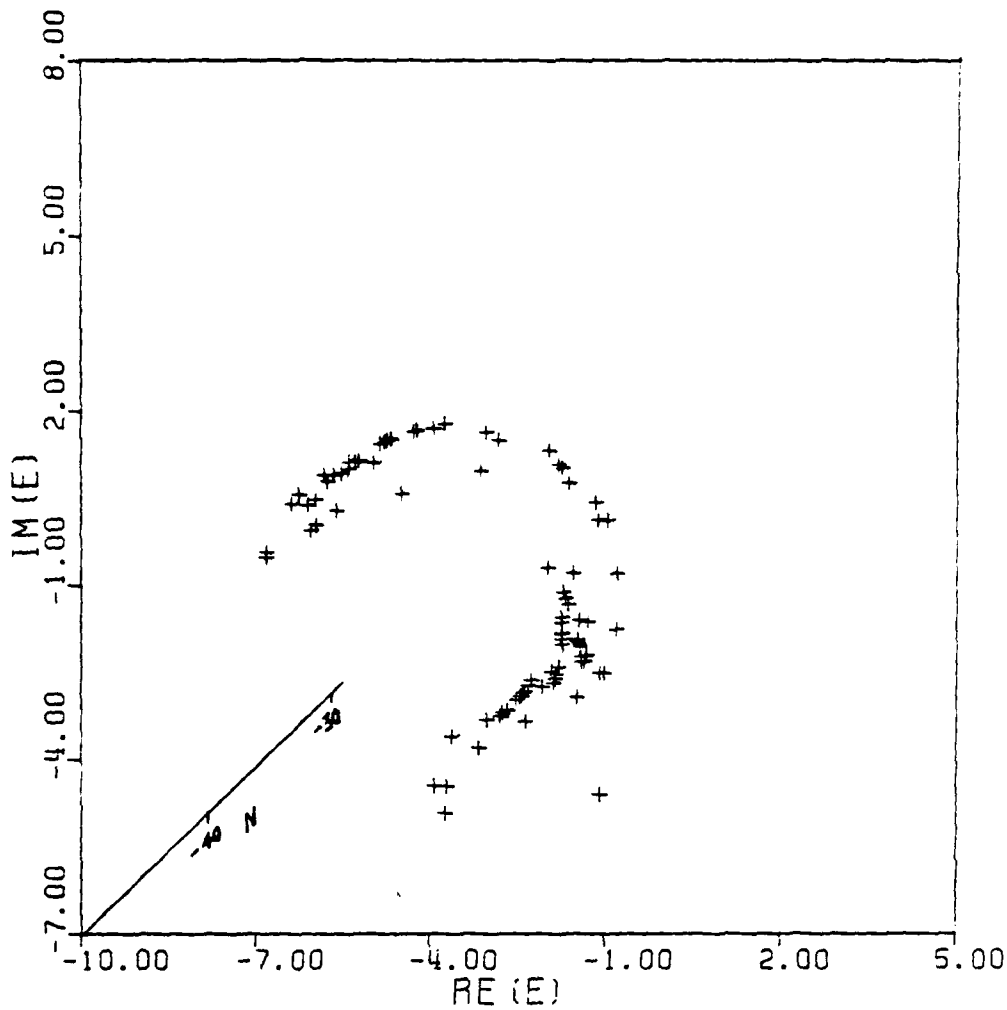

Fig.19c

Fig.19 Isometric representation of points generated by Poincaré maps onto the hyperplanes (a) $E_I = 0$; (b) $E_R = 0$; (c) $dn/dt = 0$. Angle of third axis is at 45^o; $E_o^2 = 1.625$.

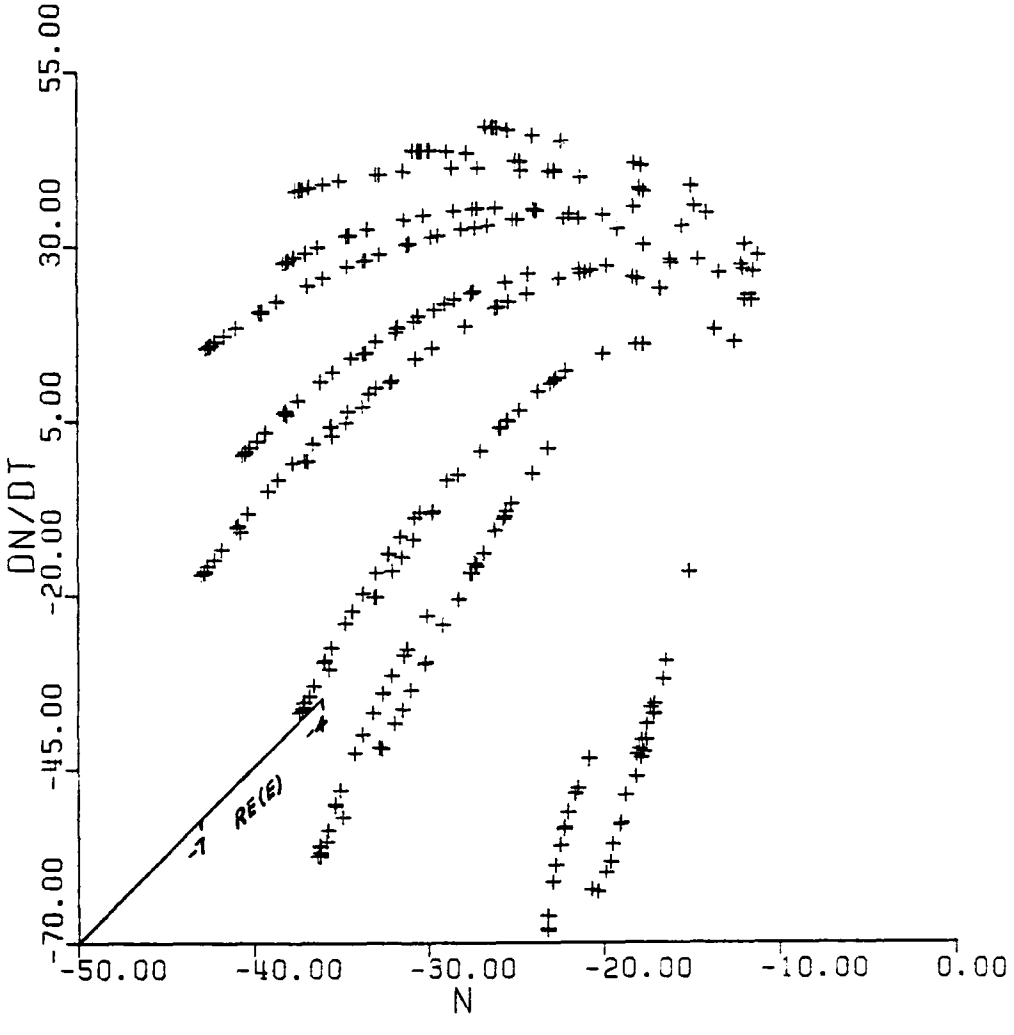
55.00
30.00
5.00
-20.00
-45.00
-70.00
DN/DT
-50.00
-40.00
-30.00
-20.00
-10.00
0.00
N
RE(E)

Fig.20a

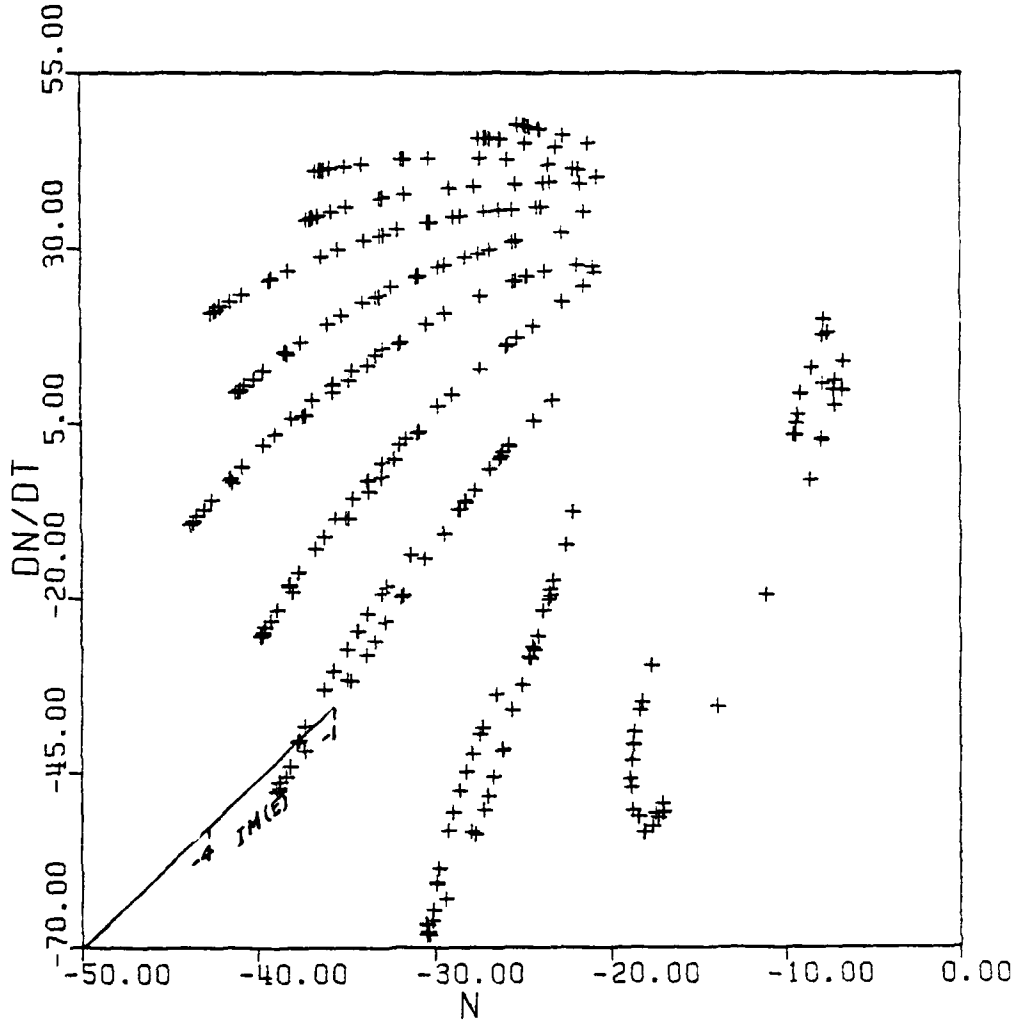
55.00
30.00
5.00
-20.00
-45.00
-70.00
DN/DT
-50.00
-40.00
-30.00
-20.00
-10.00
0.00
N
IM(E)

Fig.20b

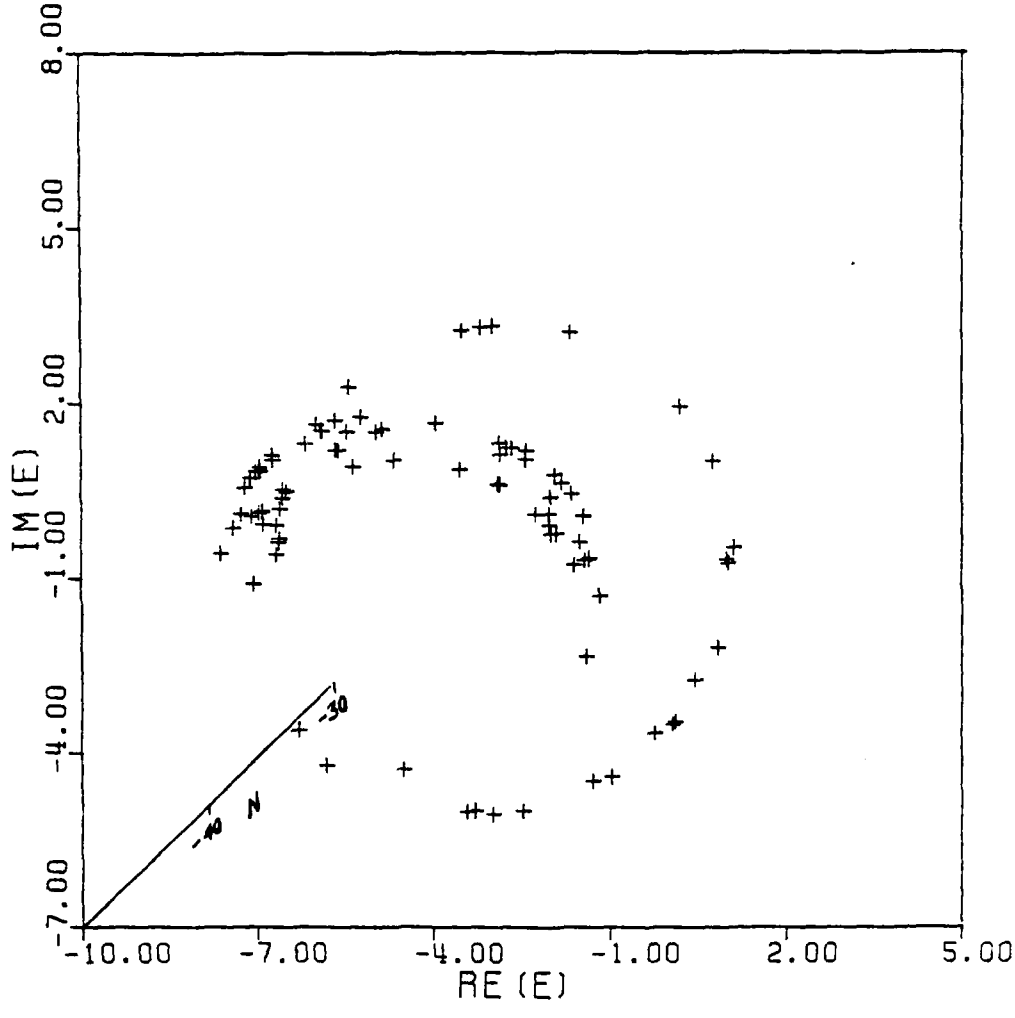

Fig.20c

Fig.20 Isometric representation of points generated by Poincaré maps onto the hyperplanes (a) $E_I = 0$; (b) $E_R = 0$; (c) $dn/dt = 0$. Angle of third axis is at 45^o; $E_o^2 = 2.669$.

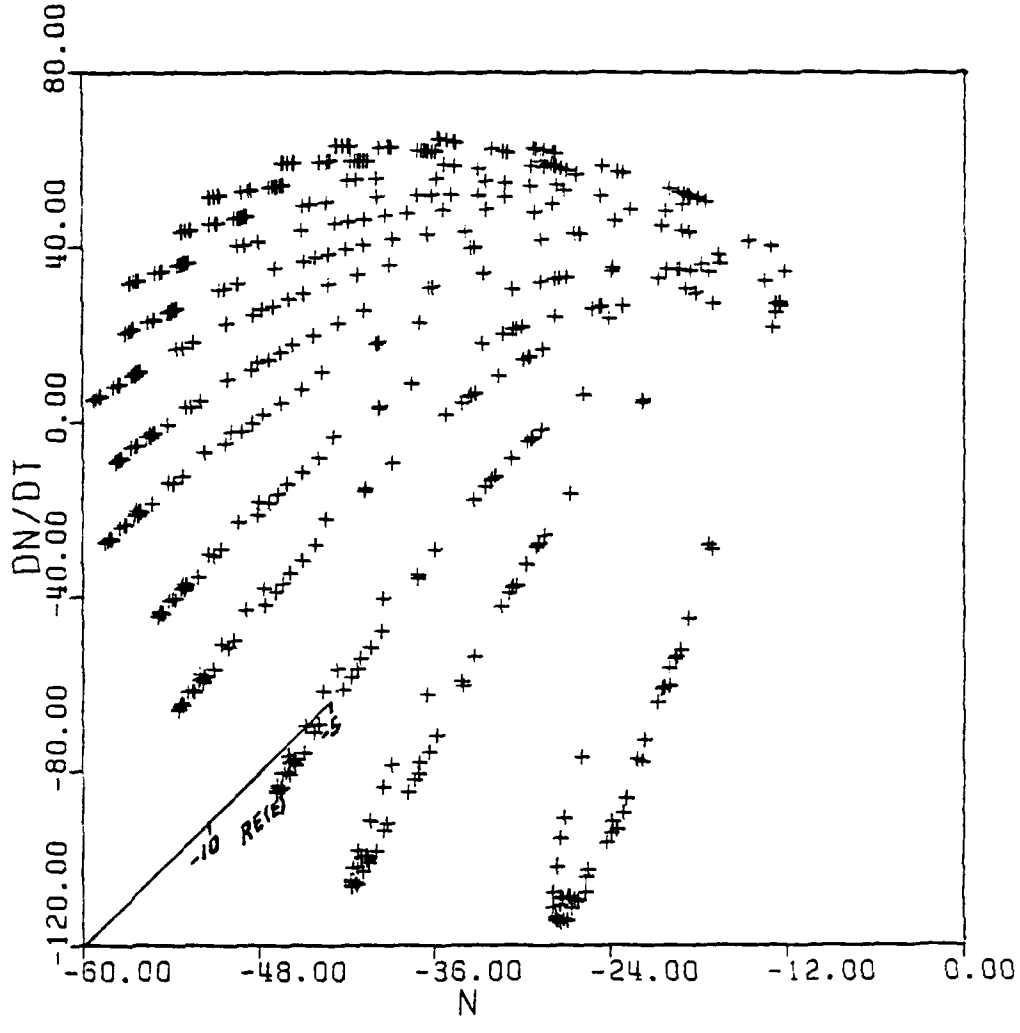
80.00
40.00
0.00
-40.00
-80.00
-120.00
DN/DT
-60.00
-48.00
-36.00
-24.00
-12.00
0.00
N
-10
RE(S)
S

Fig.21a

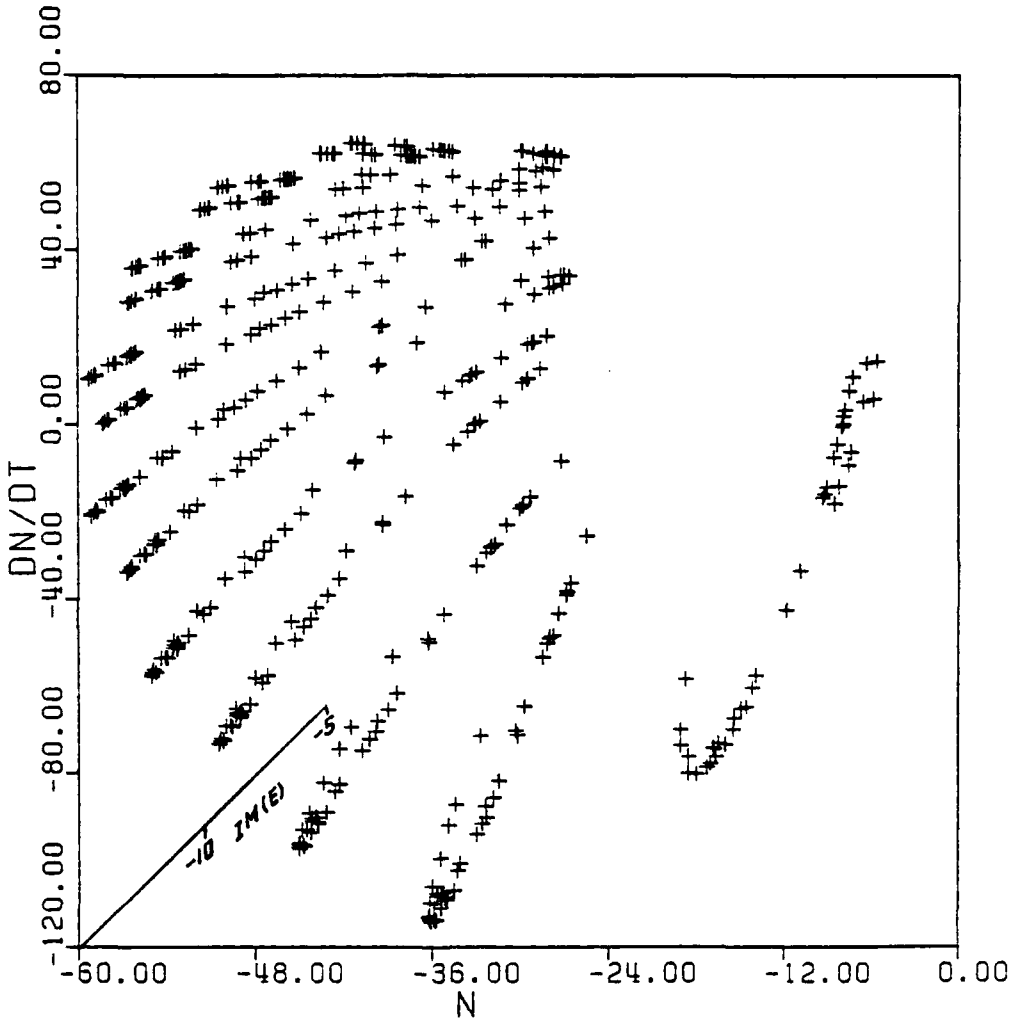
80.00
40.00
0.00
-40.00
-80.00
-120.00
DN/DT
-60.00
-48.00
-36.00
-24.00
-12.00
0.00
N
-5
-10
IM(E)

Fig.21b

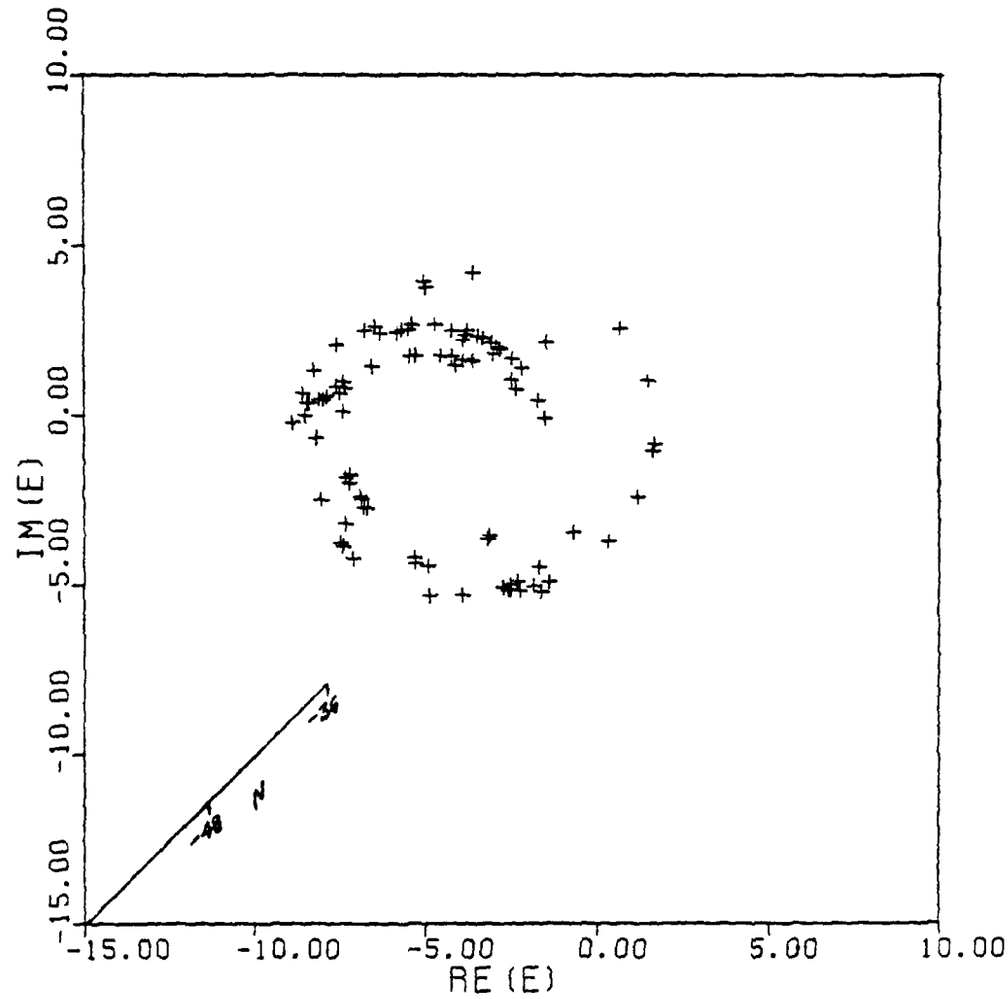

Fig.21c

Fig.21 Isometric representation of points generated by Poincaré maps onto the hyperplanes (a) $E_I = 0$; (b) $E_R = 0$; (c) $dn/dt = 0$. Angle of third axis is at 45^o; $E_o^2 = 5.05$

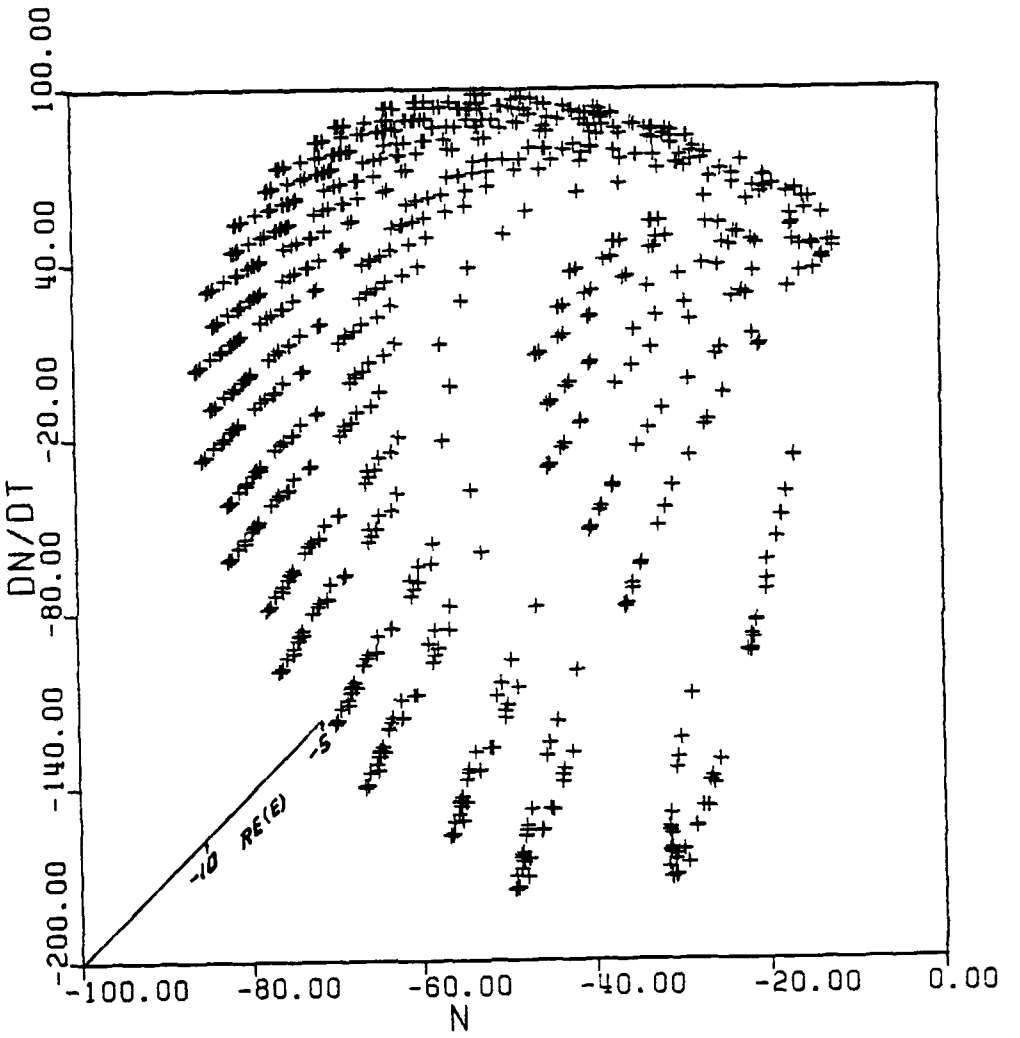
100.00
40.00
-20.00
-80.00
-140.00
-200.00
DN/DT
-100.00
-80.00
-60.00
-40.00
-20.00
0.00
N
-10
RE(E)
-5

Fig.22a

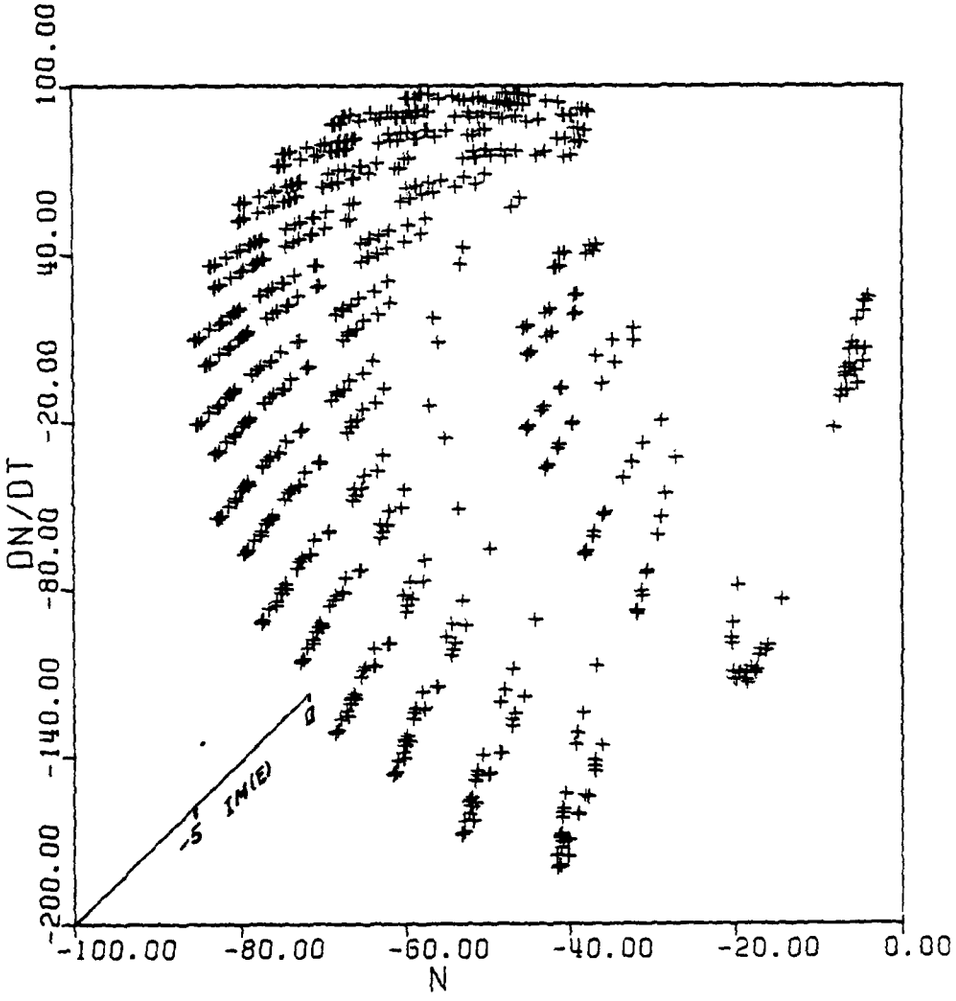
100.00
40.00
-20.00
-80.00
-140.00
-200.00
DN/DT
-100.00
-80.00
-60.00
-40.00
-20.00
0.00
N
IM(E)
.5
0

Fig.22b

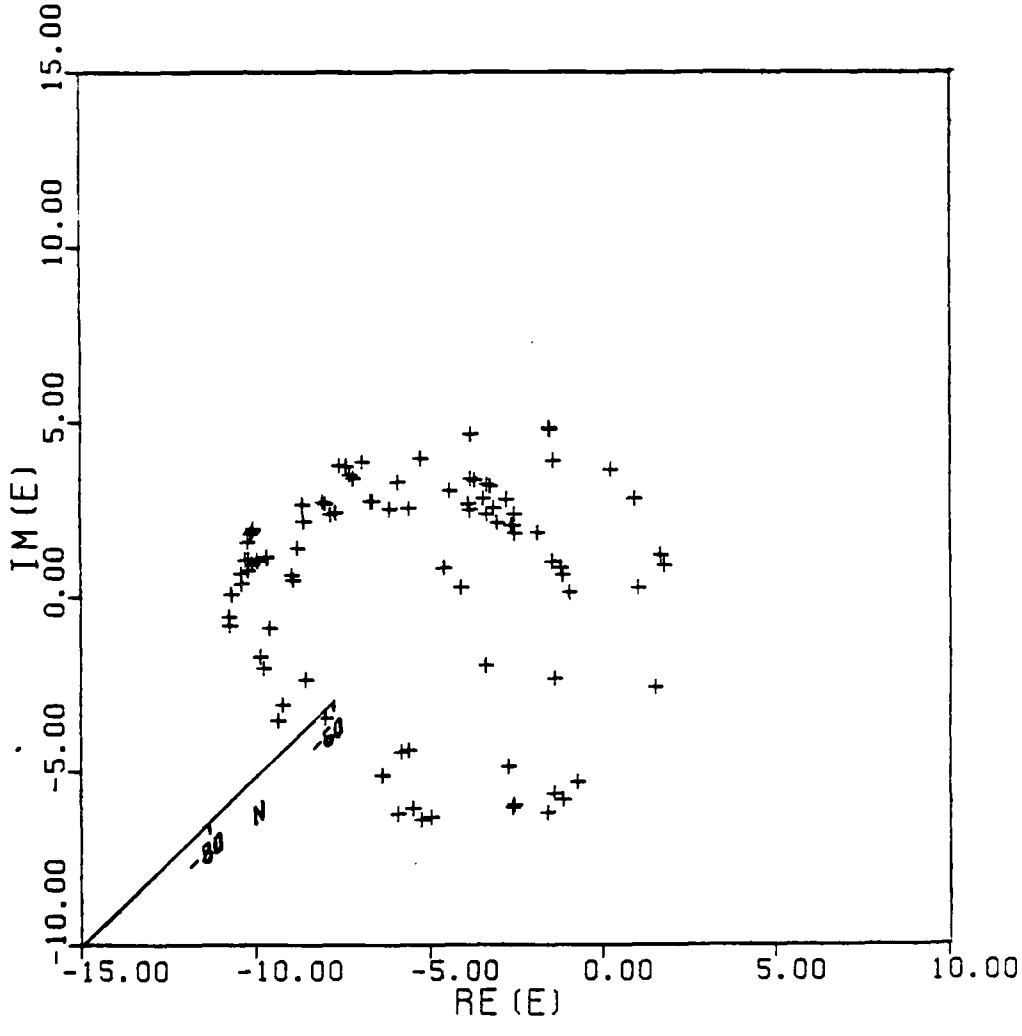

Fig.22c

Fig.22 Isometric representation of points generated by Poincaré maps onto the hyperplanes (a) $E_I = 0$; (b) $E_R = 0$; (c) $dn/dt = 0$. Angle of third axis is at 45^o; $E_o^2 = 10$.

chaotic oscillations for fixed E_o^2 and variable damping coefficient γ as compared to the case with fixed γ and variable E_o^2 studied earlier.[1] As γ is decreased from the Hopf bifurcation point $\hat{\gamma}$, the oscillatory solutions evolve from simple periodic to almost periodic solutions and to chaotic solutions. It is conjectured that the chaotic solutions appear after further bifurcation from the periodic solutions as γ decreases from $\hat{\gamma}$. The verification of this conjecture requires further study.

In this study, only the single mode model is considered. The existence of chaotic oscillations in a multiple-mode model is being investigated. The results will be reported in the near future.

REFERENCES

1. P.K.C.Wang, J. Math. Phys. 21, 398 (1980)
2. V.E.Zakharov, Zh.Eksp.Teor.Fiz. 62, 1745(1972) [Sov.Phys.JETP,35, 908 (1972)].
3. R.C.Davidson, Methods in Nonlinear Plasma Theory, Academic Press,N.Y. 1972.

APPENDIX C

CHAOTIC SOLUTIONS OF RESONANT THREE-WAVE INTERACTIONS*

Koshiro Masui and P.K.C. Wang

Department of System Science
University of California
Los Angeles, California 90024

*This research was supported by Air Force Grant AFOSR 79-0050

ABSTRACT

A numerical study is made on the chaotic solution of the nonlinear interaction of three positive-energy electrostatic waves in a plasma, where one wave is growing linearly and the remaining two are linearly damped. The reduction from the six-dimensional system to a three-dimensional system and bounds for the chaotic attractor are also discussed.

I. INTRODUCTION

In the conventional theory[1,2] of turbulence in plasmas, turbulence is described as the state in which a large number of collective degrees of freedom are strongly excited. The energy of the unstable modes is distributed to other modes by a nonlinear process and then dissipated through some form of damping mechanism. When the energy transfer between the modes is balanced, a stationary broad spectrum corresponding to stationary turbulence appears. If many collective degrees of freedom are excited simultaneously from the level of thermal fluctuation, the random character of the fluctuation is preserved to some extent. If only a small number of degrees of freedom are excited in the initial stage, there must be a randomization process by which the system goes into the turbulent state.

Recently, it has been proposed[3-5] that the turbulent state or chaotic behavior can arise in deterministic nonlinear models which have a small number of degrees of freedom. Particular examples of such models have been found in plasma physics[6-8]. In this paper, we consider a simplified model governing the nonlinear resonant interaction of three waves with both linear growth and damping rates:

$$\left.\begin{aligned} dA_1/dt &= \gamma_1 A_1 - iVA_2A_3 \\ dA_2/dt &= -\gamma_2 A_2 - iVA_1A_3^* \\ dA_3/dt &= -\gamma_3 A_3 - iVA_1A_2^* \end{aligned}\right\} , \tag{1.1}$$

where A_j's are normalized complex amplitudes of waves, V is real and γ_j's are positive numbers. System (1.1), without the growth or damping terms, has been thoroughly investigated. We shall show that, under certain

conditions on γ_j , the linear instability of the first wave could lead to a turbulence-like state without any additional assumption for randomization. A particular example in the form of system (1.1) will be studied in detail numerically.

II. DERIVATION OF BASIC EQUATIONS

We first consider three nonlinearly interacting oscillators whose equations of motion are given by

$$\left.\begin{aligned} \ddot{a}_1 - 2\gamma_1\dot{a}_1 + \omega_1^2 a_1 &= v a_2 a_3 \\ \ddot{a}_2 + 2\gamma_2\dot{a}_2 + \omega_2^2 a_2 &= v a_1 a_3 \\ \ddot{a}_3 + 2\gamma_3\dot{a}_3 + \omega_3^2 a_3 &= v a_1 a_2 \end{aligned}\right\} , \tag{2.1}$$

where v, γ_j's and ω_j's are real positive numbers. We assume that the linear damping on growth rates is small (i.e., $\gamma_j << \omega_j$) and the nonlinear coupling is small (i.e., $|a_1|v << \omega_2^2, \omega_3^2$) . Then we can express a_j in the form

$$a_j(t) = \{A_j(t)exp(i\omega_j t) + A_j^*(t)exp(-i\omega_j t)\}(v/\omega_j)^{1/2} , \tag{2.2}$$

where A_j is a slowly time-varying component. If the frequencies satisfy the resonance condition $\omega_1 = \omega_2 + \omega_3$, then substituting (2.2) into (2.1) leads to equations of the form (1.1), with $V = (v^3/4\omega_1\omega_2\omega_3)^{1/2}$.

We can also derive equations in the form of (1.1) for the nonlinear wave-wave interaction in a one-dimensional plasma involving two plasma waves

(denoted by subscripts 1 and 3) and an ion-acoustic wave (denoted by subscript 2). We assume that the resonance conditions for both the wave numbers (i.e., $k_1 = k_2 + k_3$) and the frequencies are satisfied. Here, the pair (ω_j, k_j) satisfies the linear dispersion relation associated with the j-th wave. We assume that the first plasma wave is excited by some external force and has a linear growth rate γ_1. The second plasma wave and the ion-acoustic wave are excited by the first plasma wave through nonlinear coupling and have linear damping rates γ_2 and γ_3, respectively. We also assume that $\gamma_j << \omega_j$ and that the nonlinear coupling of waves produces small shifts in frequency from the linear values. Moreover, the resonant interaction between waves and particles is negligible. Then, the equations for the interacting waves are described by (1.1). The amplitudes A_j and the parameter V are defined as follows[9]:

$$A_j(t) = \left| \left(\frac{k_j^2}{8\pi} \right) \left(\frac{\partial \mathrm{Re}\, \varepsilon^{(1)}(k)}{\partial \omega} \Big|_{k_j} \right) \right|^{1/2} \phi_j(t) , \quad j = 1,2,3, \tag{2.3}$$

$$V = - \frac{k_1^2}{8\pi} \varepsilon^{(2)}(k_1, k_2, k_3) \Bigg/ \left| \prod_{j=1}^{3} \left(\frac{k_j^2}{8\pi} \right) \left(\frac{\partial \mathrm{Re}\, \varepsilon^{(1)}(k)}{\partial \omega} \Big|_{k_j} \right) \right|^{1/2} . \tag{2.4}$$

Here, the parameter V is real, ϕ_j is the slowly varying component of the electrostatic potentional of the j-th wave, and $\varepsilon^{(1)}$ and $\varepsilon^{(2)}$ are the first and second order dielectric constants obtained from the Vlasov-Poisson equations.

In order to obtain explicit expressions for the variables and parameters, we consider the following simple model: weak electron beams are injected into both sides of an infinite plasma slab with thickness L.

We assume that there exist two eigen-modes of the plasma waves and one eigen-mode of the ion-acoustic wave, and that the velocity of the beam in the positive (resp., negative) direction is between the phase velocities of the two plasma waves propagating in the positive (resp., negative) direction. We also assume that the interaction between the beam and the fast plasma wave can be neglected. Then, it is sufficient to consider the system consisting of the beam in the positive direction, the plasma wave '1' and the ion-acoustic wave '2' traveling in the positive direction and the plasma wave '3' traveling in the negative direction.

We further assume that: (i) the electrons and ions in the plasma and the electrons in the beam have time-independent Maxwell velocity distributions in the zero-th order, (ii) the Landau damping of wave '2' is negligible as compared to the damping due to Coulomb collisions, but the Landau growth rate of wave '1' due to the beam is larger than the collision damping rate, and (iii) the plasma is nonisothermal so that the Landau damping of the ion-acoustic wave is negligible. Then, the amplitudes A_j, the parameter V and the damping on growth rates γ_j are expressed explicitly as follows:

$$A_j = \left[\frac{k_j^2}{8\pi}\,\frac{2}{\omega_{pe}}\right]^{1/2}\phi_j,\ j=1,3,\quad A_2 = \left[\frac{k_2^2}{8\pi}\,\frac{2\omega_{pi}^2}{k_2^3 c_s^3}\right]^{1/2}\phi_2\ , \tag{2.5}$$

$$V = \frac{1}{8\pi}\,\frac{\omega_{pe}^2}{v_{T_c}^2}\,\frac{c}{m_c}\,\frac{k_3}{\omega_{pe}c_s}\Bigg/\left\{\frac{|k_1k_2k_3|}{|4\pi k_2 c_s|^{3/2}}\left[\frac{m_c}{m_i}\right]\right\}^{1/2}\ , \tag{2.6}$$

$$\gamma_1 = -\gamma_{col} + \sqrt{\pi}\,\omega_{pe}\left[\frac{v_d - \omega_{pe}/k_1}{v_{T_b}}\right]\left[\frac{\omega_{pb}/k_1}{v_{T_b}}\right]^2 exp\left\{-\left[\frac{v_d - \omega_{pe}/k_1}{v_{T_b}}\right]^2\right\}\ , \tag{2.7}$$

$$\gamma_2 = \left(\frac{\pi}{8}\,\frac{m_e}{m_i}\right)^{1/2} k_2 c_s \ , \quad \gamma_3 = \gamma_{col} \ . \tag{2.8}$$

Here, γ_{col} is the collisional damping rate, m_e (resp., m_i) is the electron (resp., ion) mass, e is the electron charge, ω_{pe} (resp., ω_{pi},ω_{bi}) is the electron (resp., ion, beam) plasma frequency, v_{T_e} (resp., v_{T_b}) is the electron thermal velocity of plasma (resp., beam), c_s is the sound velocity of plasma and v_d is the beam velocity.

It can be shown that, if $A_1 = A_2 = 0$ at the initial time, then $|A_1(t)| \to \infty$ as $t \to \infty$. Hence, the solution of (1.1) is not uniformly bounded with respect to the set of initial conditions whose closure includes the set such that $A_1 = A_2 = 0$. Thus, the assumptions made in the derivation of (1.1) may be violated in some cases. Such a situation will be discussed in Section 4.

III. ANALYSIS OF THE SIMPLIFIED MODEL

We eliminate the parameter V from (1.1) by setting $X_j = -VA_j$ $(j=1,2,3)$:

$$\left.\begin{aligned} \dot{X}_1 &= \gamma_1 X_1 + iX_2X_3 \\ \dot{X}_2 &= -\gamma_2 X_2 + iX_1X_3^* \\ \dot{X}_3 &= -\gamma_3 X_3 + iX_1X_2^* \end{aligned}\right\} \ . \tag{3.1}$$

The time derivative of $\xi = \frac{1}{2}\{2X_1X_1^* + X_2X_2^* + X_3X_3^*\}$ is given by $\dot{\xi} = 2\gamma_1 X_1X_1^* - \gamma_2 X_2X_2^* - \gamma_3 X_3X_3^*$. Hence,

$$\dot{\xi}(t) \le \xi(0)\exp[2\ max\{\gamma_1,\gamma_2,\gamma_3\}|t|] \ , \quad t \in (-\infty,\infty) \ . \tag{3.2}$$

Therefore, the integral curve of (3.2) exists for all $t \in (-\infty,\infty)$.

Setting $X_j = r_j e^{i\theta_j} (j=1,2,3)$, with positive r_j , (3.1) becomes

$$\left.\begin{aligned} \dot{r}_1 + i\dot{\theta}_1 r_1 &= \gamma_1 r_1 + i r_2 r_3 e^{-i(\theta_1-\theta_2-\theta_3)} \\ \dot{r}_2 + i\dot{\theta}_2 r_2 &= -\gamma_2 r_2 + i r_1 r_3 e^{i(\theta_1-\theta_2-\theta_3)} \\ \dot{r}_3 + i\dot{\theta}_3 r_3 &= -\gamma_3 r_3 + i r_1 r_2 e^{i(\theta_1-\theta_2-\theta_3)} \end{aligned}\right\} \quad . \tag{3.3}$$

Taking the time derivative of $\eta = \mathrm{Re}(X_1 X_2^* X_3^*) = r_1 r_2 r_3 \cos(\theta_1-\theta_2-\theta_3)$, we have

$$\dot{\eta} = -(r_2 + r_3 - \gamma_1)\eta \quad . \tag{3.4}$$

Hence, if $\gamma_1 < \gamma_2 + \gamma_3$, $\eta(t) \to 0$ as $t \to \infty$.

Let $Y = (X_1, X_2, X_3)$, then the set $\Sigma = \{Y : \eta = 0\}$ is an invariant set in the sense that, if $Y(0) \in \Sigma$, then its corresponding full orbit is contained in Σ ; i.e., $Y(t) \in \Sigma$ for all $t \in (-\infty,\infty)$. The subset $\Sigma_0 = \{Y : r_j = r_k = 0,\ j \neq k,\ j,k \in \{1,2,3\}\}$ of Σ is also an invariant set.

We shall show that, if $\gamma_2 \neq \gamma_3$, the subset $\Sigma_\nu = \{Y: \cos(\theta_1-\theta_2-\theta_3) = 0, \sin(\theta_1-\theta_2-\theta_3) = \nu\} - \Sigma_0$, $\nu = 1,-1$, of Σ is an invariant set, in this case, in the sense that, if $Y(0) \in \Sigma_\nu$, then $Y(t) \in \Sigma_\nu$ for almost all $t \in (-\infty,\infty)$. Assume that $Y(0) \in \Sigma_\nu$. Since (3.1) has a unique solution for each initial condition, $Y(t) \in -\Sigma_0$ for all $t \in (-\infty,\infty)$. Hence, at any t, at most one of the $r_j(t)$'s is zero. Furthermore, all of the $r_j(t)$'s are non-zero for almost all $t \in (-\infty,\infty)$. For, if $\gamma_2 \neq \gamma_3$, Eq.(3.1) does not have a solution such that one of the $X_j(t)$'s is identically zero on some interval in $-\Sigma_0$. Since $\eta(t) = 0$ for all $t \in (-\infty,\infty)$, it follows that

$\cos(\theta_1(t) - \theta_2(t) - \theta_3(t)) = 0$ for almost all $t \in (-\infty,\infty)$. Moreover, $\sin(\theta_1(t) - \theta_2(t) - \theta_3(t)) = \nu$ for almost all $t \in (-\infty,\infty)$. For, if $\sin(\theta_1(t) - \theta_2(t) - \theta_3(t))$ has a discontinuity at t_1, then $r_j(t_1)r_k(t_1) = 0$, $j \neq k$, $j,k \in \{1,2,3\}$, since the real parts of the right-hand sides of Eq. (3.3) are continuous. This implies that $Y(t_1) \in \Sigma_0$, which is a contradiction. Hence, Σ_ν is an invariant set, in the sense defined above.

In what follows, we consider the behavior of $Y(t)$ with $Y(0) \in \Sigma_\nu$, where $\nu = 1$ or -1. For t such that $Y(t) \in \Sigma_\nu$, (3.3) reduces to

$$\left.\begin{aligned} \dot{r}_1 + i\dot{\theta}_1 r_1 &= \gamma_1 r_1 + \nu r_2 r_3 \\ \dot{r}_2 + i\dot{\theta}_2 r_2 &= -\gamma_2 r_2 - \nu r_1 r_3 \\ \dot{r}_3 + i\dot{\theta}_3 r_3 &= -\gamma_3 r_3 - \nu r_1 r_2 \end{aligned}\right\} . \tag{3.5}$$

Since $\|X_j(t)\|$ is finite at finite t, the integral curve of (3.5) for t such that $Y(t) \in \Sigma_\nu$ is identical to that of (3.4) for $t \in (-\infty,\infty)$. Hence, we can assume that Eq. (3.5) holds for $t \in (-\infty,\infty)$.

As mentioned earlier, all of the $r_j(t)$'s are non-zero for almost all $t \in (-\infty,\infty)$. Hence, $\dot{\theta}_j(t) = 0$ for almost all t except when $r_j(t) = 0$. Since $X_j(t)$ is continuously differentiable at all t, $\theta_j(t) = \theta_j(0) + \pi n_j(t)$. Here, $n_j(t)$ is an integer-valued step function which has discontinuities when $r_j(t) = 0$. Let $x_j(t) = \nu X_j e^{-i\theta_j(0)} = \nu r_j e^{i\pi n_j(t)}$, $j = 1,2,3$. Then, x_j is real and (3.5) reduces to

$$\left.\begin{aligned} \dot{x}_1 &= \gamma_1 x_1 - x_2 x_3 \\ \dot{x}_2 &= -\gamma_2 x_2 + x_1 x_3 \\ \dot{x}_3 &= -\gamma_3 x_3 + x_1 x_2 \end{aligned}\right\} . \tag{3.6}$$

The assumption that $\gamma_1 < \gamma_2 + \gamma_3$ also leads to

$$\frac{\partial \dot{x}}{\partial x} + \frac{\partial \dot{y}}{\partial y} + \frac{\partial \dot{z}}{\partial z} = -(\gamma_2 + \gamma_3 - \gamma_1) < 0 , \tag{3.7}$$

which means that the phase volume shrinks uniformly. The Lorenz system also has this property[3].

The equilibrium points of system (3.6) are easily obtainable. If $\gamma_1 < 0$, the origin P_0 is the unique equilibrium point and it is asymptotically stable in the large. If $\gamma_1 > 0$, the equilibrium points are P_0 and $P^{\nu}_{\sigma,\mu} = (\sigma(\gamma_2\gamma_3)^{1/2}, \mu(\gamma_1\gamma_3)^{1/2}, \nu(\gamma_1\gamma_2)^{1/2})$, $(\sigma,\mu,\nu) \in \Omega \triangleq \{(1,1,1), (1,-1,-1),(-1,-1,1),(-1,1,-1)\}$. The point P_0 is a stable node in the (y,z)-plane and a saddle point in a plane containing the x-axis. At $P^{\nu}_{\sigma,\mu}$, the characteristic polynomial of the linearized vector field of (3.6) is $f(\lambda) = \lambda^3 + \lambda^2(\gamma_2 + \gamma_3 - \gamma_1) + 4\gamma_1\gamma_2\gamma_3 = 0$. Since the polynomial has one negative root and a pair of complex roots, $f(\lambda) = (\lambda + c)\{\lambda - (a + ib)\}\{\lambda - (a - ib)\}$ where $c > 0$. By comparing the coefficients of polynomials, we have

$$2a - c = -(\gamma_2 + \gamma_3 - \gamma_1) , \quad a^2 + b^2 = 2ac , \tag{3.8a}$$

$$c(a^2 + b^2) = 4\gamma_1\gamma_2\gamma_3 . \tag{3.8b}$$

Eq.(3.8b) implies that $a > 0$. Hence, at each $P^{\nu}_{\sigma,\mu}$, $(\sigma,\mu,\nu) \in \Omega$, there is a bistable plane in which $P^{\nu}_{\sigma,\mu}$ is an unstable focus.

Eq.(3.6) is invariant to the interchange of subscripts 2 and 3. Hence, without loss of generality, we assume that $\gamma_2 < \gamma_3$. Let $X = (x,y,z) = (x_1,x_2,x_3)$. The time derivative of $\alpha(t) \triangleq y(t)/z(t)$ is given by

$$\dot{\alpha} = (\gamma_3 - \gamma_2)\alpha + x(1 - \alpha^2) \quad , \tag{3.9}$$

which is equal to $\mu(\gamma_3 - \gamma_2)$ at $y = \mu z$, $\mu = 1, -1$. Since $\gamma_2 < \gamma_3$, the set $\Gamma = \{X : |y| \geq |z|\}$ is a positive invariant set; namely, if $X(\hat{t}) \in \Gamma$ at some $\hat{t}$, then $X(t) \in \Gamma$ for all $t \geq \hat{t}$.

We shall show that Γ is an attractor in the sense that, for any initial point X_0 , $X(t)$ converges to Γ as $t \to \infty$ (i.e., $\lim\inf_{t\to\infty} \|X(t) - \hat{X}\| = 0$) . Since Γ is a positive invariant set, it is enough to show that, if $X(t) \in -\Gamma$ for all $t \in [0,\infty)$, $X(t)$ converges to Γ as $t \to \infty$. Let $\beta(t) = y^2(t) - z^2(t)$, then the time derivative of β is given by

$$\dot{\beta} = 2(\gamma_3 z^2 - \gamma_2 y^2) = 2(\gamma_3 - \gamma_2)z^2 - 2\gamma_2\beta \ . \tag{3.10}$$

If $X(t) \in -\Gamma$ for all $t \in [0,\infty)$, then $|y(t)| < |z(t)|$ (or $\beta(t) < 0$) and $|y(t)| < (\gamma_3/\gamma_2)^{1/2}|z(t)|$ (or $\dot{\beta}(t) > 0$) for all $t \in [0,\infty)$. Hence, $\beta(t) \to 0$ as $t \to \infty$. For, if there is a $\beta_\infty < 0$ such that $\beta(t) \to \beta_\infty$ as $t \to \infty$, then $\dot{\beta}(t) \geq -2\gamma_2\beta_\infty > 0$ from (3.10), since $-\beta(t) \leq z^2(t)$. This implies that $\beta(t)$ does not converge as $t \to \infty$, which is a contradiction. Thus, $X(t)$ converges to $\partial\Gamma \subset \Gamma$ as $t \to \infty$. Hence, Γ is an attractor.

If $X(\hat{t}) \in \Gamma$ for some $\hat{t}$, the X-trajectory is trapped in $\Gamma_+ = \Gamma \cap \{X : y > 0\}$ or $\Gamma_- = \Gamma \cap \{X : y < 0\}$ for $t \geq \hat{t}$. Only this case was observed in the computer experiment and some numerical results for such a trajectory will be presented in the next section. The set Γ_+ (resp., Γ_-) has three equilibrium points P_0 , $P^{1}_{1,1}$, and $P^{-1}_{-1,1}$ (resp., P_0 , $P^{1}_{-1,-1}$ and $P^{-1}_{1,-1}$) and the combination of these points is identical to that of the standard Lorenz attractor[3].

We shall determine the behavior of the trajectories such that $X(t) \in -\Gamma$ for all $t \in [0,\infty)$. Since Eq.(3.6) is invariant to changing the signs of any two of the three variables, it is sufficient to consider the set such that $z > 0$. Let $W_{\sigma,\mu} = \{X : |\sigma x| = \sigma x,\ |\mu y| = \mu y,\ z > 0\} - W$, $\sigma,\mu \in \{-1,0,1\}$. Here, $W = \bigcup_{(\sigma,\mu,\nu)\in\Omega} \{P^{\nu}_{\sigma,\mu}\} \cup \{x,y,z\text{-axis}\}$. The set W is the invariant set and the X-trajectory with $X_0 \notin W$ does not hit W in finite time. In what follows, the trajectory in W will be disregarded. Consider the following sets (see Figure 1):

$$\left.\begin{aligned} S &= \{X : \dot{\alpha} = 0\} \cap (W_{0,0} - \Gamma) \\ W_1 &= \{X : \dot{\alpha} > 0\} \cap (W_{0,0} - \Gamma) \\ W_2 &= \{X : \dot{\alpha} < 0\} \cap (W_{0,0} - \Gamma) \end{aligned}\right\} \quad . \tag{3.11}$$

We assume that $X(\tau_0) \in S \cap W_{1,0}$ at some τ_0. In $W_{\sigma,\mu}$, $(\sigma,\mu) = (1,-1),(-1,1)$,

$$|\dot{x}| = \sigma\dot{x} \quad , \quad |\dot{y}| = \sigma\dot{y} \quad , \quad \dot{z} < 0 \quad . \tag{3.12}$$

Hence, the X-trajectory is transverse to S and enters $W_1 \cap W_{1,-1}$. In $W_1 \cap W_{1,-1}$, $-1 < \alpha < 0$, $\dot{\alpha} > 0$, $x > 0$ and $\dot{x} > 0$. Hence, from (3.9), $\dot{\alpha}$ increases. Thus, the X-trajectory enters $W_1 \cap W_{1,1}$ in finite time. Let $X(\tau_1) \in (x,z)\text{-plane} \cap W_{1,0}$ and $X(\tau_1 + \varepsilon) \in W_1 \cap W_{1,1}$, where $X(\tau) \in W_1 \cap W_{1,1}$ for all $\tau \in [\tau_1, \tau_1 + \varepsilon]$. In $W_1 \cap W_{1,1}$, $0 < \alpha < 1$, $\dot{\alpha} > 0$ and $x > 0$. Hence, from (3.9) if $X(\tau) \in W_1 \cap W_{1,1}$ for all $\tau \in [\tau_1 + \varepsilon, t]$,

$$\dot{\alpha}(t) \geq (\gamma_3 - \gamma_2)\alpha(t) \geq (\gamma_3 - \gamma_2)\alpha(\tau_1 + \varepsilon) > 0 \ . \tag{3.13}$$

This implies that the X-trajectory enters $W_1 \cap W_{-1,1}$ in finite time, since it is transverse to the (y,z)-plane. Let $X(\tau_2) \in (y,z)\text{-plane} \cap W_{0,1}$ and $X(\tau_2 + \varepsilon) \in W_1 \cap W_{-1,1}$ where $X(\tau) \in W_1 \cap W_{-1,1}$ for all $\tau \in [\tau_2, \tau_2 + \varepsilon]$. In $W_1 \cap W_{-1,1}$, $x < 0$, $\dot{x} < 0$, $y > 0$, $\dot{y} < 0$, $z > 0$ and $\dot{z} < 0$. Hence, if $X(\tau) \in W_1 \cap W_{-1,1}$ for all $\tau \in [\tau_2 + \varepsilon, t]$,

$$\left.\begin{aligned} \dot{x}(t) &\leq \gamma_1 x(\tau_2 + \varepsilon) < 0 \\ \dot{y}(t) &\leq -\gamma_2 y(t) \\ \dot{z}(t) &\leq -\gamma_3 z(t) \end{aligned}\right\} \quad . \tag{3.14}$$

Consequently, if $X(t) \in W_1 \cap W_{-1,1}$ for all $t \in [0,\infty)$, then $x(t) \to -\infty$, $y(t) \to 0$ and $z(t) \to 0$ as $t \to \infty$. Otherwise, the X-trajectory hits $S \cap W_{-1,0}$ in finite time. Similarly, if $X(\tau_0) \in S \cap W_{-1,0}$ at some τ_0, the X-trajectory converges monotonically to the x-axis ($x(t) \to \infty$) as $t \to \infty$ or hits $S \cap W_{1,0}$ in finite time. Thus, if $X(t) \in W_{0,0} - \Gamma$ for all $t \in [0,\infty)$, then as $t \to \infty$, the X-trajectory converges to the x-axis monotonically after some oscillation about the z-axis, or oscillates about the z-axis for all $t \in [0,\infty)$ (i.e., for any large $\hat{t}$, there exist t_1 and t_2 such that $t_2 > t_1 > \hat{t}$, $X(t_1), X(t_2) \in (x,y)$-plane and the X-trajectory for $\tau \in [t_1, t_2]$ circles the z-axis).

Let us see roughly how the trajectory oscillating about the z-axis for all $t \in [0,\infty)$ behaves. Integrating (3.10),

$$0 < \int_0^\infty z^2(t)dt = \frac{1}{2(\gamma_3 - \gamma_2)} \left[-\beta(0) + 2\gamma_2 \int_0^\infty \beta(t)dt \right] < \infty \quad . \tag{3.15}$$

The second inequality holds since $\beta(t) < 0$. Likewise, $\int_0^\infty y^2(t)dt < \infty$.

By studying carefully the vector field of (3.6), we know that $y(t)$ (resp., $z(t)$) takes a larger value than $(\gamma_1\gamma_3)^{1/2}$ (resp., $(\gamma_1\gamma_2)^{1/2}$) at each time when the X-trajectory encircles the z-axis. Hence, $y^2(t) \not\to 0$ and $z^2(t) \not\to 0$ as $t \to \infty$. Therefore, for any small $\varepsilon > 0$, the time duration for which $y^2(t) > \varepsilon$ (resp., $z^2(t) > \varepsilon$) converges to zero as $t \to \infty$. Thus, $y^2(t)$ (resp., $z^2(t)$) behaves as a train of pulses whose heights are larger than $\gamma_1\gamma_3$ (resp., $\gamma_1\gamma_2$) and whose widths converge to zero as $t \to \infty$.

The X-trajectory, which is in $W_1 \cap W_{-1,1}$ or $W_2 \cap W_{1,-1}$ for all $t \in [t_1,\infty)$ for some t_1 and converges to the x-axis monotonically, is unstable in the sense that any small perturbation of α can shift X into Γ or cause X to oscillate about the z-axis. For $\dot{\alpha} = \mu(\gamma_3 - \gamma_1)$, $(|y| = \mu y)$ on $\partial\Gamma$ and the X-trajectory is transverse to S, and $\partial\Gamma$ and S approach each other as $|x| \to \infty$. The X-trajectory which oscillates about the z-axis for all $t \in [0,\infty)$ is also unstable in the sense that X is shifted into Γ by any small perturbation of α. For $\dot{\alpha} = \mu(\gamma_3 - \gamma_2)$, $(|y| = \mu y)$ on $\partial\Gamma$ and $X(t)$ converges to $\partial\Gamma$ as $t \to \infty$. Hence, from the practical standpoint, the X-trajectory which remains in $-(W \cup \Gamma)$ for all $t \in [0,\infty)$ can be disregarded. In fact, such trajectories were not observed in the computer experiment.

IV. NUMERICAL EXPERIMENT

In the numerical experiment, we used the system:

$$\left.\begin{aligned} \dot{x} &= \gamma_1 x - yz \\ \dot{y} &= -\gamma_2 y + zx \\ \dot{z} &= -z + xy \end{aligned}\right\} \quad , \tag{4.1}$$

which is obtained from (3.6) by the substitution:

$$\left.\begin{aligned} &\gamma_3 t \to t \ , \quad \gamma_j/\gamma_3 \to \gamma_j \ , \quad \text{for} \quad j = 1,2,3 \\ &x_1/\gamma_3 \to x \ , \quad x_2/\gamma_3 \to y \ , \quad x_3/\gamma_3 \to z \end{aligned}\right\} \tag{4.2}$$

We set plasma density $n_0 = 1.62 \times 10^7 (/cm^3)$, beam density $n_b = 1.85 \times 10^4$ $(/cm^3)$, plasma electron temperature $T_e = 0.25$ (eV), beam electron temperature $T_b = 0.033$ (eV) , $m_i = 1.16 \times 10^{-23}$(g), ($Li$ ion), $L = 100$ (cm) , $2\pi L/k_1 = 7$, $2\pi L/k_2 = 13$ and $2\pi L/|k_3| = 6$. Then $\gamma_j << \omega_j$ in (3.6) and $\gamma_2 = 0.4$ in (4.1). For γ_1 satisfying $0 < \gamma_1 < \gamma_2 + \gamma_3$, $V_d \cong 5.57 \times 10^8$ (cm/sec) (88.2eV).

The trajectories for various values of $\gamma_1 \in [0.2,0.6]$ are shown in Figure 2. The minimum value of $\gamma_2 + \gamma_3 - \gamma_1$ is 0.8 for $\gamma_1 \in [0,0.6]$. Hence, from (3.7), the trajectories in Figure 2 are on the set whose phase volume is almost zero and which resembles a surface.

In order to understand qualitatively the dependence of the trajectory behavior on γ_1 , we use a simple model shown in Figure 3. This model consists of two planes K_1 and K_2 containing the unstable foci F_1 and F_2 , respectively. The trajectories spiral slowly away from F_1 (resp., F_2) on

K_1 (resp., K_2) and jump from K_1 (resp., K_2) to the line L_2 (resp., L_1). Let κ be the ratio of the frequency and the growth rate of the spiral trajectory. In the actual system, $\kappa = |b|/a$ at $P^{\nu}_{\sigma,\mu}$, $(\sigma,\mu,\nu) \in \Omega$, and from (3.8),

$$(\kappa^2 - 3)^3/(\kappa^2 + 1) = (\gamma_2 + \gamma_3 - \gamma_1)^3/\gamma_1\gamma_2\gamma_3 \quad , \tag{4.3a}$$

$$\frac{d\kappa^2}{d\gamma_1} = -\frac{(\kappa^2 - 3)^2(\kappa^2 + 9)(\gamma_2 + \gamma_3 - \gamma_1)^2(2\gamma_1 + \gamma_1 + \gamma_3)}{4(1 + \kappa^2)\gamma_1^2\gamma_2\gamma_3} < 0 \quad . \tag{4.3b}$$

Hence, as γ_1 increases from 0.2 to 0.6, κ decreases from 5.56 to 3 monotonically. Furthermore, $P^{1}_{1,1}$ and $P^{-1}_{-1,1}$ move away from the x-axis perpendicularly to the x-axis. Taking into account these properties of the actual system, we consider five cases as shown in Figure 3. Here, as the system changes from (a) to (d), κ increases and F_1 and F_2 move upward. Thus, the transition from (a) to (c) in Figure 2 is similar to that from (a) to (c) in Figure 3.

In Figure 3(a), the focus F_1 (resp., F_2) is below L_1 (resp., L_2). Therefore, there may exist various types of trajectories shown in the figure and their combination leads to the trajectory as shown in Figure 2(a). Since the trajectory can be arbitrarily close to the origin, the attractor may be unbounded. In Figure 3(b), F_1 (resp., F_2) is above L_1 (resp., L_2). Consider the trajectories tangent to L_1 and L_2 at G_1 and G_2, respectively and the shaded region which they surround. This region is obviously a local attractor in the sense that any trajectory sufficiently close to the region enters the region at some time and remains there.

This case corresponds to that in Figure 2(b). As κ takes on larger values, the trajectory tangent to L_1 (resp., L_2) becomes closer to G_2 (resp., G_1). Assume that, for some value of κ, the point B_2 is above A_2, as shown in Figure 3(c). Then, the local attractor of type (b) is replaced by that of type (c). In Figure 3(c), we have omitted another local attractor which is symmetric to the one shown under 180°-rotation about the y-axis. We have also omitted the points A_1, B_1, D_1, and G_1 on L_1 and E_2 and H_2 on L_2, which are in the omitted local attractor. If the points B_j and C_j are located between E_j and H_j, $j = 1,2$, then these two attractors are separated and interlinked with each other. This case corresponds to Figure 2(c). Assuming that κ is sufficiently large so that D_2 coincides with G_2 as shown in Figure 3(d), the local attractor of type (c) disappears.

In Figure 2(d)-2(f), stable interlinked double limit-cycles and a single limit-cycle are observed. They have a small numeber of loops. In order to understand their formation, we consider the one-dimensional return maps of trajectories of the actual system. Figure 4(a) shows the graph of the value $\hat{x}$ of x on the plane $T_+ = \{X \mid z=0, x,y > 0\}$ with respect to the previous value of x on the same plane. In Figure 4(a), the circled points indicate the positions of the observed limit cycles. Actually, as shown in Figure 4(b), the mapping from a sufficiently small interval containing the circled point on the x-axis into the x-axis is a contraction mapping with respect to the length of interval. We now assume that the actual system has a transition such as that from case (c) to (e) and then to case (d), as shown in Figure 3. Figure 3(c), (e) and (d) implies that, as κ increases, A_2 and D_2 approach G_2, while B_2 and D_2 approach each other more slowly. Then, the local attractor becomes narrower

and finally the double-loop local attractor case (e) appears and lasts until case (d) occurs. It becomes more probable that the interval for contraction mapping appears as $d\hat{x}/dx$ decreases in the local attractor (indicated by a solid line) in Figure 4(a), which happens as the local attractor becomes narrower. Thus, as κ increases, limit cycles having a small number of loops appear. From Figure 4(a), a single-loop limit cycle must appear after a double-loop cycle. It cannot, however, exist in the local attractor of type (c). This may be the reason why the interlinked double limit-cycles, each of which is a single-loop, are not observed in the actual system.

In Figure 4(c), we also show the graph of values $\hat{x}$ of x on T_+ (resp., $T_- = \{X : z=0 , x<0 , y>0\}$) with respect to the previous values of x on T_- (resp., T_+) for $\gamma_1 = 0.2$ and 0.45. Figure 4(a) and (c) show that the return maps are 'folded'[10] for $\gamma_1 \in [0.2,0.489]$. The attractor produced by such a map is called a 'chaotic attractor'.[10] In this attractor, there may exist stable periodic solutions. If they exist, the attractor is not a strange attractor. Here, by a strange attractor, we mean a positive limit set of the integral curves of a differential equation which is neither empty nor an equilibrium set nor a closed orbit. Since the size of the region of attraction for the stable periodic solution is usually small, a small perturbation will expel the trajectories from the region. Hence, even if stable periodic solutions exist in the attractor, we actually cannot distinguish a chaotic attractor from a strange attractor. We cannot prove here whether our system has a stable periodic solution for $\gamma_1 \in [0.2,0.489]$. Hence, we do not know whether the attractors obtained in the experiment are strange attractors.

If the attractor Λ of a system is ergodic and $\mu(X)$ is a defined measure on Λ, then for any smooth function f,

AD-A086 456 CALIFORNIA UNIV LOS ANGELES SCHOOL OF ENGINEERING A--ETC F/G 20/9
STUDIES OF NONLINEAR PHENOMENA IN PLASMAS.(U)
MAR 80 P K WANG AFOSR-79-0050
UNCLASSIFIED UCLA-ENG-8012 AFOSR-TR-80-0502 NL

2 OF 2
AD A086456

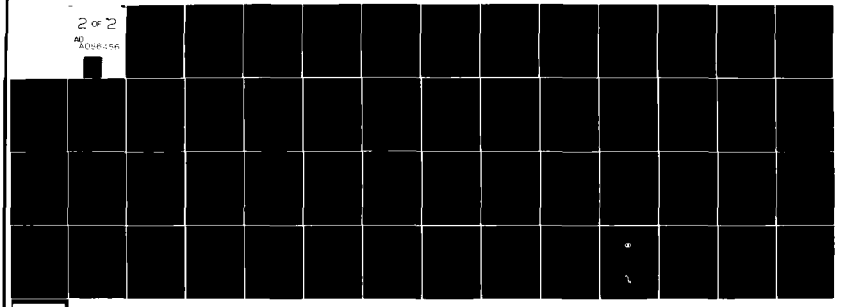

END
DATE FILMED
8-80
DTIC

$$\bar{f} = \int_{\Lambda} f(X)d\mu(X) = \lim_{T\to\infty} \frac{1}{T} \int_0^T dt\ f[X(t)] \ . \tag{4.4}$$

Also, if the time evolution of the system is mixing, then for any smooth functions f and g,

$$\begin{aligned} \zeta(\tau) &= \bar{f}\,\bar{g} - \int_{\Lambda} f[X(\tau)]\, g\,(X_0)d\mu(X_0) \\ &= \bar{f}\,\bar{g} - \lim_{T\to\infty} \frac{1}{T} \int_0^T dt\ f[X(t+\tau)]\, g\,[X(t)] \end{aligned} \tag{4.5}$$

converges to zero as $\tau \to \infty$. This property means that the time evolution of the system trajectories is highly sensitive to the initial condition. The solution with such a property is defined as a turbulent solution.[1,5] We do not know whether our system has the property of ergodicity or mixing. In order to obtain some idea on the sensitivity of our system to initial conditions, we have calculated the autocovariance functions $R(t)$ of x for $\gamma_1 = 0.2$, 0.45 and 0.49 (see Figure 5). Although we cannot draw any definite conclusions from the results, they suggest that $R(t)$ converges to zero as $t \to \infty$ and the system has the mixing property.

We shall consider whether the solution of system (3.6), with a specified initial condition which is not on the x,y or z-axis, is uniformly bounded on the time interval $[0,\infty)$. We have calculated, for some initial conditions, the ratio $P(\chi)$ of the sum of the time duration when $x(t)$ exceeds χ for $t \in [0,T)$ and T; namely, $P(\chi)$ = [length of $\{t : x(t) \geq \chi\ ,\ 0 \leq t \leq T\}$]/$T$. In Figure 6, we have plotted only those values of χ for which P is insensitive to the initial conditions. As T increases, the set of such values of χ also increases in size. Hence, it is

likely that, as $T\to\infty$, P approached P_∞, which is independent of the initial conditions. If this is true, then $P_\infty(\chi) \neq 0$ at finite values of χ, for we can choose an arbitrarily large initial condition whose corresponding trajectory also has $P_\infty(\chi)$. Thus, if P_∞ exists, the solution of (3.6) with any initial condition is not uniformly bounded on the time interval $[0,\infty)$.

If P_∞ exists and decays faster than $1/\chi^3$, then from the physical point of view, we can state as follows: the wave energy can be arbitrarily large over a finite time interval, but its time duration is so short that the time-averaged energy $\lim_{T\to\infty} (1/T)\int_0^T x^2(t)dt = \int_0^\infty \chi^2 P_\infty(\chi)d\chi$ is finite. Then, the unboundedness of system (3.6) does not contradict the physical requirement that the energy of a system must be finite.

We must show that the assumptions made in Section 2 in deriving (3.6) are consistent with the numerical results, or that the assumptions are valid for the observed values of $\|X(t)\|$. Although this is true, it is still possible that, at some t which is not realized in the experiment, $\|X(t)\|$ is so large that the assumptions are violated. If the value of $\|X(t)\|$ violating the assumptions is much larger than the observed value of $\|X(t)\|$, the violation of the assumptions rarely happens and the system (3.6) is valid most of the time.

Nonlinear terms in (1.1) produce only small shifts in frequency, since $|VA_2|$ or $|VA_3| \cong \gamma_1|x| \ll \omega_1$ for the observed values of $|x(t)| \cong \|X(t)\|$. The electrostatic potential of plasma wave '1' is given by $\phi_1 = \{\gamma_3/V(2k_1^2/8\pi\omega_{pe})\}x$. Hence, the energy density per unit wave number at k_1, which is comparable to that at k_3, is given by $E_1 = k_1^2\phi_1^2/8\pi \cong 10^{-18}\, x^2$ (erg). This is much smaller than the kinetic

energy of the electrons $E_{kin} \cong 6.15 \times 10^{-13}$(erg) for the observed values of $x(t)$. Hence, v_{Te} is constant since waves '1' and '3' are only plasma waves excited in our model. Therefore, γ_2 , γ_3 and V are constant for the observed values of $x(t)$. The bounce frequency of trapped electrons is given by $\omega_B = (ek_1^2|\phi_1|/m_e)^{1/2} = 3.37 \times 10^4 |x|^{1/2}$ (sec^{-1}). The beam particles pass through the plasma in $L/v_d = 1.8 \times 10^{-7}$ (sec) , which is much smaller than the trapping time $1/\omega_B = 2.97 \times 10^{-5} |x|^{-1/2}$ (sec) for the observed values of $x(t)$. Furthermore, the velocity distribution function of the beam is time-independent at the surface of the plasma. Hence, the velocity distribution function of the beam can be approximated to be independent of time and space in the plasma slab. Thus, γ_1 is constant for the observed values of $x(t)$.

V. CONCLUDING REMARKS

We found that the behavior of the system of resonant three-wave interaction with linear growth and damping terms is completely different from that without such terms or that approximated by a two-wave model. Although it is not proved mathematically that the system (3.6) has the statistical properties of ergodicity and mixing, numerical results show that the solution (3.6) is very sensitive to its initial condition. This suggests that a turbulent state can be produced directly by a linearly unstable wave through the interaction with two linearly damped waves. We note that, in such a mechanism, neither any additional input of randomness nor any interaction between a large number of waves is necessary to produce a turbulent state.

System (3.6) is a highly simplified model with many assumptions. In an actual plasma, however, many wave-wave and wave-particle interactions must be considered. Very little is known about the chaotic property of a system with dimension $m \geq 4$. It might be completely different from that of a three-dimensional system. Hence, at present, it is difficult to correlate the numerical results obtained for system (3.6) with the turbulence in an actual plasma.

REFERENCES

1. V.N. Tystovich, *Theory of Turbulent Plasma*, Consultants Bureau, New York, 1977.

2. S. Ichimaru, *Basic Principles of Plasma Physics: A Statistical Approach*, W.A. Benjamin, Inc., London, 1973.

3. E.N. Lorenz, "Deterministic Nonperiodic Flow," *J.Atmosph.Sci., 20* (1963) 130-141.

4. D. Ruelle and F. Takens, "On the Nature of Turbulence," *Commun.Math.Phys., 20* (1971) 167-192.

5. D. Ruelle, "Sensitive Dependence of Initial Condition and Turbulent Behavior of Dynamical Systems," in *Bifurcation Theory and Applications in Scientific Disciplines* (ed.O.Gurel and O.E. Rössler), New York Acad. Sciences, NY (1979) 408-415.

6. V.I. Dubrovin, V.R. Kogan and M.I. Rabinovich, "Decay Mechanism for the Onset of Turbulence," *Sov.J.Plasma Phys., 4:5* (1978) 658-659.

7. A.S. Picovskii, M.I. Rabinovich and V.Yu. Trakhtengents, "Onset of Stochasticity in Decay Confinement of Parametric Instability," *Sov.Phys. JETP, 47:4* (1978) 715-719.

8. P.K.C. Wang, "Nonperiodic Oscillations of Langmuir Waves," UCLA Engr. Rpt.No. *ENG-7879*, Nov. 1978.

9. A. Hasegawa, *Plasma Instabilities and Nonlinear Effects*, Springer-Verlag, New York, 1975.

10. O.E. Rössler, "Continuous-Chaos -- Four Prototype Equations," in *Bifurcation Theory and Applications in Scientific Disciplines*, (ed. O. Gurel and O.E. Rössler), New York Acad.Sciences, NY (1979) 376-392.

FIGURE CAPTIONS

Fig.1: Sketch of the surface S where $d(y/z)/dt = 0$, the sets W_1 and W_2 separated by S and the boundary $\partial\Gamma$ of the set Γ.

Fig.2: Projections of the phase-space trajectory of equation (4.1) onto the (x,z)- and (x,y)-planes for $t \in [0,3,276)$ and various values of γ_1 : (a) $\gamma_1 = 0.2$, (b) $\gamma_1 = 0.45$, (c) $\gamma_1 = 0.489$, (d) $\gamma_1 = 0.49$, (e) $\gamma_1 = 0.5$, (f) $\gamma_1 = 0.6$; tr = transient.

Fig.3: Sketch of the local attractors of the idealized system.

Fig.4: Return mappings of the actual system.

Fig.5: Autocovariance functions $R(t)$ of $x(t)$ obtained from 32,768 data points for $t \in [0,6,554)$.

Fig.6: The ratio $P(x)$ of the sum of the time durations when $x(t) \geq \chi$ for $t \in [0,T)$ and T; $T = 6,554$.

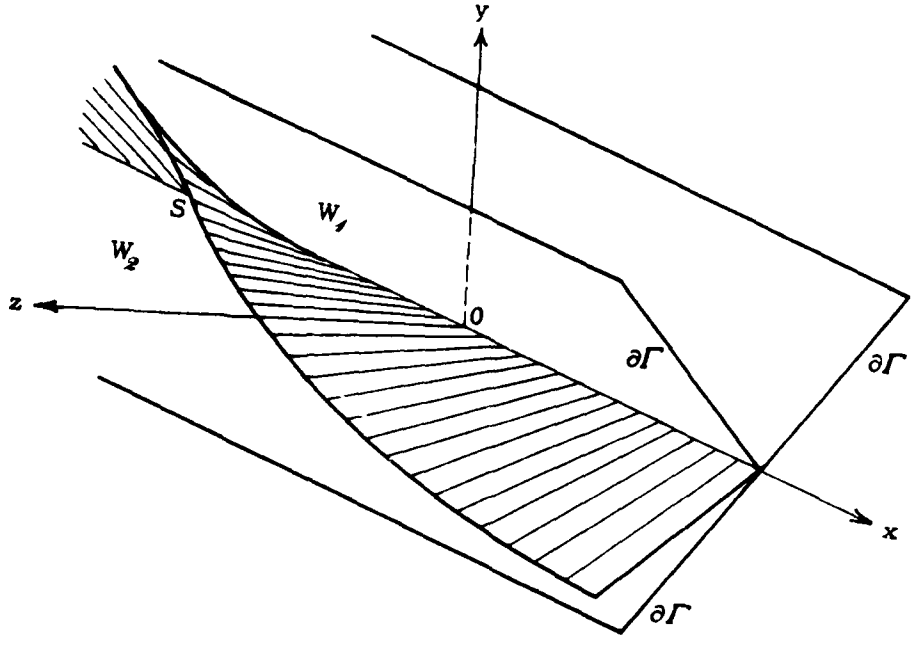

Fig. 1

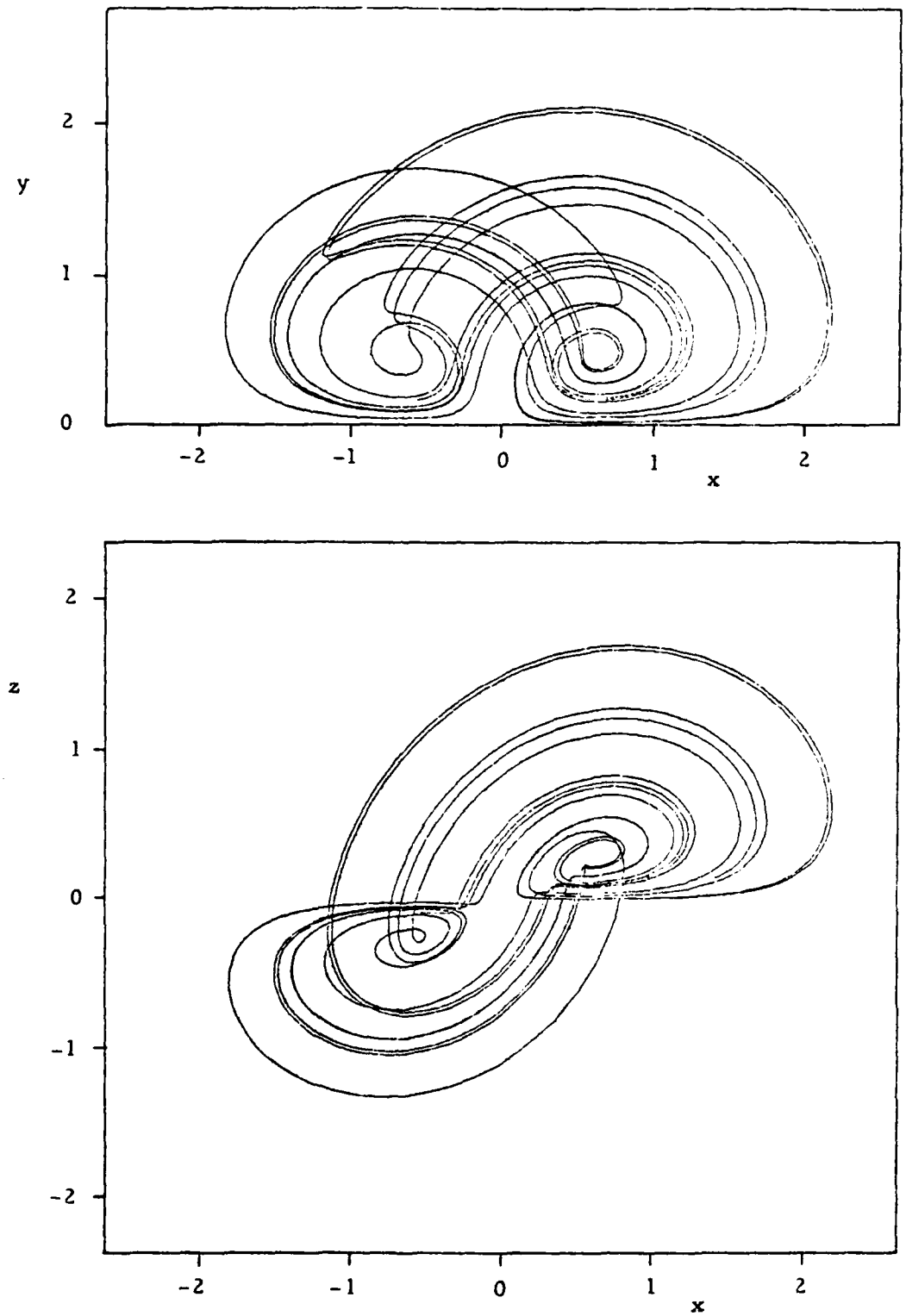

Fig. 2 (a)

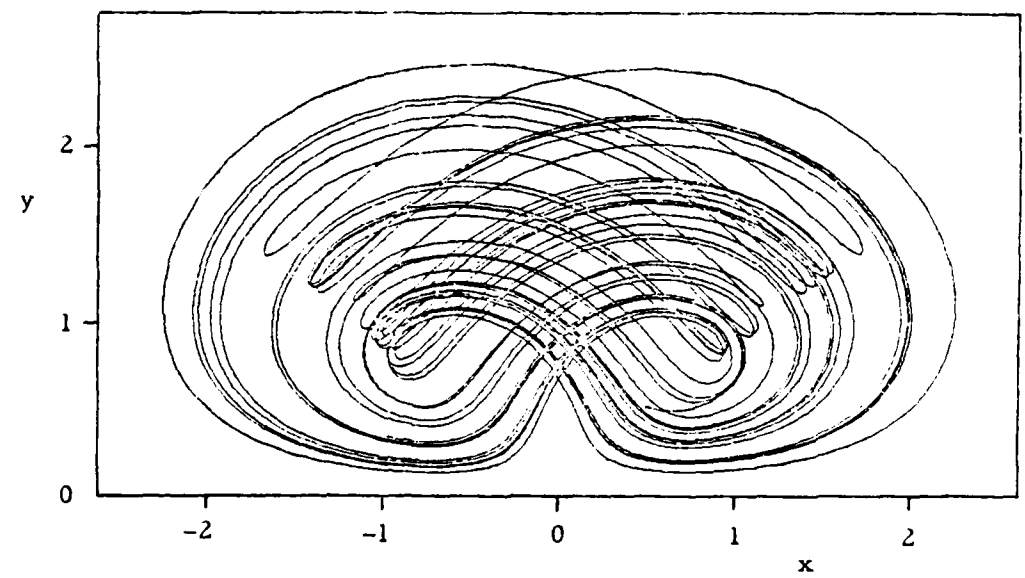

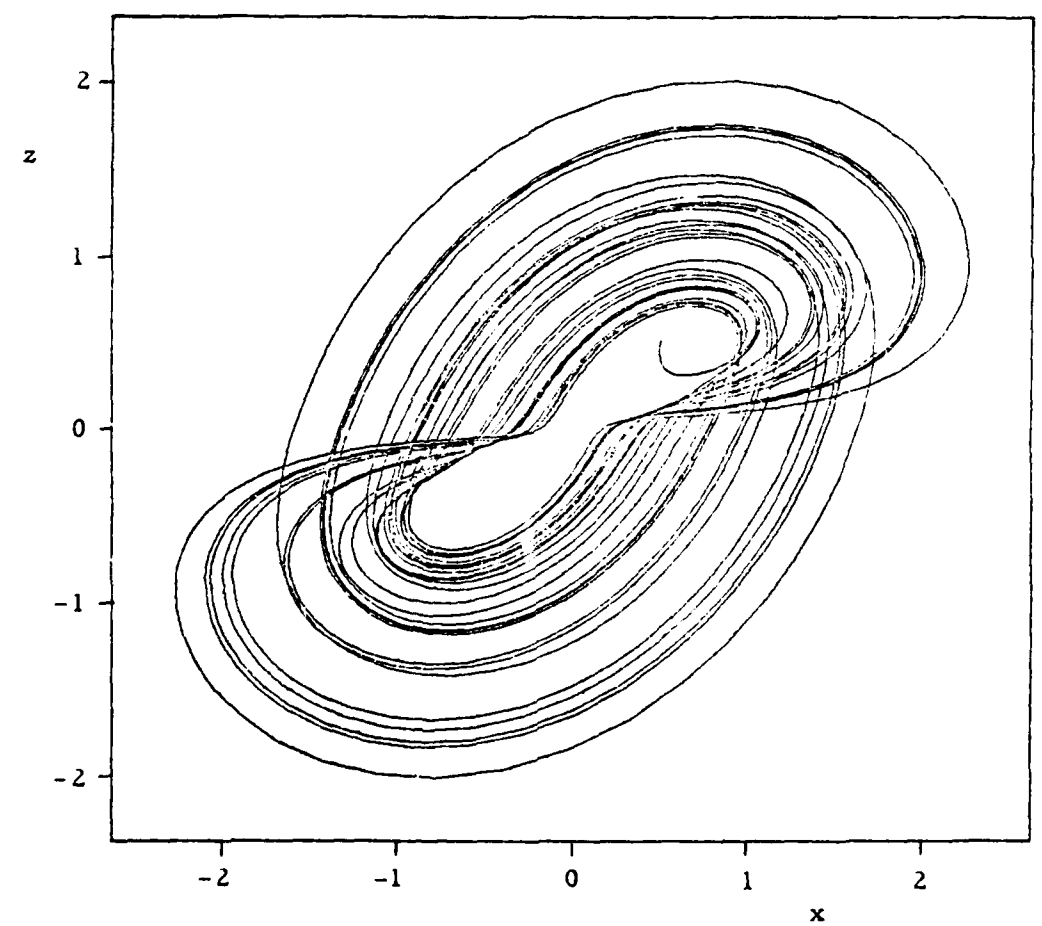

Fig. 2(6)

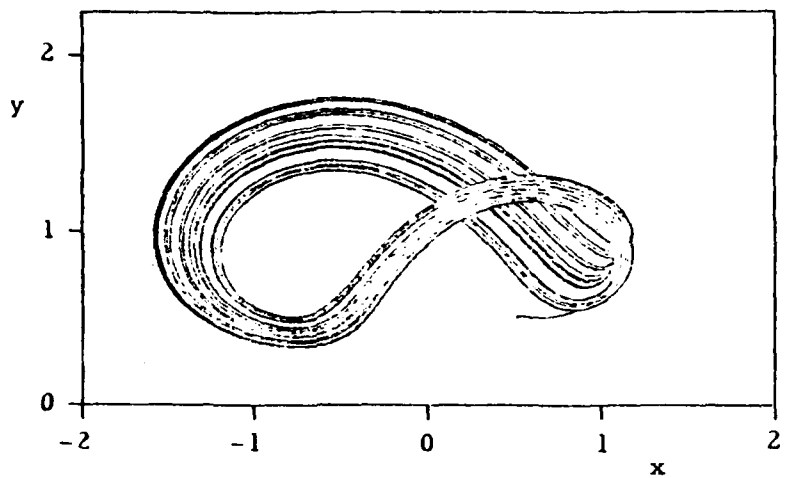

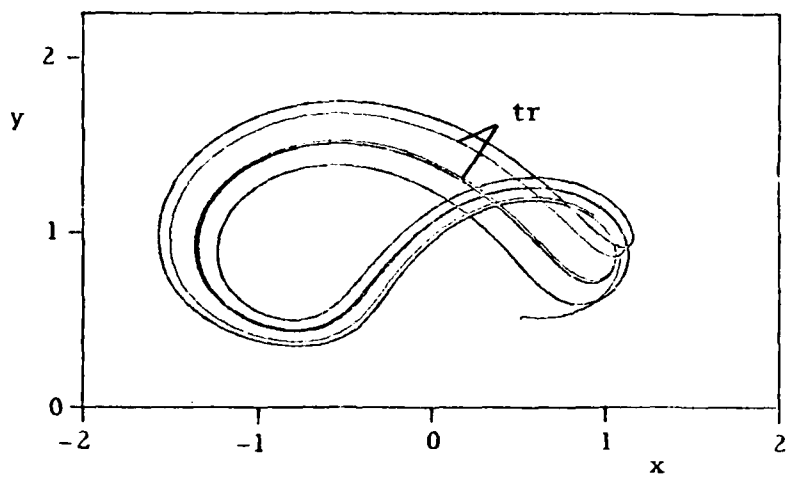

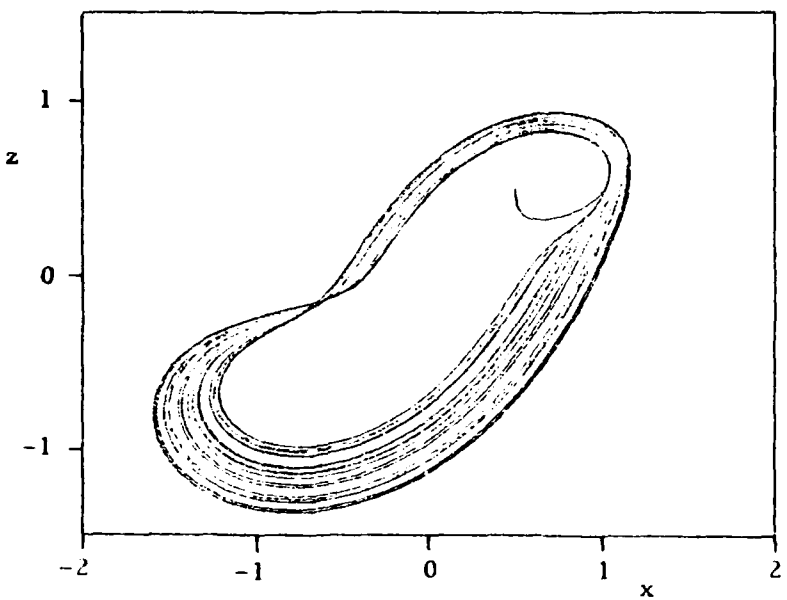

Fig. 2(c)

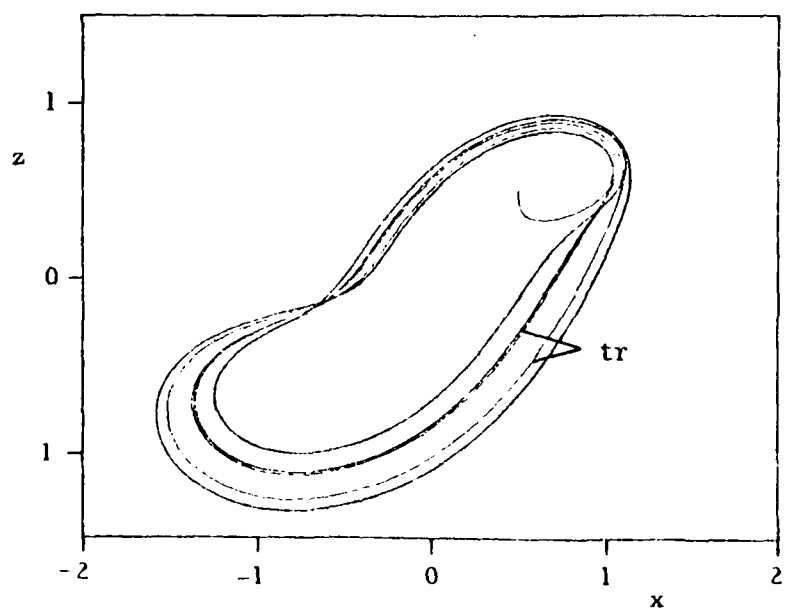

Fig. 2(d)

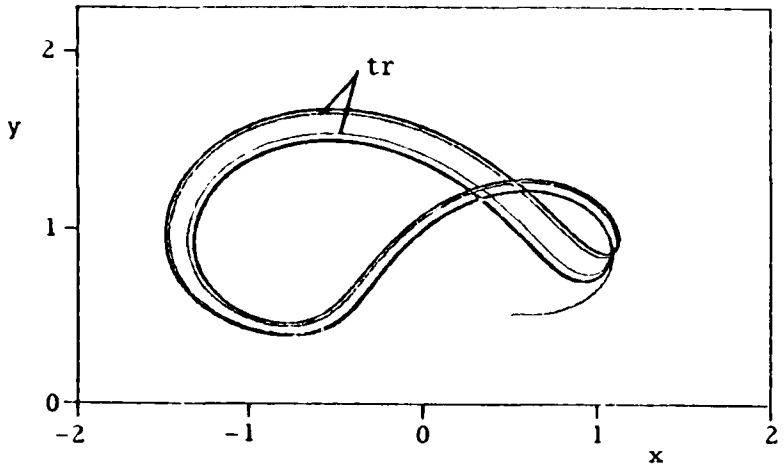

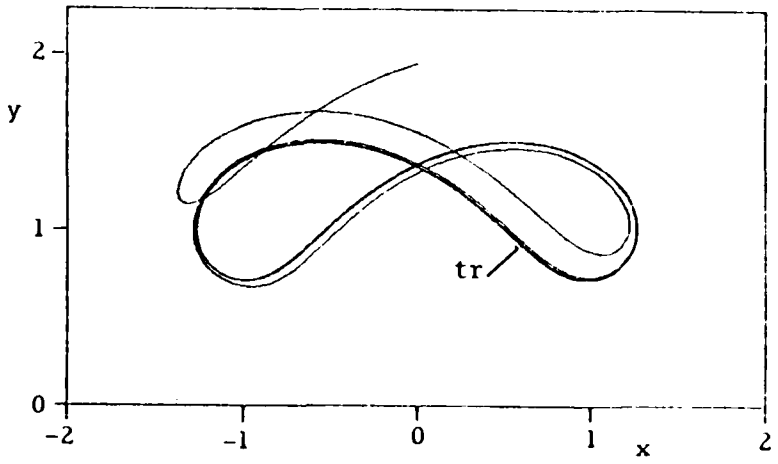

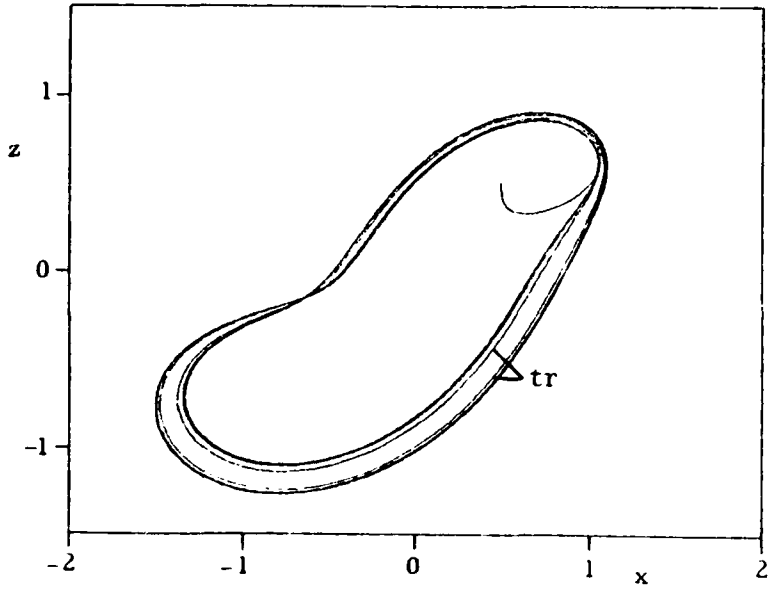

Fig. 2 (e)

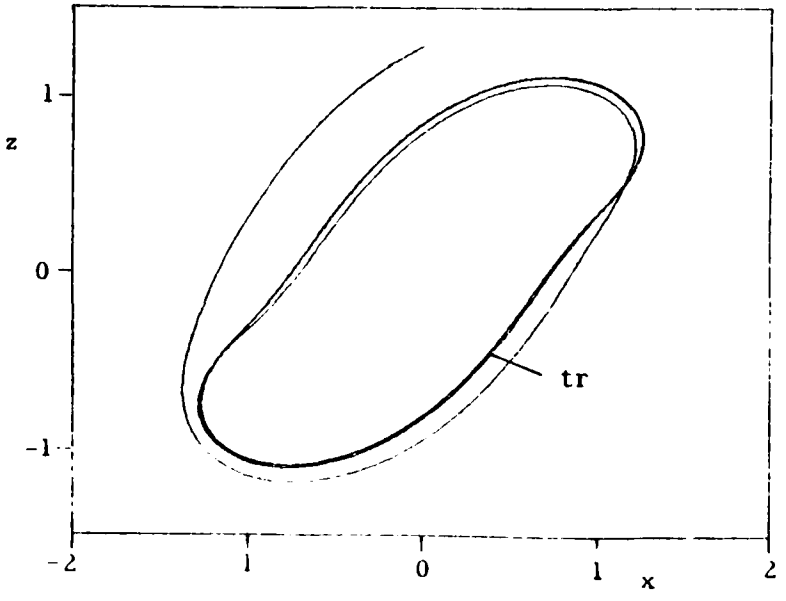

Fig. 2 (f)

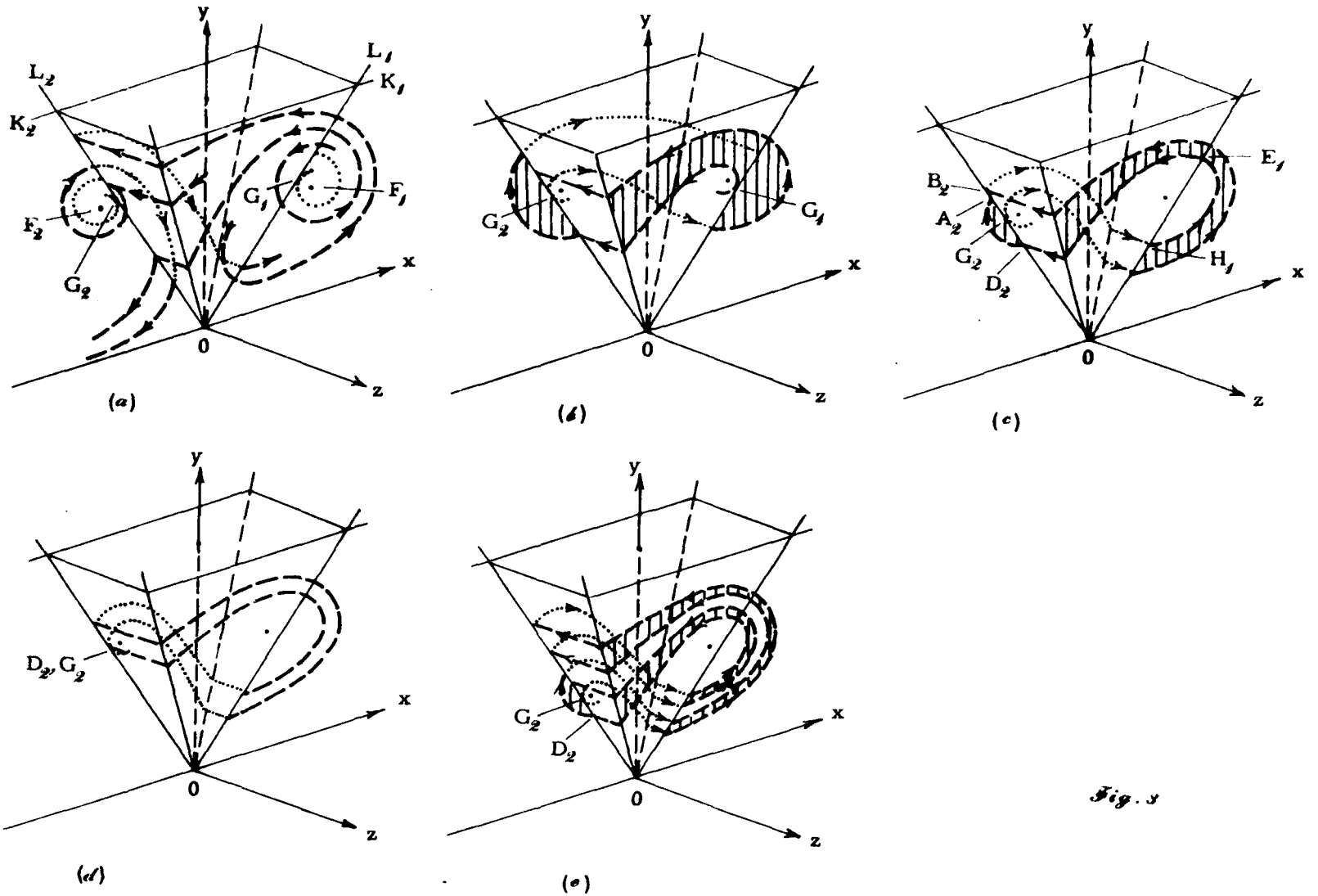

Fig. 3

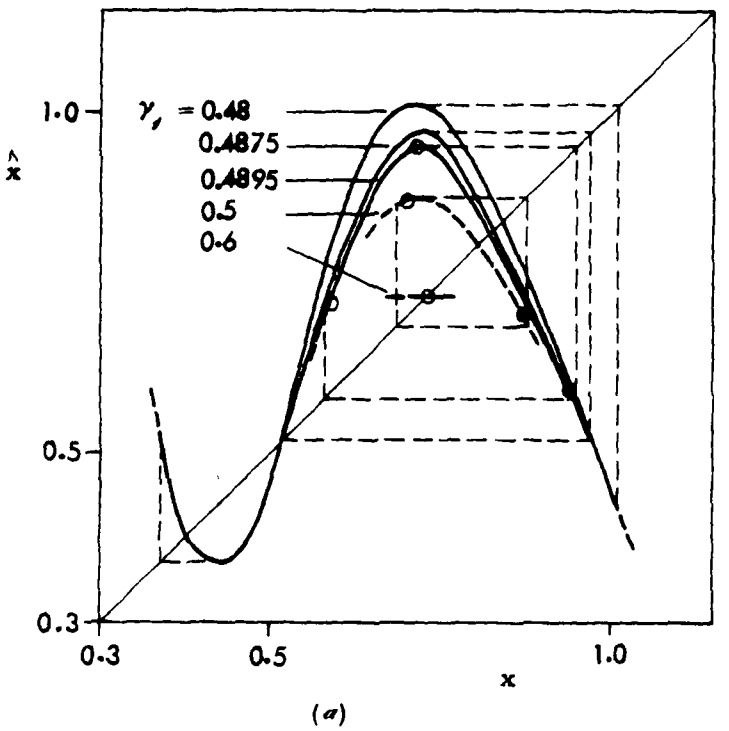
$\gamma_1 = 0.48$
0.4875
0.4895
0.5
0.6
1.0
0.5
0.3
0.3
0.5
1.0
x
$\hat{x}$

(a)

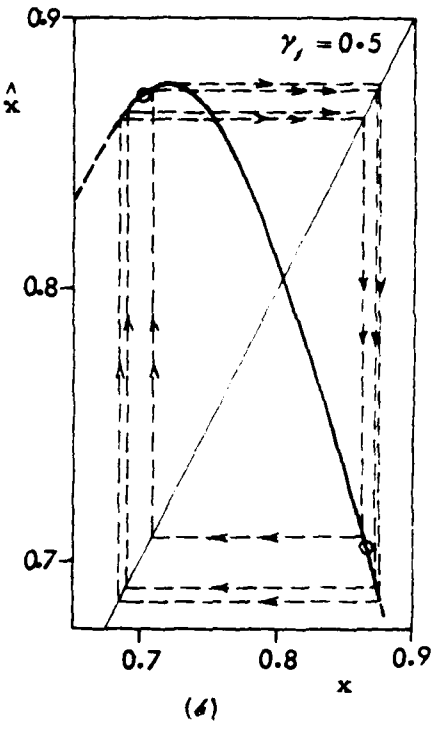
$\gamma_1 = 0.5$
0.9
0.8
0.7
0.7
0.8
0.9
x
$\hat{x}$

(b)

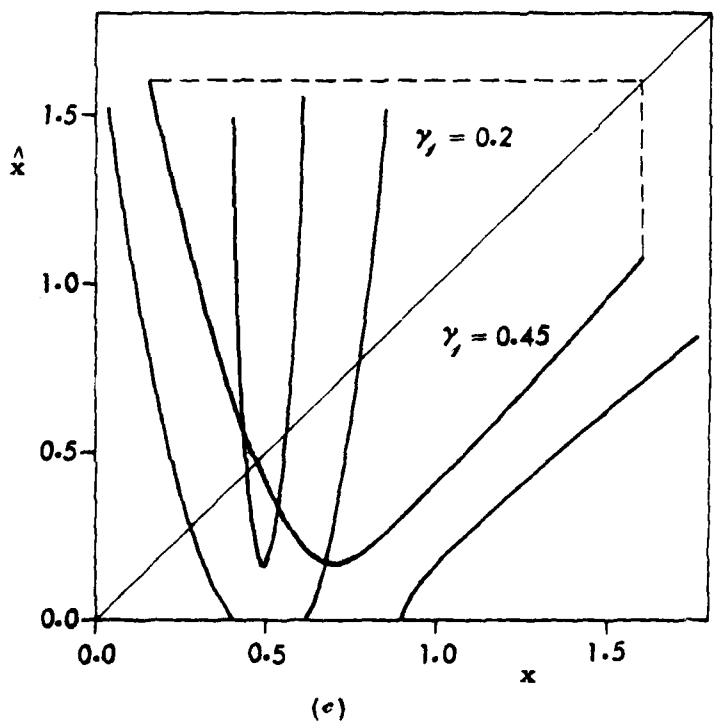
$\gamma_1 = 0.2$
$\gamma_1 = 0.45$
1.5
1.0
0.5
0.0
0.0
0.5
1.0
1.5
x
$\hat{x}$

(c)

Fig. 4

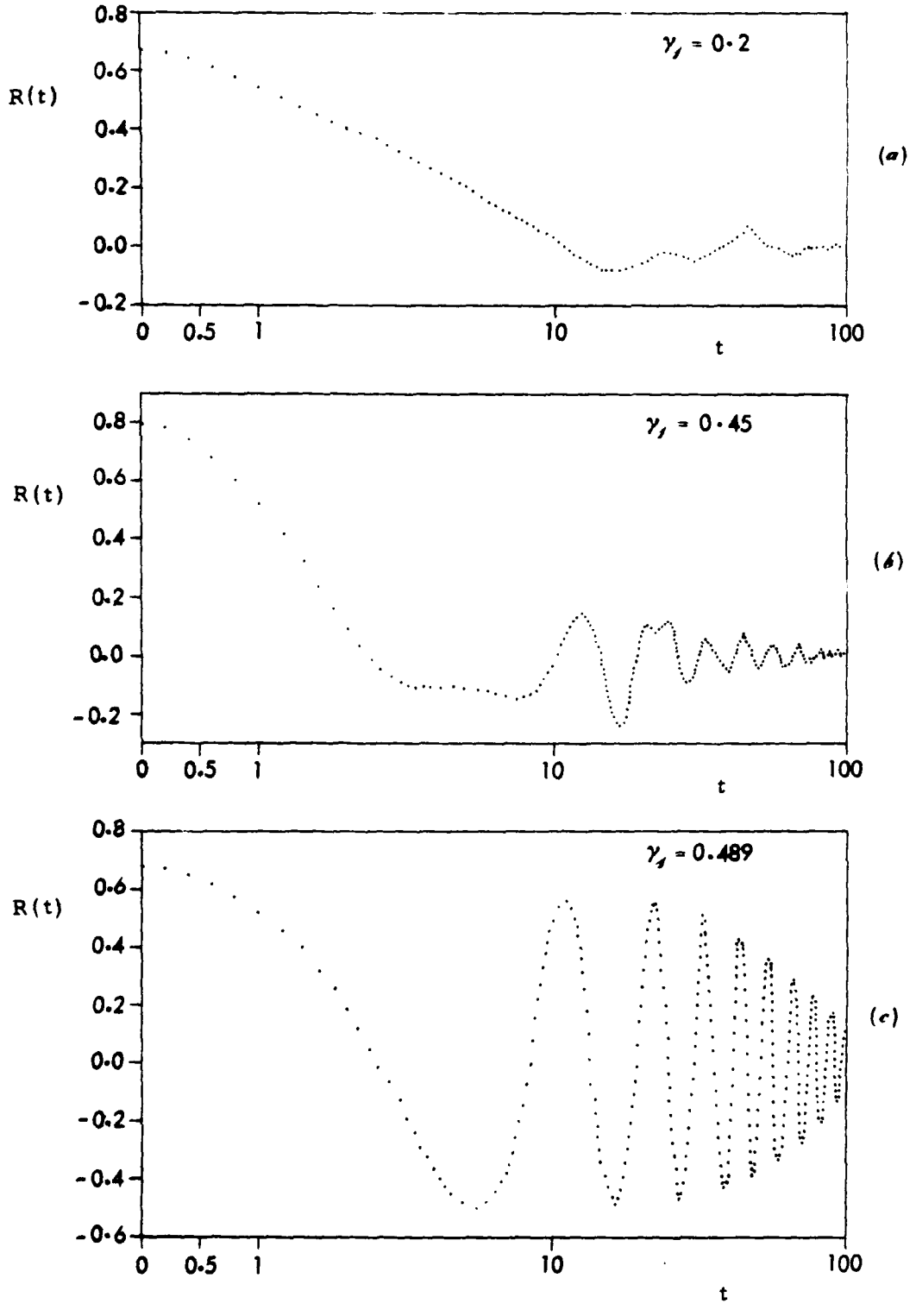
0.8
0.6
0.4
0.2
0.0
-0.2
R(t)
γ_1 = 0·2
0
0.5
1
10
100
t
(a)
0.8
0.6
0.4
0.2
0.0
-0.2
R(t)
γ_1 = 0·45
0
0.5
1
10
100
t
(b)
0.8
0.6
0.4
0.2
0.0
-0.2
-0.4
-0·6
R(t)
γ_1 = 0.489
0
0.5
1
10
100
t
(c)

Fig. 5

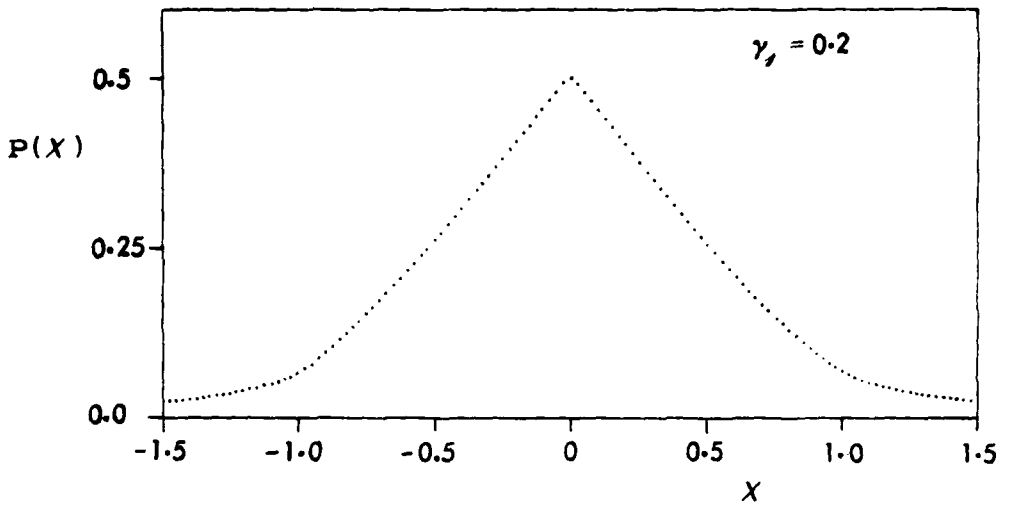

Fig. 6

APPENDIX D

STABILITY OF MODE-CONVERTED LOWER-HYBRID SOLITONS*

L.C. Himmell

Department of System Science
University of California
Los Angeles, California 90024

*This research was supported in part by Air Force Grant AFOSR-79-0050

ABSTRACT

The stability of planar, mode-converted, lower-hybrid solitons to transverse perturbations is investigated. Two classes of modes are found. In the lowest order, the stability of each class is related to a particular term of the equation governing the nonlinear evolution of these waves.

I. INTRODUCTION

It is well known that one-dimensional Langmuir solitons are modulationally unstable to transverse perturbations.[1] As a result of the instability, the soliton breaks up into collapsing bunches with longitudinal and transverse dimensions of the same order.[2,8] There is much interest in electrostatic plasma waves with frequencies near the lower-hybrid resonance frequency as a possible method of heating tokomak plasmas. According to linear theory, cold-plasma waves, excited by an rf source at the surface of a magnetically confined plasma, propagate in resonance cones[3] into the interior of the plasma until they reach the lower-hybrid resonance layer, where they may mode-convert to a slow hot-plasma wave.[4,5] Nonlinear ponderomotive effects on the cold-plasma wave[6], as well as the mode-converted lower-hybrid wave[7], have been examined in a two-dimensional geometry. Recently, the effect of a third dimension on the cold-plasma wave was studied and it was found that perturbations transverse to the soliton structure were unstable.[8] An equation governing the nonlinear dynamics of mode-converted lower-hybrid waves in three dimensions has also been presented.[9]

In this paper, we address ourselves to the stability of a mode-converted, lower-hybrid, planar soliton to perturbations in the transverse direction. We find that these solitons are also unstable.

II. EXISTENCE OF UNSTABLE MODES

The equation governing the nonlinear evolution of mode-converted, lower-hybrid waves is, according to Ref. [9],

$$i\frac{\partial}{\partial X}\psi + \alpha_o|\psi|^2\psi + \beta_o\frac{\partial^2}{\partial Z^2}\psi + \gamma_o\frac{\partial^2}{\partial Y^2}\psi + \delta_o\left(\frac{\partial}{\partial Y}|\psi|^2\right)\psi = 0 \qquad (1)$$

where

$$\alpha_o = \left[\frac{(1-K_\perp)}{2K_\perp}\left(\frac{K_\perp}{A_o}\right)^{1/2}\right], \quad \beta_o = \left[-\frac{K_\parallel}{2K_\perp}\left(\frac{A_o}{K_\perp}\right)^{1/2}\right]$$

$$\gamma_o = \frac{1}{2}(A_o/K_\perp)^{1/2}, \quad \delta_o = \frac{1}{2}(K_H/K_\perp)$$

$$K_\perp \simeq 1 + (\omega_{p_e}/\omega_{c_e})^2 - (\omega_{p_i}/\omega)^2, \quad K_\parallel = 1 - (\omega_{p_e}/\omega)^2$$

$$A_o = \frac{3}{2}(\omega_{p_i}/\omega)^2(v_i/\omega)^2 + \frac{3}{8}(\omega_{p_e}/\omega_{c_e})^2(v_e/\omega_{c_e})^2$$

$$K_H = -\frac{\omega_{p_e}^2\,\omega_{c_e}}{\omega(\omega^2-\omega_{c_e}^2)} + \frac{\omega_{p_i}^2\,\omega_{c_i}}{\omega(\omega^2-\omega_{c_i}^2)}$$

in which ω_{p_i} and ω_{p_e} denote the ion and electron plasma frequencies, ω_{c_e} and ω_{c_i} are the electron and ion cyclotron frequencies, and $v_i^2 = 2T_i/m_i$, $v_e^2 = 2T_e/m_e$. In Eq.(1), ψ is the normalized field amplitude $[K_\perp/4n_o(T_i+T_e)A_o]^{1/2}\phi$ associated with the electrostatic potential ϕ of the wave which has the form

$$\Phi = \phi\exp[i(K_\perp/A_o)^{1/2}X - i\omega t] \quad . \qquad (2)$$

We scale Eq.(1) as follows:

$$Z = \beta_o Z \ , \quad X = \beta_o \tau \ , \quad Y = y \tag{3}$$

and set

$$\kappa = \alpha_o \beta_o \ , \quad \alpha = \beta_o \delta_o \ , \quad \beta = \beta_o \gamma_o \ . \tag{4}$$

Then Eq.(1) takes the form

$$i \frac{\partial}{\partial \tau}\psi + \frac{\partial^2}{\partial z^2}\psi + \kappa|\psi|^2\psi + \alpha\left(\frac{\partial}{\partial y}|\psi|^2\right)\psi + \beta \frac{\partial^2}{\partial y^2}\psi = 0 \ , \tag{5}$$

which is the usual nonlinear Schrödinger equation with two additional terms.

For $\alpha = \beta = 0$, Eq.(5) is known to have the solution

$$\psi_o = \sqrt{\frac{2}{\kappa}} A \ \mathrm{sech}(A\xi)\exp[-i\omega_o \tau + ik_o z]$$

$$\equiv \phi(\xi)\exp[-i\omega_o \tau + ik_o z] \tag{6}$$

where

$$\xi = Z - V\tau \ , \quad V = 2k_o \ , \quad A^2 = k_o^2 - \omega_o \ , \tag{7}$$

which is stable to perturbations in the z-direction.

Next, we linearize Eq.(5), setting $\psi = \psi_o + \delta\psi$ and assume that

$$\delta\psi = [F(\xi,\tau)\cos(k_y y) + G(\xi,\tau)\sin(k_y y)]e^{-i\omega_o \tau + ik_o z} \ . \tag{8}$$

Eq.(5) then reduces to a linear combination of terms proportional to $\sin(k_y y)$ and $\cos(k_y y)$. Setting the coefficients of each of these equal to zero yields

$$i \frac{\partial}{\partial \tau} F = (L_o + \beta k_y^2)F - \kappa\phi^2(F + F^*) - k_y \alpha \phi^2 (G + G^*) \tag{9}$$

$$i \frac{\partial}{\partial \tau} G = (L_o + \beta k_y^2)G - \kappa\phi^2(G + G^*) + k_y \alpha \phi^2 (F + F^*) \tag{10}$$

where

$$L_o = - \frac{\partial^2}{\partial \xi^2} + A^2 - \kappa\phi^2$$

is a linear operator.

If we introduce

$$F = u + iv \quad , \quad G = r + is \qquad (u,v,r,s \text{ real}) \tag{11}$$

and set $\eta_1 = \begin{pmatrix} u \\ r \end{pmatrix}$ and $\zeta_1 = \begin{pmatrix} v \\ s \end{pmatrix}$, Eqs. (9-10) take the form

$$\frac{\partial}{\partial \tau} \eta_1 = (L_o + \beta k_y^2)\zeta_1 \tag{12}$$

$$- \frac{\partial}{\partial \tau} \zeta_1 = [(L_1 + \beta k_y^2)\underset{\sim}{E} - 2\alpha k_y \phi^2 \underset{\sim}{\sigma}]\eta_1 \quad , \tag{13}$$

where $L_1 = L_o - 2\kappa\phi^2$, $\underset{\sim}{E} = \begin{pmatrix} 1 & 0 \\ 0 & 1 \end{pmatrix}$ and $\underset{\sim}{\sigma} = \begin{pmatrix} 0 & 1 \\ -1 & 0 \end{pmatrix}$. We note that L_o and L_1 are self-adjoint operators and

$$L_o \phi(\xi) = 0 \ . \tag{14}$$

Assuming that

$$\eta_1 = \eta e^{-i\Omega\tau} + \text{c.c.} \ , \quad \zeta_1 = \zeta e^{-i\Omega\tau} + \text{c.c.}$$

Eqs. (12-13) reduce to

$$i\Omega\eta = (L_o + \beta k_y^2)\zeta \tag{15}$$

$$- i\Omega\zeta = [(L_1 + \beta k_y^2)\underset{\sim}{E} - 2\alpha k_y \phi^2 \underset{\sim}{\sigma}]\eta \ . \tag{16}$$

The only eigenfuction of L_o that vanishes at infinity has an eigenvalue of zero. Therefore, according to Eq.(15), $k_y = 0$ is the only marginally stable state corresponding to $\Omega = 0$.

Eqs.(15-16) can be reduced to the form

$$(L_o + \beta k_y^2)[(L_1 + \beta k_y^2)\underset{\sim}{E} - 2\alpha k_y \phi^2 \underset{\sim}{\sigma}]\eta = \Omega^2 \eta \quad , \tag{17a}$$

$$[(L_1 + \beta k_y^2)\underset{\sim}{E} - 2\alpha\phi^2\underset{\sim}{\sigma}](L_o + \beta k_y^2)\zeta = \Omega^2\zeta \quad . \tag{17b}$$

For mode-converted lower-hybrid waves, $K_\perp \sim 1$, $K_H \sim \varepsilon^{-1}$, $K_\parallel \sim \varepsilon^{-2}$, where $\varepsilon^2 \equiv m_e/m_i$. This implies that

$$\beta k_y^2/A^2 \sim \frac{\gamma_o}{\beta_o}\frac{k_y^2}{k_z^2} \sim \varepsilon^2\left(\frac{k_y}{k_z}\right)^2 << 1 \quad , \tag{18a}$$

$$\alpha k_y \phi^2/A^2 << 1 \quad , \tag{18b}$$

$$\alpha k_y \phi^2/\kappa\phi^2 << 1 \quad , \tag{18c}$$

where k_z is the component of the propagation vector in the original coordinate system. Also, $k_z^2/k^2 << \varepsilon^2$, and $k_y/k_z \lesssim 1$.[7,9] For values of k_y in this range, Eq.(17a) can be solved by expanding η and Ω^2 in the form of a perturbation series,

$$\eta = \eta_0 + \eta_1 + \eta_2 + \cdots \quad , \qquad \Omega^2 = \xi_1 + \xi_2 + \cdots \quad , \text{ etc.}$$

In lowest order, Eqs.(17a,17b) reduce to

$$L_o L_1 \eta_o = 0 \quad , \qquad L_1 L_o \zeta_o = 0 \quad . \tag{19}$$

In order to determine η_o and ζ_o, consider the functions,[2]

$$u_o^+ = -\frac{\partial}{\partial A^2}\phi \quad , \quad u_o^- = 2\frac{\partial}{\partial \xi}\phi \quad , \quad v_o^+ = 0 \quad , \quad v_o^- = -\xi\phi \quad . \tag{20}$$

According to Eq.(14),

$$L_o v_o^+ = 0 \quad . \tag{21}$$

By differentiating Eq.(14) with respect to ξ and A^2, we find that

$$L_o v_o^- = u_o^- \quad , \quad L_1 u_o^+ = v_o^+ \quad , \quad L_1 u_o^- = 0 \quad . \tag{22}$$

Eqs.(21-22) imply that

$$L_o L_1 u_o^\pm = 0 \quad , \quad L_1 L_o v_o^\pm = 0 \quad . \tag{23}$$

The only solutions of Eqs.(19) that vanish at infinity are $u_o^\pm, v_o^\pm$. Therefore,

$$\eta_o = c_1 u_o^+ + c_2 u_o^- \quad , \quad \zeta_o = c_1' v_o^+ + c_2' v_o^-$$

are the proper eigenfunctions of Eqs.(19), where c_1, c_2, c_1', c_2' are constant vectors. The parity of u_o^+, v_o^+ is even, while that of u_o^-, v_o^- is odd with respect to ξ.

In first order, Eq.(19a) takes the form

$$L_o L_1 \eta_1 + [\beta k_y^2 (L_o + L_1)\underset{\sim}{E} - L_o 2\alpha k_y \phi^2 \underset{\sim}{\sigma}]\eta_o = \xi_1 \eta_0 \quad . \tag{24}$$

We define the scalar product of two functions as follows:

$$\langle u|v\rangle \equiv \int_{-\infty}^{+\infty} d\xi uv \quad .$$

Taking scalar products of Eq.(24) with $v_o^\pm$ yields

$$\beta k_y^2 \langle v_o^+ | v_o^+ \rangle c_1 = \xi_1^+ \langle v_o^+ | u_o^+ \rangle c_1 \tag{25}$$

and

$$[\beta k_y^2 \langle u_o^- | u_o^- \rangle \underset{\sim}{E} - 2\alpha k_y \langle u_o^- | \phi^2 | u_o^- \rangle \underset{\sim}{\sigma}] c_2 = \xi_1^- \langle v_o^- | u_o^- \rangle c_2 \quad , \tag{26}$$

where we have used Eqs. (21-23) and the self-adjoint property of L_o and L_1.

We note that

$$\langle v_o^+ | v_o^+ \rangle = \frac{4A}{\kappa} \quad , \quad \langle v_o^+ | u_o^+ \rangle = -\frac{1}{2} \frac{\partial}{\partial A^2} \langle v_o^+ | v_o^+ \rangle = -\frac{1}{\kappa A} \quad , \tag{27a}$$

$$\langle u_o^- | u_o^- \rangle = \frac{16}{5} \frac{A^3}{\kappa} \quad , \langle v_o^- | u_o^- \rangle = \langle v_o^+ | v_o^+ \rangle \quad , \tag{27b}$$

$$\langle u_o^- | \phi^2 | u_o^- \rangle = \frac{64}{15} \frac{A^5}{\kappa^5} \quad . \tag{27c}$$

Therefore,

$$\Omega_+^2 \cong \xi_1^+ = -4\beta k_y^2 A^2 \quad . \tag{28}$$

The eigenvalue ξ_1^- is obtained from Eq. (26) by solving the determinantal equation

$$\begin{Vmatrix} \beta k_y^2 \langle u_o^- | u_o^- \rangle - \xi_1^- \langle v_o^- | u_o^- \rangle & -2\alpha k_y \langle u_o^- | \phi^2 | u_o^- \rangle \\ 2\alpha k_y \langle u_o^- | \phi^2 | u_o^- \rangle & \beta k_y^2 \langle u_o^- | u_o^- \rangle - \xi_1^- \langle v_o^- | u_o^- \rangle \end{Vmatrix} = 0 \tag{29}$$

from which we find

$$\xi_1^- = \frac{4}{3} \beta k_y^2 A^2 \pm i \frac{32}{15} \alpha k_y \frac{A^4}{\kappa} \tag{30a}$$

$$\Omega_- \cong \sqrt{\xi_1^-} = \pm (a^2 + b^2)^{1/4} e^{\pm i\theta/2} \tag{30b}$$

where

$$a = \frac{4}{5}\beta k_y^2 A^2 \quad , \quad b = \frac{32}{15}\alpha k_y \frac{A^4}{\kappa} \quad , \quad \theta = \arctan(b/a)$$

with growth rates

$$\gamma_+ = 2\, k_y A\sqrt{\beta}$$

$$\gamma_- = \left\{\frac{16}{15}\frac{\alpha k_y A^4}{\kappa}\left[\left[1 + \left(\frac{5}{8}\,\frac{\beta k_y \kappa}{\alpha A^2}\right)^2\right]^{1/2} - \frac{5}{8}\frac{\beta k_y \kappa}{A^2}\right]\right\}^{1/2}$$

Since the mode-conversion region is excluded $(k_z^2/k_\perp^2)|K_{||}| << 1$, from which we find that $\beta k_y \kappa/\alpha A^2 \lesssim \epsilon^2$, so that

$$\gamma_- \approx \sqrt{\frac{16}{15}\alpha k_y A^4/\kappa} \quad .$$

III. CONCLUDING REMARKS

According to Eqs. (28,30), unstable modes of either parity exist. In first order, positive parity states are driven unstable by the term $\gamma_0(\partial^2/\partial Y^2)\psi$. If δ_0 were absent, Eq. (1) would be of the same form as the equation governing the nonlinear evolution of Langmuir waves with ion inertia neglected. It is this term which is responsible for the instability of Langmuir solitons. Instabilities associated with negative parity modes are due in lowest order solely to the additional nonlinear term $\delta_0[(\partial/\partial Y)|\psi|^2]\psi$, which affects the stability of positive parity states in second order. The relative effects of these two terms can be judged by comparing growth rates of positive and negative parity modes. We find that $\gamma_+/\gamma_- \lesssim 10\,\epsilon << 1$ in regions which are not mode-converting, which indicates that the term $\delta_0[(\partial/\partial Y)|\psi|^2]\psi$ is strongly destabilizing. We therefore

expect large local values of the electric field to exist as the wave propagates away from the lower-hybrid layer, thus causing the soliton to break up into many bunches, which move apart, spreading energy throughout the plasma.

REFERENCES

1. G. Schmidt, *Phys.Rev.Lett., 34* (1975) 724.
2. V.E. Zakharov and A.M. Rubenchik, *Sov.Phys. JETP, 38* (1974) 494.
3. H.H. Kuehl, *Phys.Fluids, 5* (1962) 1095.
4. T.H. Stix, *Phys.Rev.Lett., 15* (1965) 878.
5. M.D. Simonetti, *Phys.Fluids, 18* (1975) 1524.
6. G.J. Morales and Y.C. Lee, *Phys.Rev.Lett., 35* (1975) 930.
7. H.H. Kuehl, *Phys.Fluids, 19* (1976) 1972.
8. N.R. Pereira, A. Sen, and A. Bers, *Phys.Fluids, 21* (1978) 117.
9. H.H. Kuehl, *Phys.Fluids, 21* (1978) 2120.

APPENDIX E

CHAOTIC OSCILLATIONS IN BILINEAR SYSTEMS WITH LINEAR FEEDBACK CONTROLS

P.K.C.Wang

School of Engineering and Applied Science

University of California

Los Angeles, California 90024

This work was supported by the

U.S. Air Force Office of Scientific Research

under Grant No. AFOSR 79-0050

ABSTRACT

Chaotic oscillations or strange attractors in bilinear systems with linear feedback controls are explored. A simple sufficient condition for nonexistence of such oscillations is given. Also, the construction of ellipsoidal bounds for the strange attractor is discussed. The results are applicable to the well-known Lorenz equation and other equations which are known to have chaotic oscillations.

CONTENTS

I. INTRODUCTION

Recently, it was discovered that the nonlinear mathematical models of a number of physical processes exhibit chaotic nonperiodic oscillations. A simple example is the Lorenz model [1] for thermal convection in a fluid layer given by

$$\frac{d}{dt}\begin{bmatrix} x_1 \\ x_2 \\ x_3 \end{bmatrix} = \begin{bmatrix} \sigma(x_2 - x_1) \\ rx_1 - x_2 - x_1x_3 \\ -bx_3 + x_1x_2 \end{bmatrix}, \tag{1}$$

where σ,r and b are constant parameters. It was found that for certain ranges of these parameters, the trajectories of (1) in the state space are attracted to a nonempty set which is neither an equilibrium set nor a periodic orbit. On this set, the trajectories exhibit chaotic nonperiodic oscillations. Ruelle and Takens [2] called such a set a "strange attractor". Oscillations having similar chaotic behavior were discovered in other models such as those for chemical turbulence [3], population dynamics [4], disk dynamos [5] and plasma turbulence [6]. A remarkable feature of such oscillations is that their apparent chaotic or random behavior is intrinsic to the model which is completely deterministic in nature.

In this paper, we consider a bilinear system of the form:

$$dx/dt = Ax + uBx \tag{2a}$$

defined on the n-dimensional Euclidean space E^n whose inner product is denoted by $\langle \cdot,\cdot \rangle$. A and B are real constant $n \times n$ matrices, and u is a linear feedback control given by

$$u = -K\langle c,x \rangle, \tag{2b}$$

where c is a nonzero vector in E^n, and K is a real number corresponding

to the feedback gain. We note that the Lorenz equation (1) can be re-written in the form of (2) with

$$A = \begin{bmatrix} -\sigma & \sigma & 0 \\ r & -1 & 0 \\ 0 & 0 & -b \end{bmatrix} \; ; \quad B = \begin{bmatrix} 0 & 0 & 0 \\ 0 & 0 & -1 \\ 0 & 1 & 0 \end{bmatrix} \; ; \quad c = (1,0,0)^T \tag{3}$$

and $K = -1$.

Although extensive studies have been made on bilinear control systems [7]-[10], most of the attention has been focused on optimal control, various system properties such as controllability and observability, and realization theory. Very little work has been devoted to the self-oscillation of bilinear systems with linear or nonlinear feedback controls. Here, we explore the possibility of existence of chaotic nonperiodic oscillations in system (2). We begin by studying the stability of the equilibrium states of (2), and obtaining some estimates for the solutions. Then, the existence or nonexistence of chaotic oscillations is explored.

II. STABILITY OF EQUILIBRIUM

Assuming that A is nonsingular, the equilibrium set E of system (2) consists of all fixed points of the mapping H defined by

$$H(x) = K \langle c,x \rangle A^{-1}Bx. \tag{4}$$

Obviously, the zero vector belongs to E. Let x_e be a nonzero vector in E. Then,

$$\|x_e\| = |K| |\langle c,x \rangle| \|A^{-1}Bx_e\| \leq |K| \|c\| \| A^{-1}B \| \|x_e\|^2. \tag{5}$$

Hence, any nonzero equilibrium state must lie outside or on the sphere with radius $\rho = (|K| \|c\| \|A^{-1}B\|)^{-1}$. Also, since H is an even operator

(i.e. $H(-x) = H(x)$ for all $x \in E^n$), hence for any nonzero $x_e \in E$, $-x_e \notin E$,

Now, consider the equation

$$x = H(x) \tag{6}$$

for determining the equilibrium states. Since $K\langle c,x\rangle$ is a real number, any nonzero solution x_e of (6) must be an eigenvector of $A^{-1}B$ corresponding to some nonzero real eigenvalue. Moreover, $\langle c,x_e\rangle \neq 0$. Hence, any nonzero equilibrium state x_e must belong to $\eta(A^{-1}B)^{\perp} \cap \{x \in E^n: \langle c,x\rangle \neq 0\}$, where $\eta(A^{-1}B)$ denotes the null space of $A^{-1}B$. Let v_i be an eigenvector of $A^{-1}B$ associated with the nonzero real eigenvalue λ_i. Then, its corresponding equilibrium state x_e has the form αv_i, where the scalar α can be determined by substituting αv_i into (6), i.e.

$$\alpha v_i = K\langle c,\alpha v_i\rangle\ A^{-1}B(\alpha v_i) = \lambda_i K\alpha^2 \langle c,v_i\rangle v_i$$

or

$$\alpha = 1/(\lambda_i K\ \langle c,v_i\rangle), \tag{7}$$

provided that $K\ \langle c,v_i\rangle \neq 0$.

Evidently, if $A^{-1}B$ has n distinct nonzero real eigenvalues λ_i with corresponding eigenvectors v_i, then the equilibrium set E is given by

$$E = \{0\} \bigcup \{v_i/(\lambda_i K\ \langle c,v_i\rangle): K\langle c,v_i\rangle \neq 0,\ i=1,\ldots,n\}\ . \tag{8}$$

Since $\{v_i, i=1,\ldots,n\}$ is linearly independent and $c \neq 0$, there exists at least one i, say i=k, such that $\langle c,v_k\rangle \neq 0$. Thus, for any nonzero K, E has at least two and at most (n+1) distinct points. In the case where $A^{-1}B$ is a simple linear transformation with repeated real eigenvalues, say $\lambda_i = \lambda$ with eigenvectors v_i, $i \in I \subseteq \{1,\ldots,n\}$. Then, for $K \neq 0$ and $c \notin [\text{span}\{v_i, i \in I\}]^{\perp}$, E has an infinite number of equilibrium points, since any nontrivial linear combination v of such v_i's is again an eigen-

vector of $A^{-1}B$ with $\langle c,v\rangle \neq 0$.

To study the stability of an isolated equilibrium state x_e, we consider the following linearized system about x_e:

$$d\delta x/dt = J_f(x_e)\delta x, \tag{9}$$

where $J_f(x_e)$ is the Jacobian matrix of $f(x) = Ax - K\langle c,x\rangle Bx$ at x_e given by

$$J_f(x_e) = A - KB\{\langle c,x_e\rangle I + x_e c^T\} . \tag{10}$$

Obviously, the stability of the origin is determined only by the eigenvalues of A. At a nonzero equilibrium state $x_e = v_i/(\lambda_i K \langle c,v_i\rangle)$, we have $A^{-1}Bx_e = \lambda_i x_e$ or $Bx_e = Av_i/(K \langle c,v_i\rangle)$. Thus, $J_f(x_e)$ can be rewritten as

$$J_f(x_e) = A \{I - \langle c,v_i\rangle^{-1} v_i c^T\} - \lambda_i^{-1} B \tag{11}$$

which is independent of the feedback gain K. This is evident from the fact that for $K\neq 0$, we may introduce the scaling $x=\hat{x}/K$. Thus, (2) is equivalent to the system

$$d\hat{x}/dt = A\hat{x} - \langle c,\hat{x}\rangle B\hat{x}. \tag{2'}$$

III. ESTIMATES FOR SOLUTIONS; INVARIANT SETS

First, we derive a few elementary estimates for the solutions of (2) under various assumptions on A and B.

Proposition 1: Let μ_i and λ_j denote the eigenvalues of $(A + A^T)$ and $(B + B^T)$ respectively, and $\mu = \max_i\{\mu_i\}$, $|\lambda| = \max_j\{|\lambda_j|\}$. Assume that $\nu \triangleq |K|\|c\||\lambda| > 0$. Then, a solution of (2) starting with x_o at $t = 0$ satisfies one of the following estimates:

(i) for $\hat{\mu}=0$:

$$\|x(t)\| \leq \|x_o\|(1 - \nu\|x_o\|t/2)^{-1} \text{ for all } t\in[0,2(|x_o|\nu)^{-1}[;$$

(ii) for $\hat{\mu}>0$:

$$\|x(t)\| \leq \|x_o\|[(\hat{\mu} + \nu|x_o|)\exp(-\hat{\mu}t/2) - \nu|x_o|]^{-1}$$

for all $t\in[0,t_1[$, where

$$t_1 = 2\hat{\mu}^{-1}\ell n[1 + \hat{\mu}(\nu\|x_o\|)^{-1}];$$

(iii) for $\hat{\mu}<0$ and $\|x_o\| \leq |\hat{\mu}|/\nu$, $\|x(t)\| \leq |x_o\|$ for all $t\geq 0$. Moreover, $\|x(t)\| \to 0$ as $t\to\infty$.

Proof: Let $V(t) = \|x(t)\|^2$. By direct computation

$$dV/dt = \langle x,(A + A^T)x\rangle - K\langle c,x\rangle\langle x,(B + B^T)x\rangle$$
$$\leq \hat{\mu}V + |K|\|c\|\|x\|\,|\langle x,(B + B^T)x\rangle| \leq (\hat{\mu} + \nu V^{\frac{1}{2}})V \triangleq h(V) \qquad (12)$$

with $V(0) = \|x_o\|^2$.

For $\hat{\mu}>0$, h is a strictly monotone increasing function of V. Consequently, $V(t) = \|x(t)\|^2 \leq w(t)$, where w is the solution of

$$dw/dt = (\mu + \nu w^{\frac{1}{2}})w, \quad w(0) = \|x_o\| . \qquad (13)$$

Solving the above equation for each case with $\hat{\mu}=0$ or $\hat{\mu}>0$ leads directly to the estimates (i) and (ii). When $\hat{\mu}<0$, $dV/dt < 0$ for $0 < V < (|\hat{\mu}|/\nu)^2$. Result (ii) follows.||

In the special case where B is skew-symmetric (i.e. $B=-B^T$), we have the exponential estimate:

$$\|x(t)\| \leq |x_o\|\exp(\hat{\mu}t/2) \text{ for all } t\geq 0, \qquad (14)$$

which implies that no solution has finite escape time. Finally, when both A and B are skew-symmetric, $|x(t)|=|x_o\|$ for all t or the solution remains

on the sphere with radius $\|x_o\|$ at all time.

Now, we give lower bounds for the solutions.

Proposition 2: Let $\check{\mu}$ denote the minimum eigenvalue of $(A + A^T)$ and $|\lambda|, \nu$ be as defined in Proposition 1. Then the solution of (2) starting from x_o at t=0 satisfies one of the following lower bounds:

(i) for $\check{\mu}=0$,

$$\|x(t)\| \geq \|x_o\|/(1 + \nu|x_o|t/2) \text{ for all } t\geq 0; \tag{15}$$

(ii) for $\check{\mu}\neq 0$,

$$\|x(t)\| \geq \check{\mu}\|x_o\|/[(\check{\mu} - \nu\|x_o\|)\exp(-\check{\mu}t/2) + \nu|x_o|] \text{ for all } t\geq 0. \tag{16}$$

Proof: Let $V(t) = \|x(t)\|^2$. Then,

$$dV/dt \geq \check{\mu}V - K\langle c,x\rangle\langle x,(B + B^T)x\rangle \geq (\mu - \nu V^{\frac{1}{2}})V \tag{17}$$

with $V(0) = \|x_o\|^2$. Consequently, $V(t) = \|x(t)\|^2 \geq w(t)$, where w is the solution of

$$dw/dt = (\mu - \nu w^{\frac{1}{2}})w, \qquad w(0) = \|x_o\|^2. \tag{18}$$

Solving (16) leads to estimates (15) and (16).||

We observe that for $\check{\mu}>0$ and $\check{\mu}<0$, the lower bound (16) tends to $\check{\mu}/\nu$ and zero respectively as $t\to\infty$. Also, the lower bound (15) tends to zero as $t\to\infty$.

Now, we consider the existence of linear subspaces in E^n which are invariant sets of the system.

Proposition 3: Let A represent a simple linear transformation on E^n with distinct real eigenvalues $\tilde{\lambda}_i$ and their corresponding eigenvectors $\tilde{v}_i$, i=1,...,n. Let $J\subset\{1,...,n\}$ denote the index set such that $\{\tilde{\lambda}_i : i\in J\}$ represents all the uncontrollable modes of (A,B) and all the unobservable modes of (A,c^T). Then, $\text{span}\{\tilde{v}_i; i\in J\}$ is an invariant set of (2).

Proof: Let $T = [\tilde{v}_1 | \cdots | \tilde{v}_n]$. Since A is simple, T^{-1} exists and $T^{-1}AT = \Lambda = \text{diag}[\tilde{\lambda}_1, \ldots, \tilde{\lambda}_n]$. Let $x = Tz$. Then, (2) is transformed into the following form:

$$dz/dt = \Lambda z - K\langle c, Tz\rangle T^{-1}BTz. \tag{19}$$

If $\tilde{\lambda}_j$ is an uncontrollable mode of (A,B), then the j-th row of $T^{-1}B$ must be zero. Also, if $\tilde{\lambda}_j$ is an unobservable mode of (A,c^T), then the j-th column of c^TT must be zero. In either case, the equation corresponding to the j-th mode reduces to $dz_j/dt = \tilde{\lambda}_j z_j$. Thus, the subspace spanned by $\tilde{v}_j$ is an invariant set of (2), and the desired result follows.||

For a general linear transformation A, we can introduce the usual canonical decomposition of the state space of the linear system: $dx/dt = Ax + Bu$, $y = \langle c,x\rangle$ according to its controllable, uncontrollable, observable and unobservable modes. It is easy to see that the subspace corresponding to the uncontrollable and/or unobservable modes of the foregoing linear system is an invariant set of (2).

IV. CHAOTIC OSCILLATIONS

The existence of chaotic oscillations or strange attractors depends on the manner in which the stable and unstable manifolds intersect with each other. Given a system such as (2), suppose we could find all the bounded invariant manifolds of the system, then we could seek chaotic oscillations by deleting those invariant manifolds which correspond to the equilibrium set and periodic orbits. The remaining ones, if they exist, may consist of solutions which are almost periodic, pseudo-random or chaotic functions of time. The distinction between the almost periodic solutions from the pseudo-random solutions can be accomplished by investigating the asymptotic properties of their correlation functions, provided that these solutions are known. The

foregoing approach, although conceptually simple, represents a formidable task from the analytical and/or computational standpoints. So far, chaotic oscillations in certain nonlinear systems were discovered through numerical computation and bifurcation analysis. It is desirable to have readily verifiable analytical conditions for determining the existence of chaotic oscillations directly in terms of the right-hand-sides of the system equations. Lacking such results at the present time, we shall restrict ourselves to the less ambitious tasks of establishing simple sufficient conditions for the nonexistence of chaotic oscillations, and obtaining bounds for the amplitudes of the chaotic oscillations when they exist.

Theorem 1: If $A+A^T$ is negative definite; B is skew-symmetric, and $c \in \eta(A^{-1}B)$, then system (2) has no periodic, almost periodic or chaotic oscillations.

Proof: Since any nonzero equilibrium state of (2) must belong to $\eta(A^{-1}B)^{\perp} \cap \{x \in E^n : \langle c,x \rangle \neq 0\}$, hence the zero state is the only equilibrium state if c $\eta(A^{-1}B)$. Since A+A is negative definite, $\langle x, (A+A^T)x \rangle \leq \mu \|x\|^2$ for all $x \in E$, where is the minimum eigenvalue of $A+A^T$. Since B is skew-symmetric, x(t) has a decaying exponential upper bound given by (14), implying that the origin is asymptotically stable in the large. Hence, no periodic, almost periodic or chaotic oscillations can exist. ||

Assuming the existence of chaotic oscillations, we proceed to construct an ellipsiodal domain Ω in E^n which contains the invariant manifold generated by the chaotic oscillations. This invariant manifold does not contain any equilibrium states.

Consider a quadratic form in x given by

$$V(x) = \langle x-\tilde{x}, Q(x-\tilde{x}) \rangle, \tag{20}$$

where $\tilde{x}$ is a constant vector in E^n and Q is a positive definite symmetric

matrix. We shall make use of V to establish conditions under which Ω is an attractor of (2) in the sense that every trajectory initiated from the exterior of Ω eventually enters Ω at some finite time $t_1>0$ and remains in Ω for all $t>t_1$, or tends to Ω as $t\to\infty$. Clearly, such a Ω contains all the trajectory points of the chaotic oscillations when they exist.

Theorem 2: Suppose that A is nonsingular and there exist a nonzero vector $\tilde{x}\in E^n$ and a positive definite symmetric matrix Q such that

(i) QB is skew-symmetric;

(ii) $G\overset{\Delta}{=}A^TQ+QA+KP$ is negative definite, where $P = c\tilde{x}^TQB+B^TQ\tilde{x}c^T$,

then there exists an ellipsoidal set $\Omega=\{x\in E^n: V(x) \leqslant \alpha\}$ which is an attractor of system (2) containing the manifold generated by the chaotic oscillations when they exist.

Proof: Consider dV/dt given by

$$dV/dt = \langle x,(A^TQ+QA)x\rangle - K\langle c,x\rangle\langle x,(B^TQ+QB)x\rangle - 2\langle x,A^TQ\tilde{x}\rangle + K\langle c,x\rangle(\langle x,B^TQ\tilde{x}\rangle + \langle \tilde{x},QBx\rangle). \tag{21}$$

In view of condition (i), the second term in the right-hand-side of (21) vanishes. Rewriting the last term in (21) as $K\langle x,Px\rangle$, (21) reduces to

$$dV/dt = \langle x,Gx\rangle - 2\langle x,A^TQ\tilde{x}\rangle. \tag{22}$$

From (ii), G^{-1} exists. We can rewrite (22) as

$$dV/dt = \langle x-x_s,G(x-x_s)\rangle - C, \tag{23}$$

where $x_s = G^{-1}A^TQ\tilde{x}$ and $C = \langle x_s,Gx_s\rangle$. Since A is nonsingular, Q is positive definite and $\tilde{x}\neq 0$, hence $x_s \neq 0$. Evidently, at any point exterior to the ellipsoidal set $\tilde{\Omega} \overset{\Delta}{=} \{x\in E^n: -\langle x-x_s,G(x-x_s)\rangle\leqslant|C|\}$, $dV/dt < 0$. Also, since $\tilde{\Omega}$ is bounded, there exists a real number α such that the ellipsoidal set $\Omega\overset{\Delta}{=}\{x\in E^n: V(x) \leqslant \alpha\}$ contains $\tilde{\Omega}$. Consequently, we have dV/dt <0 along any trajectory exterior to Ω, which implies that Ω is an attractor of (2).||

Remarks:

(R-1) Condition (i) requires the existence of a positive definite symmetric matrix Q such that

$$B^TQ + QB = 0. \tag{24}$$

Rewriting (24) in the usual form of a linear equation $Sq = 0$ with $S = B^T \otimes I + I \otimes B^T$ and $q = (q_1^T,\ldots,q_n^T)^T$, where q_i is the i-th column of Q and $\otimes$ denotes the Kronecker product, we see that for the existence of a nonzero q or Q satisfying (24), S must be singular. Since the eigenvalues of S have the form $\lambda_i + \lambda_j$, where λ_i and λ_j are eigenvalues of B, there must exist λ_i and λ_j such that $\lambda_i + \lambda_j = 0$. This is possible if and only if at least one of the following conditions holds: (i) B is singular; (ii) B has real eigenvalues symmetric about the origin, and (iii) B has one or more complex conjugate pairs of pure imaginary eigenvalues. For the special case where B is skew-symmetric, all its eigenvalues lie on the imaginary axis. Hence (24) has nontrivial solutions Q. The requirement that Q be positive definite imposes further restrictions on B. Results for a special form of B were given in [11] and [12].

(R-2) Condition (ii) requires the negative definiteness of G. We note that if B is singular, then for all $x \in \eta(QB)$ (the null space of QB), $\langle x,Px\rangle = 0$ regardless of the choice of $\tilde{x}$. Therefore, in this case, a necessary condition for G to be negative definite is that $\Pi^T(A^TQ + QA)\Pi$ be negative definite, where the matrix Π represents the projection onto $\eta(QB)$.

(R-3) Given a pair $(\tilde{x},Q)$ satisfying conditions (i) and (ii) of Theorem 1, the smallest ellipsoidal set Ω containing $\tilde{\Omega}$ can be found by solving the following standard constrained optimization problem: Maximize

$V(x) = \langle x-\tilde{x}, Q(x-\tilde{x})\rangle$ over the ellipsoid $\partial\tilde{\Omega} = \{x\in E^e : \langle x-x_s, G(x-x_s)\rangle = C\}$. Although this problem can be solved exactly, it is useful to construct an ellipsoidal set Ω' (not necessarily the smallest one) which contains $\tilde{\Omega}$. Let $w = Q^{\frac{1}{2}}(x-\tilde{x})$ so that $V = \|w\|^2$ and $\tilde{\Omega} = \{w\in E^n : -\langle w-Q^{\frac{1}{2}}(x_s-\tilde{x}), Q^{-\frac{1}{2}}GQ^{-\frac{1}{2}}(w-Q^{\frac{1}{2}}(x_s-\tilde{x}))\rangle \leq |C|\}$. Since

$$\gamma\|w-Q^{\frac{1}{2}}(x_s-\tilde{x})\|^2 \leq -\langle w-Q^{\frac{1}{2}}(x_s-\tilde{x}), Q^{-\frac{1}{2}}GQ^{-\frac{1}{2}}(w-Q^{\frac{1}{2}}(x_s-\tilde{x}))\rangle \leq |C|, \tag{25}$$

where γ is the minimum eigenvalue of the positive definite symmetric matrix $-Q^{-\frac{1}{2}}GQ^{-\frac{1}{2}}$, we have

$$\|w\| - \|Q^{\frac{1}{2}}(x_s-\tilde{x})\| \leq \|w-Q^{\frac{1}{2}}(x_s-\tilde{x})\| \leq (|C|/\gamma)^{\frac{1}{2}} \tag{26}$$

or

$$\|w\| \leq (|C|/\gamma)^{\frac{1}{2}} + \|Q^{\frac{1}{2}}(x_s-\tilde{x})\| \triangleq \sqrt{\alpha'}. \tag{27}$$

Thus, the ellipsoidal set

$$\Omega' = \{x\in E^n : \langle x-\tilde{x}, Q(x-\tilde{x})\rangle \leq \alpha'\} \tag{28}$$

contains $\tilde{\Omega}$.

An alternate approach is to find a pair $(\tilde{x},Q)$ satisfying conditions (i) and (ii) such that the ellipsoidal set containing $\tilde{\Omega}$ has the smallest volume. This problem is not so straightforward.

(R-4) If system (2) has invariant sets of the form $\text{span}\{\tilde{v}_i; i\in J\}$ as described in Proposition 3, then their intersection with the invariant manifold generated by the chaotic oscillations must be empty. Moreover, the invariant sets $\text{span}\{\tilde{v}_i\}$ associated with the positive eigenvalues $\tilde{\lambda}_i$, $i\in J$ can have at most the zero vector in common with the ellipsoidal set Ω in Theorem 2.

V. EXAMPLES

First,we consider an equivalent version of the Lorenz equation in the form of (2) with variable feedback gain K, and A,B,c given by (3). Assuming that $b\neq 0$ and $\sigma(1-r)\neq 0$, A is invertible. The eigenvalues of $A^{-1}B$ given by

$$A^{-1}B = \begin{bmatrix} 0 & 0 & (1-r)^{-1} \\ 0 & 0 & (1-r)^{-1} \\ 0 & -b^{-1} & 0 \end{bmatrix} \tag{29}$$

are

$$\lambda_1 = 0, \quad \lambda_{2,3} = \pm[b(1-r)]^{-\frac{1}{2}} . \tag{30}$$

Thus, the equilibrium set E consists of the zero state and

$$\begin{aligned} v_2/(\lambda_2 K\langle c,v_2\rangle) &= K^{-1}(\sqrt{b(r-1)},\sqrt{b(r-1)},1-r)^T, \\ v_3/(\lambda_3 K\langle c,v_3\rangle) &= K^{-1}(-\sqrt{b(r-1)},-\sqrt{b(r-1)},1-r)^T, \end{aligned} \tag{31}$$

where v_2 and v_3 are eigenvectors of $A^{-1}B$ corresponding to λ_2 and λ_3 respectively. Also, the eigenvalues of A are given by

$$\tilde{\lambda}_1 = [-(1+\sigma)+\Delta^{\frac{1}{2}}]/2, \quad \tilde{\lambda}_2 = [-(1+\sigma)-\Delta^{\frac{1}{2}}]/2, \quad \tilde{\lambda}_3 = -b \tag{32}$$

and their corresponding eigenvectors $\tilde{v}_i$ are

$$T = [\tilde{v}_1 | \tilde{v}_2 | \tilde{v}_3] = \begin{bmatrix} 2\sigma/(\sigma-1+\Delta^{\frac{1}{2}}) & 2\sigma/(\sigma-1-\Delta^{\frac{1}{2}}) & 0 \\ 1 & 1 & 0 \\ 0 & 0 & 1 \end{bmatrix} \tag{33}$$

where $\Delta=(1+\sigma)^2-4\sigma(1-r)$. If σ and Δ are nonzero, then T^{-1} exists and

$$T^{-1}B = \begin{bmatrix} 0 & 0 & -4\sigma r\Delta^{-\frac{1}{2}}[\sigma-1-\Delta^{\frac{1}{2}}]^{-1} \\ 0 & 0 & 4\sigma r\Delta^{-\frac{1}{2}}[\sigma-1+\Delta^{\frac{1}{2}}]^{-1} \\ 0 & 1 & 0 \end{bmatrix} \tag{34}$$

$$C^T T = [2\sigma/(\sigma-1+\Delta^{\frac{1}{2}}), 2\sigma/(\sigma-1-\Delta^{\frac{1}{2}}), 0].$$

Evidently, (A,B) is completely controllable and $\tilde{\lambda}_3$ is the only unobservable mode of (A,c^T). From Proposition 3, span$\{\tilde{v}_3\}$ is an invariant set of the system. Since B is skew-symmetric, the solutions have an exponential upper bound (14) with $\hat{\mu} = \max\{-2b, -(1+\sigma) \pm [(1-\sigma)^2+(\sigma+r)^2]^{\frac{1}{2}}\}$.

Now, we apply Theorem 2 to construct an ellipsoidal set Ω which contains the orbits of the chaotic oscillations when they exist. To simplify the computations, we make use of a function V of the form (20) with a diagonal matrix $Q = \text{diag}[q_{11}, q_{22}, q_{33}]$. To satisfy condition (i) of Theorem 2, we must have $q_{22} = q_{33}$. Let $\tilde{x} = (\tilde{x}_1, \tilde{x}_2, \tilde{x}_3)^T$. Then, the matrix G in condition (ii) of Theorem 2 is given explicitly by

$$G = \begin{bmatrix} -2\sigma q_{11} & \sigma q_{11} + (r+K\tilde{x}_3)q_{33} & -Kq_{33}\tilde{x}_2 \\ \sigma q_{11} + (r+K\tilde{x}_3)q_{33} & -2q_{33} & 0 \\ -Kq_{33}\tilde{x}_2 & 0 & -2bq_{33} \end{bmatrix} \tag{35}$$

We must choose $q_{11}, q_{33} > 0$ and $\tilde{x}$ such that G is negative definite. For expedience, we set

$$\tilde{x}_2 = 0, \quad \tilde{x}_3 = -(\sigma q_{11} + r q_{33})/(Kq_{33}) \tag{36}$$

so that G reduces to a diagonal matrix. For $\sigma, b > 0$, G is negative definite for any positive q_{11} and q_{33}. Now, we have $dV/dt < 0$ at any point exterior to the ellipsoidal set $\tilde{\Omega} = \{x \in E^3 : -\langle x-x_s, G(x-x_s)\rangle \leq |C|\}$, where

$$\begin{aligned} x_s &= G^{-1}A^T Q\tilde{x} = (\tilde{x}_1/2, -\sigma q_{11}\tilde{x}_1/(2q_{33}), -(\sigma q_{11}+rq_{33})/(2Kq_{33}))^T, \\ C &= \langle x_s, Gx_s\rangle = -(1/2)q_{33}^{-1}\{\sigma q_{11}\tilde{x}_1^2(q_{33}+\sigma q_{11}) + b(\sigma q_{11}+rq_{33})^2/K^2\}. \end{aligned} \tag{37}$$

The remaining task is to construct an ellipsoidal set

$$\Omega = \{x \in E^3 : \langle x-\tilde{x}, Q(x-\tilde{x})\rangle = q_{11}(x_1-\tilde{x}_1)^2 + q_{33}x_2^2 + q_{33}[x_3+(\sigma q_{11}+rq_{33})/(Kq_{33})]^2 \leq \alpha\} \tag{38}$$

which contains $\tilde{\Omega}$. Such a set is given by Ω' in (28) with

$$\sqrt{\alpha'} = (|C|/\gamma)^{\frac{1}{2}} + \|Q^{\frac{1}{2}}(x_s-\tilde{x})\| = [|C|/(2\min\{1,b,\sigma\})]^{\frac{1}{2}}$$

$$+ (1/2)\{q_{11}\tilde{x}_1^2(1+\sigma^2 q_{11}q_{33}^{-1}) + (\sigma q_{11}+rq_{33})^2/(K^2 q_{33})\}^{\frac{1}{2}}, \qquad (39)$$

where C is defined in (37). We wish to choose q_{11}, q_{33} and $\tilde{x}_1$ such that the volume of Ω'

$$V_{\Omega'} = \frac{4\pi}{3}[(\alpha')^3/q_{11}]^{\frac{1}{2}}q_{33}^{-1} = \frac{4\pi}{3q_{33}\sqrt{q_{11}}}\left\{(|C|/\gamma)^{\frac{1}{2}} + \frac{1}{2}\left[q_{11}\tilde{x}_1^2\left(1+\frac{\sigma^2 q_{11}}{q_{33}}\right) + \frac{(\sigma q_{11}+rq_{33})^2}{K^2 q_{33}}\right]^{\frac{1}{2}}\right\}^3 \qquad (40)$$

is minimized. Since for any fixed $q_{11}, q_{33}>0$, $V_{\Omega'}$ is a strictly monotone increasing function of $\tilde{x}_1$ for $\tilde{x}_1 \geq 0$, hence we set $\tilde{x}_1=0$ in (40). The resulting $V_{\Omega'}$ can be rewritten in terms of the ratio $q=q_{33}/q_{11}$

$$V_{\Omega'} = (4\pi/3)[\sqrt{b/(2\gamma)} + 1/2]^3 |K|^{-3} q^{-\frac{5}{2}}(\sigma+rq)^3, \qquad (41)$$

which has a minimum point in $[0,\infty[$ given by $\hat{q} = 5\sigma/r$.

This specifies a $\Omega'=\{x\in E^3 : x_1^2+\hat{q}x_2^2+\hat{q}[x_3+6r/(5K)]^2 \leq (9/5)(\sigma r K^{-2})(\sqrt{2b/\lambda}+1)^2\}$ which contains the manifold generated by the chaotic oscillations.

It is known [1] that for K=-1, σ=10 and b=8/3, chaotic oscillations or a strange attractor exist for $r > 24.06$. Since for $K\neq 0$, systems (2) and (2') are equivalent, we conclude that chaotic oscillations exist for the foregoing values of σ,b and r and any $K\neq 0$. The peak magnitudes $|x_1|$ of the oscillations or the size of the strange attractor are inversely proportional to $|K|$.

Figure 1 shows a typical buildup of the chaotic oscillations in the time domain for the foregoing values of σ,b,K=1 and r=30. The projections of the trajectory onto the (x_1,x_2) and (x_3,x_2) planes are shown in Fig.2. For these parameter values, $V_{\Omega'}$ given by (41) has a minimum point $\hat{q}=5/3$

which gives $\Omega' = \{x \in E^3: x_1^2/(61.185)^2 + x_2^2/(47.394)^2 + (x_3+36)^2/(47.394)^2 \leq 1\}$ containing the strange attractor. The ellipses corresponding to the boundary of Ω' in its principal-axes planes are also shown in Fig.2. It should be mentioned that nonellipsoidal bounds for the strange attractor of the Lorenz equation have been obtained using certain invariants of the equation with $\sigma=0$ [13],[14].

Besides the Lorenz equation, there are a number of other nonlinear systems which are known to exhibit chaotic oscillations and can be written in the form of (2). An example is given by Rössler [15] where A,B and c are

$$A = \begin{bmatrix} 0 & -1 & -1 \\ 1 & \sigma & 0 \\ b & 0 & -r \end{bmatrix}, \quad B = \begin{bmatrix} 0 & 0 & 0 \\ 0 & 0 & 0 \\ 0 & 0 & 1 \end{bmatrix}, \quad c = (1,0,0)^T, \tag{42}$$

and $K=-1$. Here, A is nonsingular if $\sigma b \neq r$. The equilibrium set $\bar{E}$ consists of the origin and the point $(-\sigma b+r, b-r\sigma^{-1}, r\sigma^{-1}-b)^T$. It can be readily verified that (A,B) is completely controllable and if $\sigma \neq r$, (A,c^T) is completely observable. Also,there does not exist nontrivial linear invariant subspaces if $\sigma \neq r$.

It is known that this system has chaotic oscillations for $b=0.4$, $r=4.5$ and $0.36 \leq \sigma \leq 0.5$. Again, Using Theorem 2, we can construct an ellipsoidal set Ω which contains the chaotic orbits. We omit the details here. A typical solution corresponding to chaotic oscillations is shown in Figs. 3 and 4.

VI. CONCLUDING REMARKS

The existence of chaotic oscillations in deterministic nonlinear dynamical systems is an intriguing phenomenon which is inherent in a number of mathematical models for real-world systems. For models of population

dynamics and economic systems, chaotic oscillations imply the absence of predictable "cycles". In fluid models, such oscillations could provide a mathematical explanation of various turbulence phenomena. Chaotic oscillations could also arise in bilinear systems with linear feedback controls as demonstrated here. They cannot be predicted or analyzed using conventional methods. Although at the present time, there are a number of mathematical results pertaining to various strange attractors in abstract dynamical systems [16],[17]. However, they are not readily applicable for determining the existence of chaotic oscillations even for the relatively simple class of nonlinear systems considered here. The establishment of sufficient conditions for the existence of chaotic oscillations or strange attractors is a difficult challenging problem in nonlinear system theory.

Here, we have considered only continuous-time systems. Similar results can be obtained for discrete-time bilinear systems with linear feedback controls of the form:

$$\begin{aligned} x(k+1) &= Ax(k) + u(k)Bx(k), \\ u(k) &= -K\langle c, x(k)\rangle. \end{aligned} \tag{43}$$

It is known that chaotic oscillations can exist in such systems also. In fact, the scalar equation: $x(k+1) = ax(k) - ax^2(k)$ has chaotic oscillations for $3.57<a\leq 4.0$ [18].

A problem of practical interest is the extension of nonturbulent regime in a fluid system to a broader range of Reynold's numbers. If fluid turbulence is indeed explainable by the theory of chaotic oscillations, then it may be possible to achieve the desired result by introducing appropriate feedback controls into the system. Finally, it is of interest to synthesize nonlinear systems to generate chaotic oscillations or pseudo-random functions having certain desired properties, This idea has al-

ready been utilized in a number of pseudo-random number algorithms in digital computation.

REFERENCES

[1] E.N.Lorenz,"Deterministic Nonperiodic Flow", J. of the Atmospheric Sciences, Vol.20,pp.130-141,March,1963.

[2] D.Ruelle and F.Takens,"On the Nature of Turbulence", Commun.Math. Phys. Vol.20,pp.167-192,1971.

[3] O.E.Rössler,"Chemical Turbulence:Chaos in a Simple Reaction-Diffusion System", Z.Naturforch. Vol.31,pt.a,p.1168,1976.

[4] R.M.May (Editor), Theoretical Ecology:Principles and Applications, Blackwell,Oxford,1976.

[5] E.Bullard,"The Disk Dynamo", in Topics in Nonlinear Dynamics (Edited by S.Jorna), Am. Inst. of Physics, AIP Conf. Proc. No.46,1978, pp.373-389.

[6] P.K.C.Wang,"Nonperiodic Oscillations of Langmuir Waves", UCLA Engr. Rpt. No. ENG-7879, Nov. 1978, Submitted to J.Math.Physics.

[7] R.R.Mohler, Bilinear Control Processes with Applications to Engineering,Ecology and Medicine, Academic Press, N.Y.1973.

[8] C.Bruni, G. DiPillo and G.Koch, "Bilinear Systems: An Appealing Class of Nearly Linear Systems in Theory and Applications", IEEE Trans. on Auto. Control, Vol.AC-19,No.4,pp.334-348, Aug.1974.

[9] A.Isidori and A.Ruberti,"Realization Theory of Bilinear Systems", in Geometric Methods in System Theory,(Edited by D.Q.Mayne and R.W. Brockett), D.Reidel,Dordrecht,Holland,1973.

[10] R.E.Rink and R.R.Mohler,"Completely Controllable Bilinear Systems", SIAM J. Control, Vol.6,No.3, pp.477-486,1968.

[11] J.Walker,"On the Application of Liapunov's Direct Method to Linear Lumped Parameter Elastic Systems", J.Appl.Mech. Vol.41,pp.278-284,1974.

[12] M.Slemrod,"Stabilization of Bilinear Control Systems with Applications to Nonconservative Problems in Elasticity", SIAM J. Control and Opti-

mization,Vol.16,No.1,pp.131-141,1978.

[13] Y.M.Treve,"Boxing-in the Lorenz Attractor", Preprint,1978.

[14] H.Haken and A.Wunderlin,"New Interpretation and Size of Strange Attractor of the Lorenz Model of Turbulence",Phys..Letters, Vol.62A, No.3, pp.133-134,1977.

[15] O.E.Rössler,"Continuous Chaos--Four Prototype Equations", in Bifurcation Theory and Applications in Scientific Disciplines,(Edited by O.Gurel and O.E.Rössler),New York Acad. of Sciences,N.Y.1979,pp.376-392.

[16] S.Smale,"Differentiable Dynamical Systems",Bull.Am.Math.Soc. Vol.73, pp.747-817,1967.

[17] S.Newhouse,D.Ruelle and F.Takens,"Occurrence of Strange Axiom A Attractors Near Quasi Periodic Flows on T^m,$m\geq 3$", Comm. Math. Phys. Vol.64, pp.35-40,1978.

[18] T-Y. Li and J.A.Yorke,"Period Three Implies Chaos", Am.Math.Monthly, Vol.82,pp.985-992,1975.

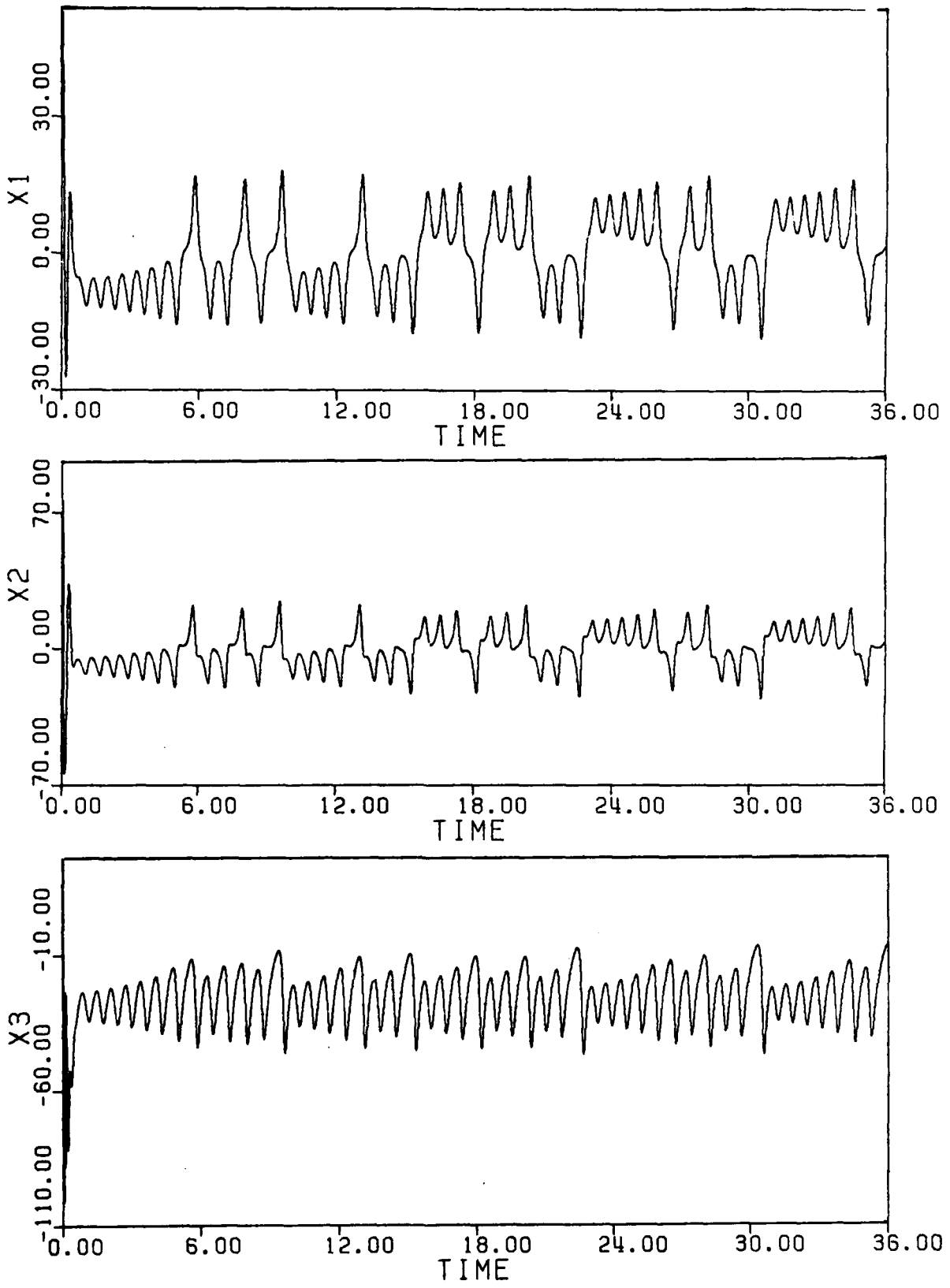
X1
30.00
0.00
-30.00
0.00
6.00
12.00
18.00
24.00
30.00
36.00
TIME
X2
70.00
0.00
-70.00
0.00
6.00
12.00
18.00
24.00
30.00
36.00
TIME
X3
-10.00
-60.00
-110.00
0.00
6.00
12.00
18.00
24.00
30.00
36.00
TIME

Figure 1

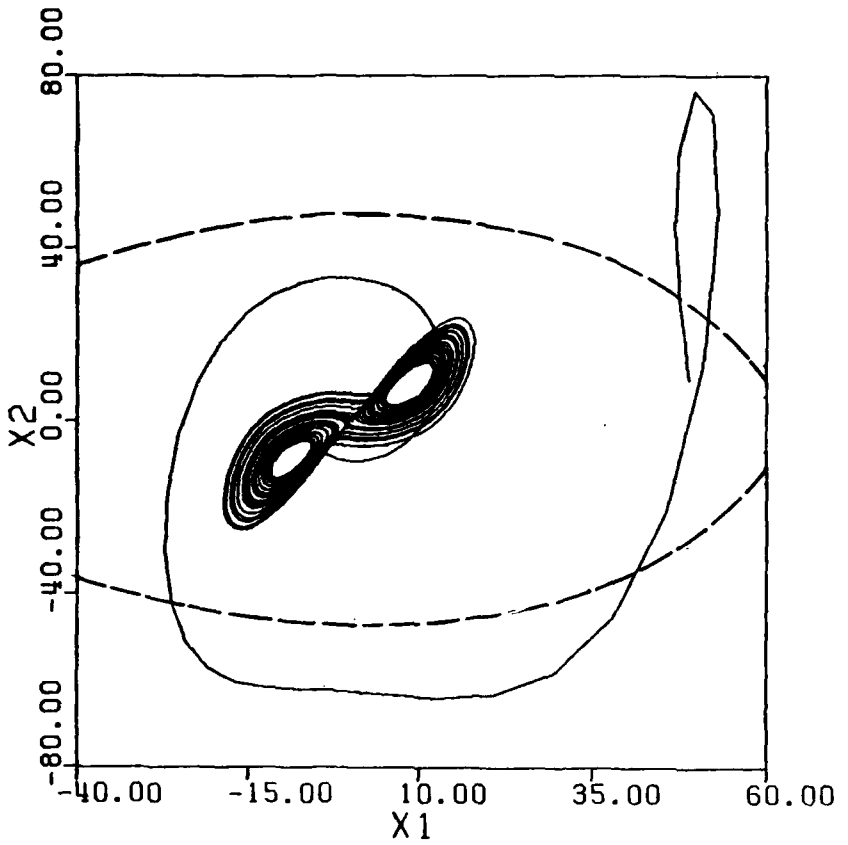
80.00
40.00
0.00
-40.00
-80.00
X2
-40.00
-15.00
10.00
35.00
60.00
X1

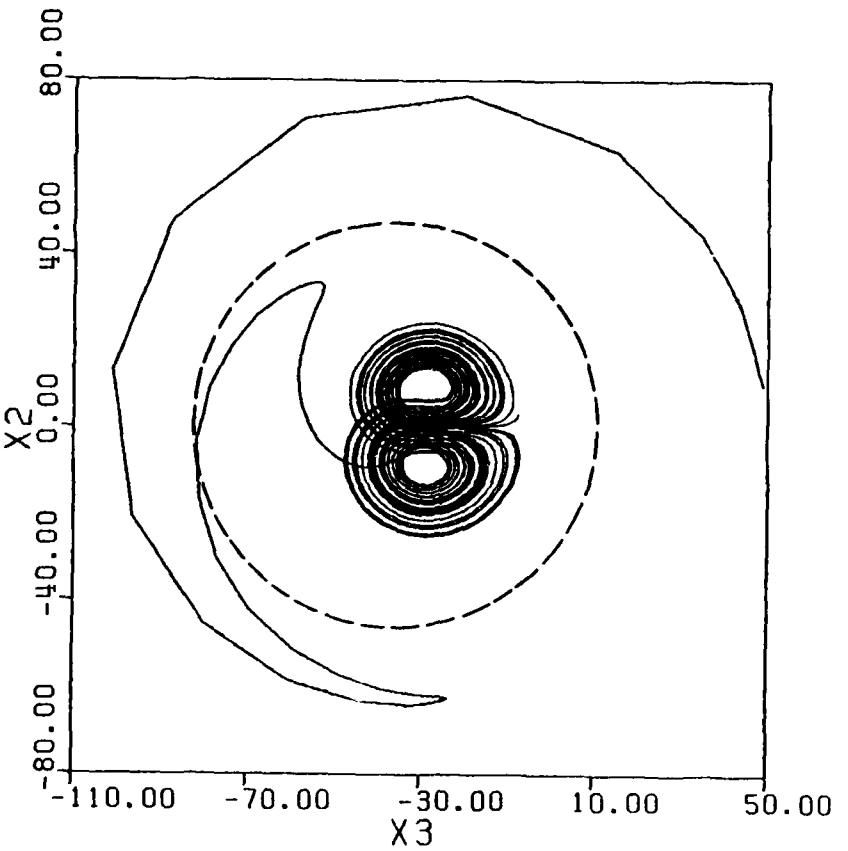
80.00
40.00
0.00
-40.00
-80.00
X2
-110.00
-70.00
-30.00
10.00
50.00
X3

Figure 2:

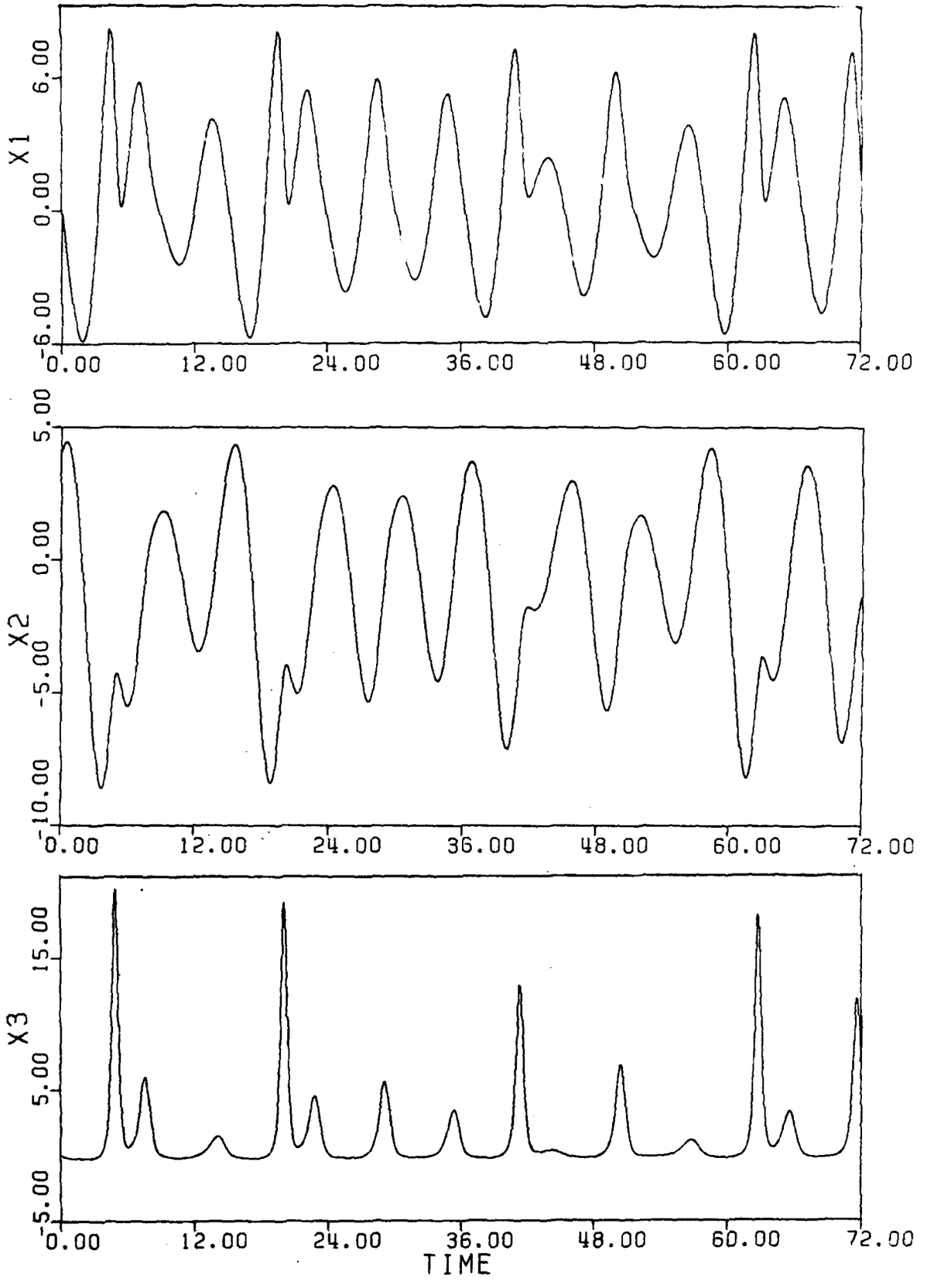
X1
6.00
0.00
-6.00
0.00
12.00
24.00
36.00
48.00
60.00
72.00
X2
5.00
0.00
-5.00
-10.00
0.00
12.00
24.00
36.00
48.00
60.00
72.00
X3
15.00
5.00
-5.00
0.00
12.00
24.00
36.00
48.00
60.00
72.00
TIME

Figure 3

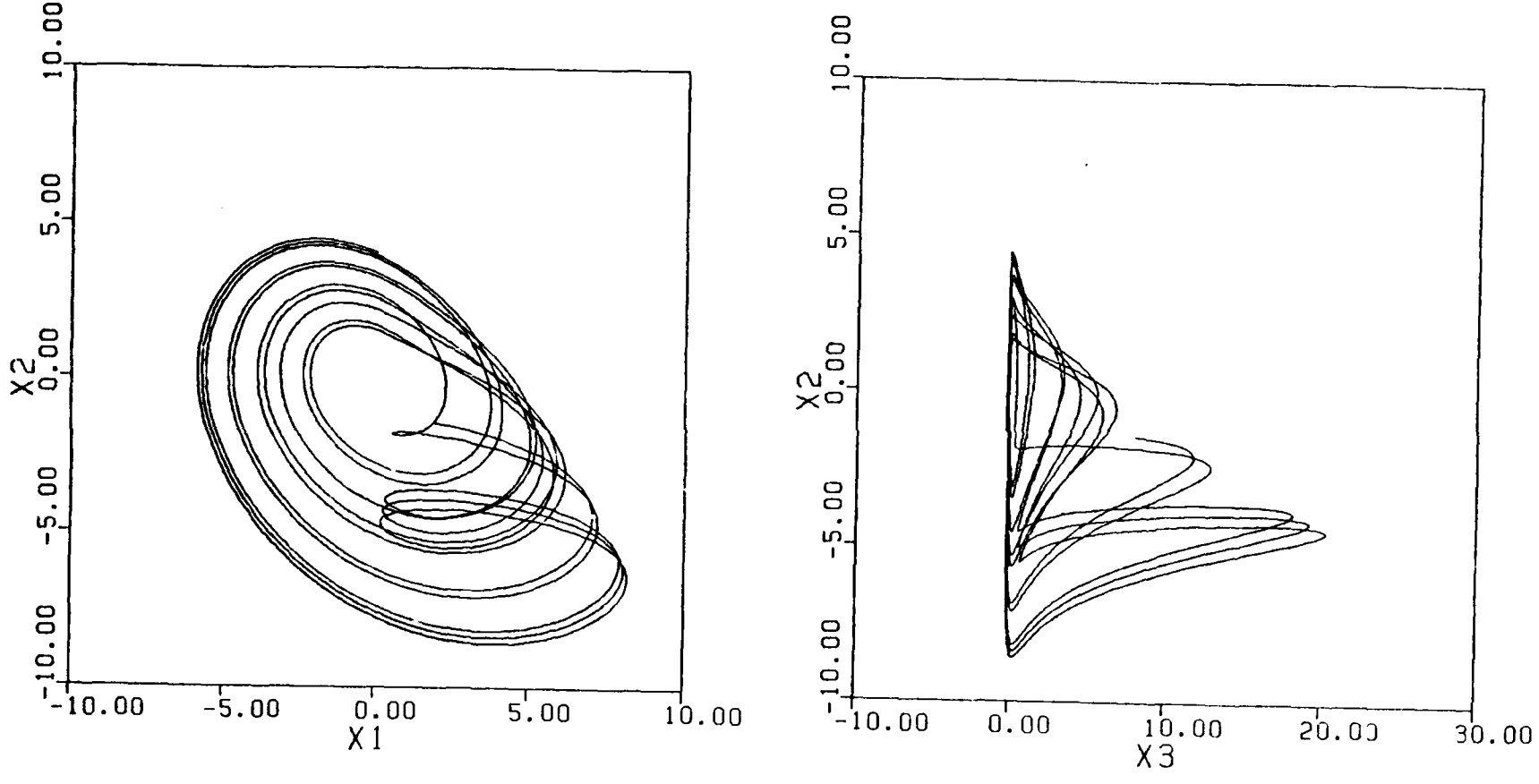
10.00
5.00
0.00
-5.00
-10.00
X2
-10.00
-5.00
0.00
5.00
10.00
X1
10.00
5.00
0.00
-5.00
-10.00
X2
-10.00
0.00
10.00
20.00
30.00
X3

Figure 4

FIGURE CAPTIONS

Figure 1: Time domain solution of Lorenz equation with K=1,σ=10,b=8/3 and r=30; initial conditions: $x_1(0)=x_2(0)=50, x_3(0)=0$.

Figure 2: Projections of the trajectory of Lorenz equation (with parameters given in Fig.1) in the state space onto the (x_2,x_1) and (x_2,x_3) planes, and the ellipses corresponding to the boundary of Ω' in its principal-axes planes indicated by dashed curves.

Figure 3: Time domain solution of eq. (2) (with matrices (42)) for b=0.4, r=4.5,σ=4.0 and K=-1; initial conditions: $x_1(0)=x_3(0)=0$, $x_2(0)=4.0$.

Figure 4: Projections of the trajectory of eq.(2) (with matrices (42) and parameters given in Fig.3) in the state space onto the (x_2,x_3) and (x_2,x_1) planes.

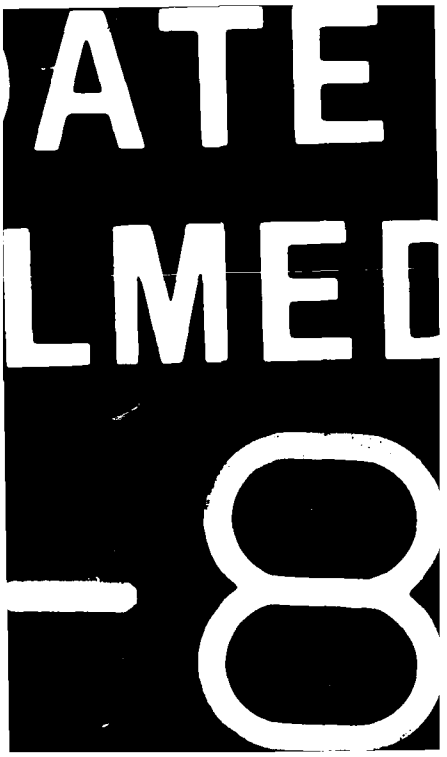
ATE
LMED
8